



Search for singly produced vector-like top partners in multilepton final states with 139 fb^{-1} of pp collision data at $\sqrt{s} = 13 \text{ TeV}$ with the ATLAS detector

The ATLAS Collaboration

A search for the single production of a vector-like top partner (T) with mass greater than 1 TeV decaying into a Z boson and a top quark is presented, using the full Run 2 dataset corresponding to 139 fb^{-1} of pp collisions at $\sqrt{s} = 13 \text{ TeV}$, collected in 2015–2018 with the ATLAS detector at the Large Hadron Collider. The targeted final state is characterized by the presence of a pair of electrons or muons with opposite-sign charges which form a Z -boson candidate, as well as by the presence of b -tagged jets and forward jets. Events with exactly two or at least three leptons are categorized into two independently optimized analysis channels. No significant excess above the background expectation is observed and the results from the two channels are statistically combined to set exclusion limits at 95% confidence level on the masses and couplings of T . The results are interpreted in several benchmark scenarios to set limits on the mass and universal coupling strength (κ) of the vector-like quark. For singlet T quarks, κ values between 0.22 and 0.64 are excluded for masses between 1000 and 1975 GeV. For T quarks in the doublet scenario, where the production cross section is much lower, κ values between 0.54 and 0.88 are excluded for masses between 1000 and 1425 GeV.

1 Introduction

The discovery of the Higgs boson by the ATLAS and CMS experiments at the Large Hadron Collider (LHC) [1, 2] was a major milestone for the Standard Model (SM), the framework for understanding the fundamental constituents of our universe and their interactions. While finding the Higgs boson completed the SM, this model leaves many questions unaddressed about the physical nature of our universe. One of these questions is about the measured Higgs boson mass—specifically, the many orders of magnitude that separate it from the Planck scale, requiring quadratically divergent finely tuned corrections [3]. These large corrections are mitigated in some beyond Standard Model (BSM) theories. Vector-like Quarks (VLQs), colored spin- $\frac{1}{2}$ fermions with identical electroweak (EW) representation for both left and right chiralities, are predicted by a large subset of these theories [4–13]. The usual four VLQ species are denoted by $X_{+\frac{5}{3}}, T_{+\frac{2}{3}}, B_{-\frac{1}{3}}$ and $Y_{-\frac{4}{3}}$, where the subscript indicates the electric charge of the corresponding particle. Their renormalizable EW representation consists of (T) or (B) singlets, (X, T) , (T, B) , or (B, Y) doublets and (X, T, B) or (T, B, Y) triplets. In most representations, they couple to the SM quarks via an exchange of charged (W^\pm) or neutral (Z, H) bosons. The interaction of the VLQs with the SM quarks can be summarized with the following simplified Lagrangian [14]:

$$\mathcal{L} = \sum_{Q,q,\zeta} \left[\frac{g_w}{2c_w} \tilde{\kappa}_\zeta^{Qq} \bar{Q} \not{Z} P_\zeta q + \frac{g_w}{\sqrt{2}} \kappa_\zeta^{Qq} \bar{Q} \not{W} P_\zeta q - \hat{\kappa}_\zeta^{Qq} H \bar{Q} P_\zeta q \right] + \text{h.c.}, \quad (1)$$

where Q represents a VLQ, ζ represents the chirality with P_ζ being the corresponding projection operator, q represents a SM quark of up or down type, and the electroweak couplings $\tilde{\kappa}_\zeta^{Qq}$, κ_ζ^{Qq} , and $\hat{\kappa}_\zeta^{Qq}$ determine the coupling strengths between Q and q when mediated by the Z , W , and H bosons respectively. The mass hierarchy of the SM quarks suggests that VLQs interact predominantly with the third-generation SM quarks [15, 16]. Hence, VLQ interactions with lighter generations are set to zero in the simplified representation of Eq. (1) and the VLQ species T and B are referred to as top and bottom partners respectively in the following discussion.

At the LHC, the dominant modes of VLQ production are pair and single production. During Run 1 (2010–2012) of the LHC, the VLQ searches at center-of-mass energies of $\sqrt{s} = 7$ and 8 TeV typically probed VLQ masses lower than 1 TeV where VLQ pair production dominates [16]. Since the pair production of VLQs proceeds through QCD interactions, the cross-section under the narrow-width approximation only depends on the VLQ mass and not on the species nor its EW representation. No significant excess was observed by the Run 1 searches looking for pair production of VLQs and lower exclusion limits on VLQ mass were reported in the range of approximately 600–1000 GeV, depending on the search [17–22]. The searches for single production of T or B also reported similar limits in Run 1 for a range of couplings probed in the singlet and doublet benchmarks [19, 23].

Run 2 (2015–2018) searches at $\sqrt{s} = 13$ TeV for pair production of top and bottom partners from ATLAS and CMS have set lower limits on the VLQ masses in the range of 800–1400 GeV [24–34]. Since the single production of VLQs can have a larger cross-section at high masses for reasonably large couplings [16], the Run 2 searches are increasingly focusing on this production mode [35–45]. However, unlike pair production, single production of VLQs is mediated by electroweak processes. Both the kinematics and cross-sections of the single VLQ processes depend on the representation and the choice of couplings that determine the relative strength of these particles interacting with SM quarks and vector/Higgs bosons.

This paper focuses on the search for a singly produced T decaying to a Z boson and a top quark using the complete Run 2 dataset collected by the ATLAS detector. As shown in Figure 1, the electroweak interaction can produce a T in the s - and t -channel topologies. These processes are referred to as $WTZt$ and $ZTZt$ processes, where the first W or Z refers to the vector boson scattered off of the incoming parton, T refers to the VLQ exchanged in the intermediate stage, and Zt refers to the production of the Z boson and t quark. The $WTZt$ mode dominates in the singlet representation of T since the smaller coupling between the T and the Z boson and the kinematically disfavored $g \rightarrow t\bar{t}$ splitting suppress the contribution from $ZTZt$. On the other hand, the latter is the dominant mode in the doublet representation since the T 's coupling with the W boson is suppressed by the mass diagonalization matrix [16]. A model-independent approach [46–48] that allows probing a wide range of couplings for the W , Z , and H -mediated interactions of these heavy quarks is adopted in this search.

The analysis is performed across two channels spanning decays of T quarks with mass in the range between 1.0 and 2.7 TeV. The dilepton (2ℓ) channel selects events with exactly one pair of opposite-sign leptons, i.e. electrons or muons and a hadronically decaying top quark in the final state. The trilepton (3ℓ) channel requires, in addition to the pair of opposite-sign leptons, at least a third lepton from a leptonically decaying top quark. The reconstructed Z -boson from the pair of leptons is expected to have large transverse momentum while the hadronic decay of the boosted top quark in the 2ℓ channel would constitute wide-radius jet signatures. These results improve on a previous ATLAS search [35] with a data sample corresponding to an integrated luminosity of 36.1 fb^{-1} , by benefiting from the larger data sample of 139 fb^{-1} , improved kinematic selections and introducing a method to identify hadronically decaying top quarks.

The paper is organized as follows. Section 2 provides a brief overview of the ATLAS detector. The data and simulated background and signal samples are described in Section 3. Section 4 describes the object definition while event selection, categorization, and the analysis strategy are outlined in Section 5. The systematic uncertainties are discussed in Section 6. Results obtained from this search are reported in Section 7 and conclusions are presented in Section 8.

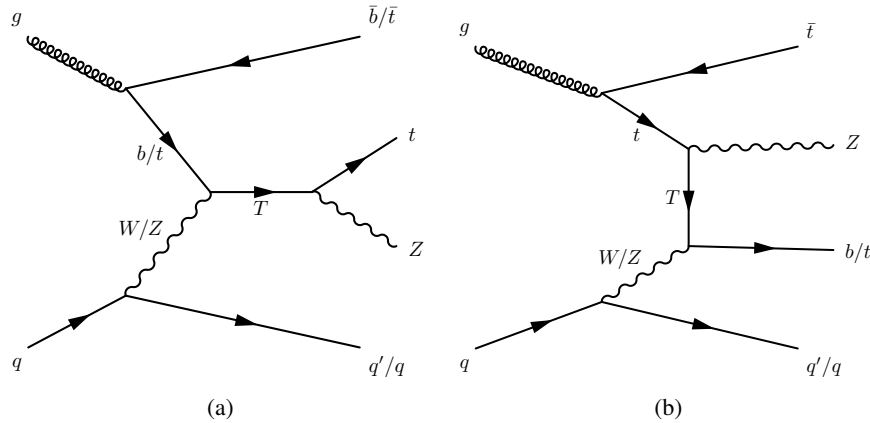


Figure 1: Illustrative (a) s -channel and (b) t -channel Feynman diagrams for $WTZt$ and $ZTZt$ processes.

2 ATLAS detector

The ATLAS detector [49] at the LHC covers nearly the entire solid angle around the collision point.¹ It consists of an inner tracking detector surrounded by a thin superconducting solenoid, electromagnetic and hadronic calorimeters, and a muon spectrometer incorporating three large superconducting air-core toroidal magnets.

The inner-detector system (ID) is immersed in a 2 T axial magnetic field and provides charged-particle tracking in the range of $|\eta| < 2.5$. The high-granularity silicon pixel detector covers the vertex region and typically provides four measurements per track, the first hit normally being in the insertable B-layer (IBL) installed before Run 2 [50]. It is followed by the silicon microstrip tracker (SCT), which usually provides eight measurements per track. These silicon detectors are complemented by the transition radiation tracker (TRT), which enables radially extended track reconstruction up to $|\eta| = 2.0$. The TRT also provides electron identification information based on the fraction of hits (typically 30 in total) above a higher energy-deposit threshold corresponding to transition radiation.

The calorimeter system covers the pseudorapidity range of $|\eta| < 4.9$. Within the region $|\eta| = 3.2$, electromagnetic calorimetry is provided by barrel and endcap high-granularity lead/liquid-argon (LAr) calorimeters, with an additional thin LAr presampler covering $|\eta| < 1.8$ to correct for energy loss in material upstream of the calorimeters. Hadron calorimetry is provided by the steel/scintillator-tile calorimeter, segmented into three barrel structures within $|\eta| = 1.7$, and two copper/LAr hadron endcap calorimeters. The solid angle coverage is completed with forward copper/LAr and tungsten/LAr calorimeter modules optimised for electromagnetic and hadronic energy measurements respectively.

The muon spectrometer (MS) comprises separate trigger and high-precision tracking chambers measuring the deflection of muons in a magnetic field generated by the superconducting air-core toroidal magnets. The field integral of the toroids ranges between 2.0 and 6.0 T m across most of the detector. Three layers of precision chambers, each consisting of layers of monitored drift tubes, cover the region $|\eta| < 2.7$, complemented by cathode-strip chambers in the forward region, where the background is highest. The muon trigger system covers the range of $|\eta| < 2.4$ with resistive-plate chambers in the barrel, and thin-gap chambers in the endcap regions.

Interesting events are selected by the first-level trigger system implemented in custom hardware, followed by selections made by algorithms implemented in the software-based high-level trigger (HLT) [51]. The first-level trigger reduces the incoming data rate from the 40 MHz bunch crossings to a design value of 100 kHz, which is further reduced by the HLT to record events to disk at a rate of about 1 kHz.

An extensive software suite [52] is used in data simulation, in the reconstruction and analysis of real and simulated data, in detector operations, and in the trigger and data acquisition systems of the experiment.

¹ ATLAS uses a right-handed coordinate system with its origin at the nominal interaction point (IP) in the center of the detector and the z -axis along the beam pipe. The x -axis points from the IP to the center of the LHC ring, while the y -axis points upwards. Cylindrical coordinates (r, ϕ) are used in the transverse plane, ϕ being the azimuthal angle around the z -axis. The pseudorapidity is defined in terms of the polar angle θ as $\eta = -\ln \tan(\theta/2)$. Angular distance (ΔR) is defined as $\Delta R \equiv \sqrt{(\Delta\eta)^2 + (\Delta\phi)^2}$.

3 Data and simulated event samples

The data sample was collected by the ATLAS detector in proton–proton (pp) collisions at a center-of-mass energy of $\sqrt{s} = 13$ TeV during Run 2 with all detector subsystems operational and with the LHC operating in stable beam conditions with 25 ns bunch spacing. The dataset corresponds to an integrated luminosity of 139 fb^{-1} with an average of about 34 simultaneous interactions per bunch crossing (pileup).

All of the nominal Monte Carlo (MC) simulation samples used in the analysis were processed with the ATLAS simulation framework [53], using a detailed simulation based on GEANT4 [54]. The effect of pileup was modeled by overlaying the simulated hard-scattering event with inelastic pp events generated with PYTHIA 8.186 [55] using the NNPDF2.3_{LO} set of parton distribution functions (PDF) [56] and the A3 set of tuned parameters (tune) [57]. The pileup is reweighted in the MC event samples to match the pileup conditions in data.

The nominal MC sample for Z boson production with jets (Z +jets) was generated with SHERPA 2.2.1 [58] and the nominal diboson (VV) sample was generated with SHERPA 2.2.2. Both the samples were generated using the NNPDF3.0 [59] next-to-next-to-leading-order (NNLO) PDF set. The Z +jets sample includes events generated with up to two partons at next-to-leading-order (NLO) and up to four partons at leading-order (LO) and is normalized to the NNLO cross-section [60]. The VV sample is normalized to the SHERPA NLO cross-section and includes $q\bar{q}$ -initiated events with up to one parton at NLO and up to three partons at LO and gg -initiated processes simulated using LO matrix elements for up to one additional jet. For both samples, COMIX [61] and OPENLOOPS [62–64] were used and the matrix element (ME) was merged with the SHERPA parton shower [65] according to the MEPS@NLO prescription [66–69]. To estimate modeling uncertainties for these backgrounds, additional samples were produced with MADGRAPH5_AMC@NLO 2.2.3 [70], using the NNPDF3.0_{NLO} PDF set and interfaced to PYTHIA 8.210 [71] with the A14 tune [72] and the NNPDF2.3_{LO} PDF for showering. In the 2ℓ channel, the simulated Z +jets events are categorized into Z +Light Flavor (LF) and Z +Heavy Flavor (HF) events in accordance with the absence or presence of heavy flavor jets in the MC generator record of these simulated events in the kinematic acceptance defined in Sections 4 and 5. An additional set of Z +jets events was generated with SHERPA 2.2.11 to compare the modeling of the Z +jets background in the 2ℓ channel.

The nominal $t\bar{t}$ background sample uses the POWHEG method [73, 74] implemented in POWHEG BOX v2 [75, 76] with the NNPDF3.0_{NNLO} PDF set. POWHEG BOX was interfaced with PYTHIA 8.230 with the A14 tune for showering and hadronization. The sample is normalized to the NNLO cross-section in QCD including resummation of next-to-next-to-leading-logarithmic (NNLL) soft gluon terms calculated with TOP++ [77–83]. For the evaluation of modeling uncertainties, samples were produced with the same matrix element generator as the nominal sample, but HERWIG 7 was used with the H7-UE-MMHT tune [84] for showering and hadronization. To assess the uncertainty in the matching of NLO matrix elements to the parton shower, additional samples were generated with MADGRAPH5_AMC@NLO 2.6.0 and the NNPDF3.0_{NNLO} PDF set, interfaced with PYTHIA 8.230 using the same showering configuration as the nominal sample.

The nominal sample for $t\bar{t}$ production with a vector boson ($t\bar{t} + W$ and $t\bar{t} + Z$) was generated with MADGRAPH5_AMC@NLO 2.3.3 interfaced with PYTHIA 8.210 for showering and hadronization, using the NNPDF2.3_{LO} PDF set and the A14 tune. These events were normalized to the NLO cross-sections calculated with MADGRAPH5_AMC@NLO [85, 86]. To evaluate modeling uncertainties, alternative samples were produced where either the A14 tune was varied or HERWIG 7 was used with the H7-UE-MMHT tune for the showering. Additional samples were produced using SHERPA 2.2.1 to evaluate the uncertainty

due to the choice of matrix element generator. The production of $t\bar{t}\bar{t}$ and $t\bar{t}WW$ events was modeled using the MADGRAPH5_AMC@NLO generator at LO with the NNPDF3.1_{NLO} PDF, interfaced with PYTHIA 8.230 using the A14 tune and the NNPDF2.3_{LO} PDF set. These samples were normalized to cross-sections calculated with NLO QCD and EW corrections [85]. These four processes are merged into a single process labeled $t\bar{t} + X$ in which the contribution from $t\bar{t} + Z$ dominates due to the requirement of an opposite-sign same-flavor (OS-SF) lepton pair with an invariant mass close to that of a Z boson in the final state.

The single-top-quark processes were simulated with POWHEG BOX [87, 88] using the NNPDF3.0_{NLO} PDF set and interfaced to PYTHIA 8.234 with the A14 tune. The samples are normalized to their respective NLO QCD cross-sections [89, 90] for the t -channel and s -channel, and with additional NNLL soft gluon terms for Wt production [91–93]. The production of tZq and tWZ events was modeled using the MADGRAPH5_AMC@NLO generator at NLO with the NNPDF3.0_{NLO} PDF and interfaced with PYTHIA 8.212 using the A14 tune and the NNPDF2.3_{LO} PDF set. The diagram-removal scheme [94] was used in the generation of Wt and tWZ events to address their overlaps with $t\bar{t}$ and $t\bar{t} + Z$ samples. These samples were also merged into a single process labeled as single-top.

Signal samples for the $WTZt$ and $ZTZt$ processes were generated at LO using MADGRAPH5_AMC@NLO with the Universal FeynRules Output (UFO) model [95] from Ref. [14], interfaced with PYTHIA 8.244 and using the NNPDF3.0_{LO} PDF set and the A14 tune. This model uses the four-flavor scheme. Top partner samples were obtained for various masses, ranging from 1.0 TeV and 2.7 TeV in steps of 100 GeV. For each mass point, the coupling strength κ was varied between 0.1 and 1.0 with a step of 0.05 (0.1) for couplings less (greater) than 0.5. The relative strength of the three coupling modes were obtained from $\vec{\xi} = (\xi_W, \xi_Z, \xi_H) = (0.5, 0.25, 0.25)$.² The MC samples were produced for a subset of the mass and coupling points. Those samples were used for other masses and couplings by implementing an event-by-event matrix element reweighting [96]. While the left- and right-handed couplings dominate in the singlet and doublet representations of T , the current analysis was found to be insensitive to the choice of chirality for the signal MC generation and all signal samples were generated using the left-handed couplings. The signal samples were normalized to the NLO cross-section calculated with the narrow-width approximation [97]. Due to the requirement of at least one jet containing a b -hadron in the signal region the kinematic differences between the 4 flavor scheme and 5 flavor scheme are expected to be small. However, since the top partner can have large width based on the choice of coupling, additional correction factors were applied to evaluate the cross-section at finite width [98]. The contribution from the non-resonant t -channel diagram was also taken into account [99].

4 Object reconstruction

Events are required to have at least one vertex with at least two tracks with transverse momentum $p_T > 0.5$ GeV. The primary vertex (PV) is defined as the one with the largest Σp_T^2 , where the sum is performed over all the tracks matched to the vertex.

Electrons are reconstructed from energy clusters in the EM calorimeter matched with ID tracks and must fulfill the *tight likelihood* identification criteria [100]. Electrons are calibrated [100] and required to have

² The parameterization of VLQ Lagrangian in terms of the κ and $\vec{\xi}$ parameters was introduced in Ref. [47] and is used for the interpretation of the search presented in this paper. Its conversion to the coupling convention in Eq. (1) is obtained by doing a one-to-one mapping of the tree level couplings in the Lagrangian. The ξ_W, ξ_Z, ξ_H parameters satisfy the constraint $\xi_W + \xi_Z + \xi_H = 1$ and asymptotically represent the branching ratios of T decaying into Wb, Zt , and Ht in the narrow-width limit.

$p_T > 28$ GeV and to be reconstructed within $|\eta| = 2.47$, excluding the calorimeter barrel–endcap transition regions ($1.37 < |\eta| < 1.52$). A high acceptance for the expected signal events is maintained by not applying an isolation requirement to electron candidates beyond those implicit in the trigger requirements, which are explained in Section 5. Furthermore, the track matched with the candidate electron is required to have a longitudinal impact parameter with respect to the PV which satisfies $|z_0 \cdot \sin \theta| < 0.5$ mm and a transverse impact parameter with respect to the beamline (d_0) with a significance $|d_0|/\sigma(d_0) < 5$.

Muons are reconstructed [101] from combined tracks in the MS and the ID and must fulfill the *medium* identification criteria [101]. Muons are calibrated and required to have $p_T > 28$ GeV and to be reconstructed within $|\eta| = 2.5$. Muon candidates must also satisfy the track-based isolation requirements defined by the *FixedCutTightTrackOnly* working point [101]. This isolation requirement does not significantly reduce the acceptance. This working point uses the scalar sum of the p_T of all tracks that are inside of a cone of size $\Delta R = \min\{0.3, 10 \text{ GeV}/p_T(\mu)\}$ around the muon candidate, where $p_T(\mu)$ is the candidate muon p_T . The track matched with the muon candidate under consideration is excluded from the sum. The muon is selected if this sum is less than 15% of $p_T(\mu)$. Finally, muon candidates are required to have a matched track with $|z_0 \cdot \sin \theta| < 0.5$ mm and a significance $|d_0|/\sigma(d_0) < 3$.

Jets are reconstructed from particle-flow objects [102] using the anti- k_r algorithm [103, 104] with a radius parameter of $R = 0.4$. Jets are calibrated to the particle level from a combination of simulation-based corrections and measurements in data [105] and are required to fulfill $p_T > 25$ GeV for $|\eta| < 2.5$ and $p_T > 35$ GeV for $2.5 < |\eta| < 4.5$. These two jet categories are respectively called central and forward jets. To reduce jet contributions from pileup, a ‘jet vertex tagger’ algorithm using a two-dimensional likelihood discriminant [106] is applied to jets with $|\eta| < 2.4$ and $p_T < 60$ GeV. The DL1r algorithm [107] is used to identify jets in the central region ($|\eta| < 2.5$) containing b -hadrons (b -tagging) with a working point corresponding to a b -tagging efficiency in simulated $t\bar{t}$ events of 77%, a c -jet rejection factor of ~ 6 , and a light-jet rejection factor of ~ 192 .

The missing transverse momentum [108], with magnitude E_T^{miss} , is defined as the negative vectorial sum of the transverse momenta of all the calibrated reconstructed lepton and jet candidates in the event and includes a ‘soft term’ with contributions from tracks emanating from the PV but not matched with any of the reconstructed objects.

A procedure to remove potential overlaps between reconstructed lepton and jet candidates is performed sequentially as follows. First, any electron sharing an ID track with one of the muons is removed. Next, any jet within $\Delta R = 0.2$ of an electron is removed, followed by the removal of electrons within $\Delta R = 0.4$ of any remaining jet. Then any jet with at most two tracks with $p_T > 0.5$ GeV within $\Delta R = 0.2$ of a muon is removed, unless it is b -tagged. At the end of the procedure, any muon within $\Delta R = \min\{0.4, 0.04 + 10 \text{ GeV}/p_T(\mu)\}$ of any remaining jet is removed.

To identify hadronically decaying boosted top-quark jets, variable-radius reclustered jets (vRC jets) are reconstructed using the variable-radius jet algorithm [109] from calibrated jets with $R = 0.4$ where the effective radius of the jet cone is chosen as $R_0 = \frac{2m_t}{p_T}$, m_t and p_T representing the mass of the top quark and the jet transverse momentum respectively. These vRC jets are known to provide stable top-tagging performance for a wide range of jet p_T [110]. The vRC jets are called top-tagged (top-vetoed) if the vRC jet mass is greater (less) than 140 GeV. Top-tagged and top-vetoed jets are required to have $p_T > 200$ GeV and to contain at least two $R = 0.4$ jets as jet constituents when their transverse momentum is less than 700 GeV.

5 Event selection

A common initial event selection is performed for both the 2ℓ and 3ℓ channels where events are required to have passed the single lepton trigger selections [51, 111, 112]. For muons, triggers with a p_T threshold of 20 GeV (26 GeV) in 2015 (2016–2018) and isolation requirements, are combined in logical OR with triggers with a 50 GeV p_T threshold with no isolation requirement. A complementary barrel region only trigger with a 60 GeV p_T threshold is added for the 2017–2018 data taking period. Similarly, electron triggers with isolation and identification requirements (tight likelihood identification in 2016–18, with a less restrictive requirement in 2015) and p_T thresholds of 24–26 GeV are combined with triggers with higher p_T thresholds between 120 GeV and 140 GeV, less restrictive identification criteria, and no isolation requirements.

Events are additionally required to have at least one OS-SF lepton pair with the transverse momentum of each lepton being greater than 28 GeV. The pair of OS-SF leptons with invariant mass $m(\ell\ell)$ closest to the mass of the Z -boson (m_Z) is identified as the Z -boson candidate. Based on the expected hadronic activity of the signal topologies, events are also required to have at least one vRC jet (in the 2ℓ channel) or at least two central jets (in the 3ℓ channel).

5.1 Dilepton channel

The preselection of events for the 2ℓ channel (2ℓ PS) requires the Z -boson candidate to have an invariant mass satisfying $|m(\ell\ell) - m_Z| < 10$ GeV. Given that the search is sensitive to energetic final-state objects, additional background reduction is achieved by requiring the Z -boson candidate to have a transverse momentum ($p_T(\ell\ell)$) of at least 200 GeV and the scalar sum of transverse momenta of jets in the event, denoted by H_T , to be at least 300 GeV. Since signal events are expected to contain a hadronically decaying boosted top quark, events without any vRC jets are rejected. The four momentum of the leading vRC jet (J), defined as the vRC jet with the highest p_T , is combined with that of the Z -boson candidate to obtain an estimate of the mass of T , $m_{\ell\ell J}$. To reduce sensitivity to VLQ pair-production and to allow for a consistent phenomenological interpretation of observed data counts, a requirement of $H_T + E_T^{\text{miss}} < m_{\ell\ell J}$ is also placed on preselection events [35].

The main background for the 2ℓ channel is comprised of Z +jets events, with minor contributions from VV and $t\bar{t}$ processes. Measurements of differential cross sections have recently shown that the current simulations of Z +jets processes overestimate both the upper tail of the H_T spectrum and the cross section at high jet multiplicities [113]. This leads to discrepancies in the shapes of the $H_T + E_T^{\text{miss}}$ and jet multiplicity spectra between the data and expected background in the kinematic regimes relevant for this search. Data-driven reweighting factors are therefore used to correct the observed discrepancies in these processes. These corrections are derived using the following procedure.

To improve the background modeling, a reweighting factor is extracted for the Z +jets samples by comparing data with simulated events in the 2ℓ PS region for the jet multiplicity and $H_T + E_T^{\text{miss}}$ distributions. These reweighting factors are separately derived for 2ℓ PS events with and without b -tagged jets. Since the shapes of the Z +LF and Z +HF samples were found to be similar in these regions, these factors are applied on the Z +jets template obtained by combining these samples together. The reweighting function is defined bin-by-bin by the formula

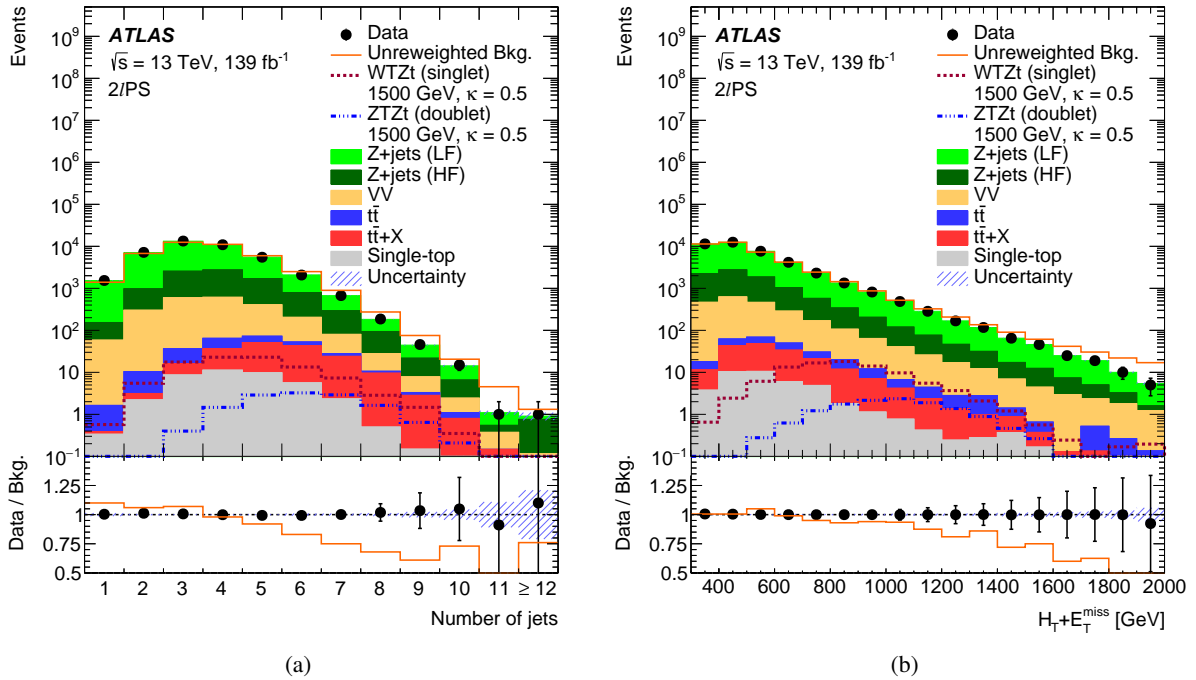


Figure 2: Distributions of (a) jet multiplicity and (b) $H_T + E_T^{\text{miss}}$ in the $2\ell\text{PS}$ region after reweighting. The overlaid solid line shows the total background prediction before the reweighting and the corresponding data-over-background ratio in the bottom panel. The red and blue dotted lines show the signal contributions from $WTZt$ and $ZTZt$ processes with $M_T = 1.5$ TeV and $\kappa = 0.5$ in the singlet and doublet representations respectively. The last bin in each distribution contains the overflow.

$$R_{Z+\text{jets}}(x) = \frac{\text{Data}(x) - \text{MC}^{\text{non-}Z+\text{jets}}(x)}{\text{MC}^{Z+\text{jets}}(x)}, \quad (2)$$

where x represents the binning in each kinematic variable. After reweighting in jet multiplicity, a second reweighting is applied on $H_T + E_T^{\text{miss}}$ using Eq. (2). The joint reweighting factors are applied on an event-by-event basis to estimate the MC contribution of Z -jets events for this channel. The jet multiplicity and $H_T + E_T^{\text{miss}}$ distributions in the $2\ell\text{PS}$ region are shown in Figure 2. In the bins of jet multiplicity and $H_T + E_T^{\text{miss}}$ distributions, the contribution of non- Z -jets processes is less than 15% before reweighting. The predicted signal contribution is also quite small. For a benchmark $WTZt$ process with $M_T = 1.5$ TeV and $\kappa = 0.5$ in the singlet representation, the bin-by-bin signal-over-background ratio (S/B) varies between 4–7% for most bins and is always less than 9%.

Figure 3 shows the distributions of the key kinematic variables for the expected background and benchmark signal processes in the $2\ell\text{PS}$ region. Events with a singly produced T have a distinctive signature with a forward jet scattering off of a vector boson from one of the incoming partons. Events are additionally expected to have b -tagged jets. Hence, in addition to the preselection, the signal-enriched kinematic phase space, called the *signal region* ($2\ell\text{SR}$), requires events with at least one forward jet, at least one b -tagged jet, and at least one top-tagged jet, as shown in Table 1. The distribution of the transverse momentum of the Z -boson candidate, $p_T(\ell\ell)$, was the variable that offered maximum sensitivity and, hence, is used as the final discriminant in this channel to perform the statistical fit described in Section 7.

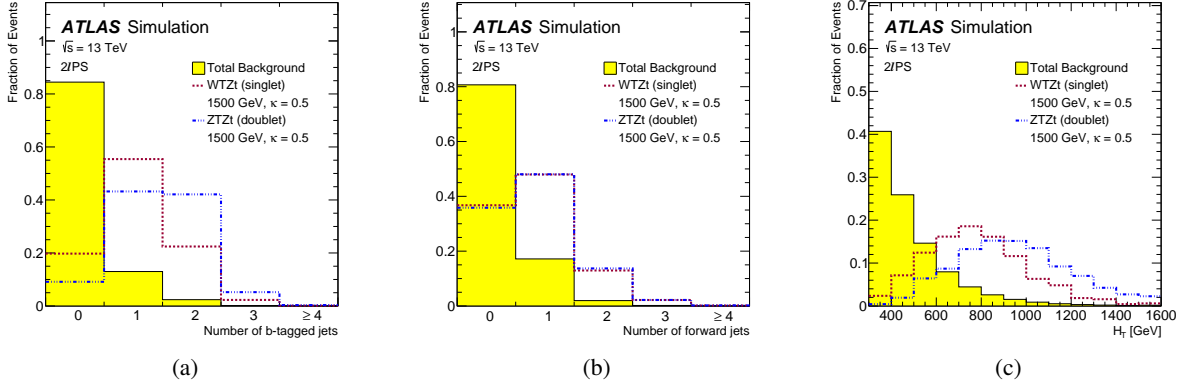


Figure 3: Simulated distributions of (a) b -tagged jet multiplicity, (b) forward jet multiplicity, and (c) H_T for total background (solid area) and benchmark signal processes (dashed lines) in the 2ℓ PS region before reweighting is performed in jet multiplicity and $H_T + E_T^{\text{miss}}$ distributions. Each distribution is separately normalized to unit area. The signal contributions are from $WTZt$ and $ZTZt$ processes with $M_T = 1.5$ TeV and $\kappa = 0.5$ in the singlet and doublet representations respectively. The last bin in each distribution contains the overflow.

Three control regions (CRs) are defined to improve the background modeling and reduce its uncertainties. Two validation regions (VRs) are defined to validate the background prediction in the distribution of the final discriminant. The event selection criteria for these regions are summarized in Table 1. Each of the control regions is obtained by inverting exactly two of the three jet cuts of the 2ℓ SR shown in Table 1. The regions 2ℓ CR1, 2ℓ CR2, and 2ℓ CR3 are defined to have the same selection as 2ℓ SR in multiplicities of forward jets, b -tagged jets, and top-tagged jets respectively. The inversion of the requirement of the presence of top-tagged jets requires the presence of at least one top-vetoed tagged jet. Both the validation regions are required to have at least one top-tagged jet to maintain their kinematic similarity with the signal region. Identified as 2ℓ VR1 and 2ℓ VR2, they are made orthogonal to the 2ℓ SR by requiring zero b -tagged jets and zero forward jets respectively.

Table 1: Summary of selections applied to define the control, validation, and signal regions for the 2ℓ channel.

	2ℓ CR1	2ℓ CR2	2ℓ CR3	2ℓ VR1	2ℓ VR2	2ℓ SR
Preselection	$= 2$ OS-SF leptons with $ m(\ell\ell) - m_Z < 10$ GeV $p_T(\ell\ell) > 200$ GeV, $H_T > 300$ GeV ≥ 1 vRC jet $H_T + E_T^{\text{miss}} < m_{\ell\ell J}$					
forward jets	≥ 1	0	0	≥ 1	0	≥ 1
b -tagged jets	0	≥ 1	0	0	≥ 1	≥ 1
top-tagged jets	–	–	≥ 1	≥ 1	≥ 1	≥ 1
top-vetoed jets	≥ 1	≥ 1	–	–	–	–

5.2 Tripleton channel

As the name of the channel suggests, events with at least three leptons passing the preselection are selected. Although the selection is inclusive of events with four or more leptons, their overall contribution is quite

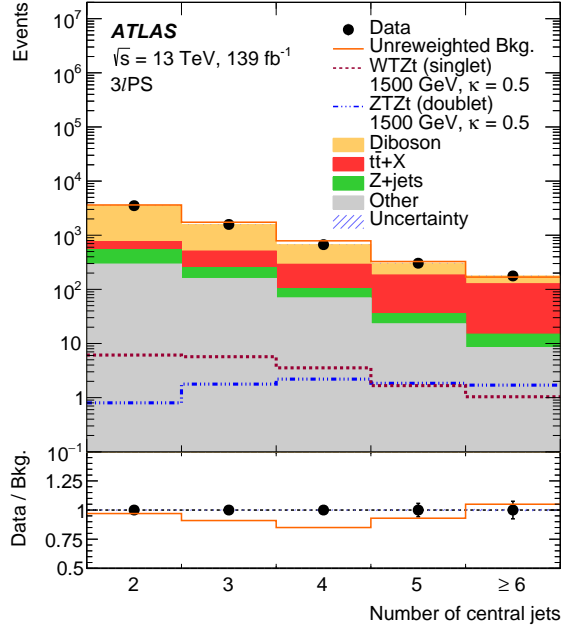


Figure 4: Distribution of central jet multiplicity in the $3\ell PS$ region after reweighting. The overlaid solid line shows the total background prediction before the reweighting and the corresponding data-over-background ratio in the bottom panel. The red and blue dotted lines show the signal contributions from $WTZt$ and $ZTZt$ processes with $M_T = 1.5$ TeV and $\kappa = 0.5$ in singlet and doublet representations respectively.

small ($< 5\%$). The lepton with highest p_T that does not comprise the Z -boson candidate is labeled as the third lepton (ℓ_3) in this channel. The main sources of background are diboson processes and $t\bar{t}+X$, the latter being primarily composed of $t\bar{t} + Z$ and other small contributions from $t\bar{t} + W$ and $t\bar{t}t\bar{t}$ processes. Minor contributions result from background processes like single-top and Z +jets. To improve the quality of MC background modeling, a data-driven reweighting factor is determined for the VV and $t\bar{t} + X$ samples in this channel. This reweighting is performed for the central jet multiplicity distribution for events passing the $3\ell PS$ criteria. These events are classified into separate regions according to the presence or absence of b -tagged jets in the event. A pair of simultaneous linear equations can be formulated for these two sets of data and MC distributions:

$$\begin{aligned}
 n_{0,i}^{\text{data}} &= \alpha_i^{VV} n_{0,i}^{VV} + \alpha_i^{t\bar{t}X} n_{0,i}^{t\bar{t}X} + n_{0,i}^{\text{others}} \\
 n_{1,i}^{\text{data}} &= \alpha_i^{VV} n_{1,i}^{VV} + \alpha_i^{t\bar{t}X} n_{1,i}^{t\bar{t}X} + n_{1,i}^{\text{others}}
 \end{aligned} \tag{3}$$

where n^{data} denotes the data yield and n^{VV} , $n^{t\bar{t}X}$, and n^{others} denote the predicted yields from VV , $t\bar{t} + X$, and other backgrounds respectively. The subscripts 0/1 refer to events with $0/\geq 1$ b -tagged jets and the index i runs over the bins of the central jet multiplicity distribution. The $(\alpha_i^{VV}, \alpha_i^{t\bar{t}X})$ factors for each bin are obtained by simultaneously solving the pair of equations in Eq. (3) and applied to estimate the MC contributions of VV and $t\bar{t} + X$ processes. The central jet multiplicity distribution in the $3\ell PS$ is shown in Figure 4. In the regions where the reweighting factors are derived, the overall contribution of the minor backgrounds is up to 29%, reaching a bin-by-bin maximum of 37%. The predicted signal contributions in these regions are small. For a benchmark $WTZt$ process with $M_T = 1.5$ TeV and $\kappa = 0.5$ in the singlet representation, the bin-by-bin S/B is less than 2%.

Figure 5 shows distributions of some of the kinematic variables for the expected background and benchmark

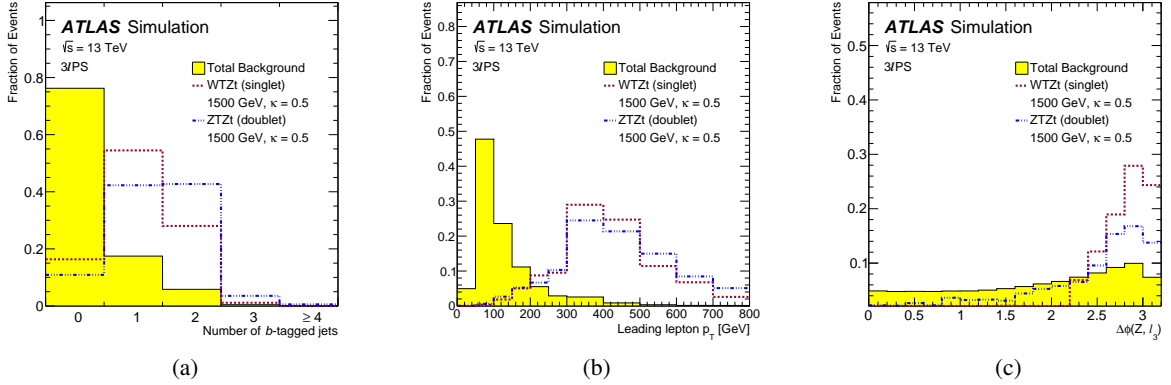


Figure 5: Simulated distributions of (a) b -tagged jet multiplicity, (b) p_T of the leading lepton, and (c) $\Delta\phi$ between the Z candidate and the third lepton for total background (solid area) and benchmark signal processes (dashed lines) in the 3ℓ PS region before reweighting is performed in the central jet multiplicity distribution. Each distribution is separately normalized to unit area. The signal contributions are from $WTZt$ and $ZTZt$ processes with $M_T = 1.5$ TeV and $\kappa = 0.5$ in the singlet and doublet representations respectively. The last bin in each distribution contains the overflow.

signal processes in the 3ℓ PS region. Exploiting the distinctive signature of signal events, which are expected to have b -tagged and forward jets, the signal region in this channel (3ℓ SR) requires events to have at least one of each of these jet types. To further increase the signal-to-background ratio, additional requirements are applied on the Z -boson candidate p_T , $p_T(\ell\ell) > 300$ GeV and the leading lepton p_T , $\max(p_T(\ell)) > 200$ GeV. The decay products of T , the Z boson and the top-quark, are expected to have large angular separation between them. Requiring the azimuthal separation of the Z candidate from the third lepton ($\Delta\phi(Z, \ell_3)$) to be at least $\frac{\pi}{2}$ significantly improves the signal purity in the signal region (Figure 5(c)). For similar reasons, the azimuthal separation between the Z candidate and the leading b -tagged jet, defined as the b -tagged jet with the largest p_T which is expected to emerge from the decay of the top quark, is required to satisfy $\Delta\phi(Z, b_{\text{lead}}) > \frac{\pi}{2}$.

Finally, to allow for a consistent phenomenological interpretation, the product of H_T and jet multiplicity, $H_T \cdot n(\text{jets})$, is required to be less than 6 TeV in the signal region to reduce potential contamination from pair production of VLQs [35].

The statistical analysis in this channel also uses $p_T(\ell\ell)$ as the final discriminant. Three control regions and one validation region are defined in this channel. The diboson control region (3ℓ VV) is defined by rejecting events with any b -tagged jet. The mixed control region (3ℓ Mixed) and the $t\bar{t} + X$ control region (3ℓ ttX), are defined by accepting events with exactly one b -tagged jet and at least two b -tagged jets respectively. To maintain orthogonality with the signal region, both regions reject events with forward jets and require $\Delta\phi(Z, \ell_3) < 2.6$. Finally, a validation region (3ℓ VVR) is defined to validate the background modeling by requiring the same set of selections on the b -tagged jet and forward jet multiplicities as the signal region, but made orthogonal to it by requiring that at least one of the $\Delta\phi$ requirements is reversed, i.e., $\Delta\phi(Z, \ell_3) < \frac{\pi}{2}$ or $\Delta\phi(Z, b_{\text{lead}}) < \frac{\pi}{2}$. The definitions of these regions are summarized in Table 2.

Table 2: Summary of selections applied to define the control, validation, and signal regions for the 3ℓ channel.

	$3\ell VV$	$3\ell \text{Mixed}$	$3\ell t\bar{t}X$	$3\ell V\bar{V}$	$3\ell \text{SR}$
Preselection	≥ 3 leptons ≥ 1 pair of OS-SF leptons with $ m(\ell\ell) - m_Z < 10$ GeV ≥ 2 central jets				
b -tagged jets	0	1	≥ 2	≥ 1	≥ 1
forward jets	–	0	0	≥ 1	≥ 1
$\Delta\phi$ selections	–	$\Delta\phi(Z, \ell_3) < 2.6$	$\Delta\phi(Z, \ell_3) < 2.6$	$\Delta\phi(Z, \ell_3) < \frac{\pi}{2}$ OR $\Delta\phi(Z, b_{\text{lead}}) < \frac{\pi}{2}$	$\Delta\phi(Z, \ell_3) > \frac{\pi}{2}$ AND $\Delta\phi(Z, b_{\text{lead}}) > \frac{\pi}{2}$
other selections	–	–	–	–	$\max(p_T(\ell)) > 200$ GeV $p_T(\ell\ell) > 300$ GeV $H_T \cdot n(\text{jets}) < 6$ TeV

6 Systematic uncertainties

Uncertainties from experimental and theoretical sources are introduced in the normalization or shape of the final discriminant in the two analysis channels. Experimental uncertainties include effects on the electron energy scale and energy resolution, the muon momentum scale and resolution, and uncertainties in the data-to-MC correction factors for the electron and muon trigger, reconstruction, identification, and isolation efficiencies [100, 101]. Jet energy scale and resolution uncertainties are also included, as obtained from studies in data and simulation [105]. Flavor-tagging uncertainties include uncertainties in the b -jet tagging, c -jet mis-tagging, and light-jet mis-tagging efficiencies, and uncertainties due to extrapolations to regions not covered by the data used for the efficiency measurements [114–116]. Subdominant uncertainties include uncertainties related to the soft term in the E_T^{miss} calculation [117] and to the E_T^{miss} energy scale and resolution, uncertainties in the reweighting of the MC event samples to match the pileup conditions in data and a 1.7% [118] uncertainty in the integrated luminosity of the 2015–2018 data sample, obtained using the LUCID-2 detector [119] for the primary luminosity measurements.

Theoretical uncertainties include cross-section and other modeling uncertainties for all background samples. The cross-section uncertainties considered are between 5 – 6% for the Z +jets, $t\bar{t}$, and $V\bar{V}$ samples [77, 120, 121] and between 10 – 12% for the $t\bar{t} + Z$ sample [122]. Uncertainties associated with missing higher orders are estimated by varying the renormalization and factorization scales by factors of 0.5 and 2 and then, constructing upward and downward varying envelopes by considering the largest positive and negative fluctuation on a bin-by-bin basis. PDF uncertainties when comparing distributions obtained with events generated with different PDF sets are obtained using the PDF4LHC recommendations [123]. For the 2ℓ channel, the Z +jets scale and PDF variations are decorrelated between Z +LF and Z +HF events. For the 3ℓ channel, the $V\bar{V}$ scale-variation uncertainties are broken down into their normalization and shape components, and treated as uncorrelated across regions with different b -jet multiplicities.

Uncertainties due to the choice of generator or showering algorithm are estimated by comparing additional samples from alternative generators. Generator uncertainties for $t\bar{t} + X$ are obtained from comparing the nominal MADGRAPH5_AMC@NLO samples with the alternative SHERPA samples. For the 3ℓ channel where Z +jets is a minor background and mainly contributes via jets mis-identified as leptons, generator uncertainties are estimated by comparing nominal samples with alternative MADGRAPH5_AMC@NLO samples and only taking the shape difference into account. For the 2ℓ channel where Z +jets is the main background, generator uncertainties are taken into account by comparing the SHERPA 2.2.1 sample with the SHERPA 2.2.11 sample where an independent reweighting based on jet multiplicity and $H_T + E_T^{\text{miss}}$ distribution, as explained in Section 5.1, is applied on the latter. To estimate the uncertainties due to

the modeling of initial-state radiation, final-state radiation, and the choice of parton shower algorithm, either additional event weights for the nominal samples or alternative MC samples were produced. These uncertainties were calculated by comparing the nominal MC distribution with the distributions obtained from these additional event weights or the alternative samples.

A conservative uncertainty of 30% on the fraction of VV and Z +jets events with heavy-flavor jets is applied in both the channels. This uncertainty is based on variations of the factorization and renormalization scales and the multijet merging scale [124]. Also, a shape uncertainty is introduced in the 3ℓ channel for VV and $t\bar{t} + X$ by comparing the distributions before and after implementing jet multiplicity based reweighting explained in Section 5.2. In the 2ℓ channel, bin-by-bin variations in the reweighting factors due to the statistical fluctuations in the MC samples are calculated and these variations are used to obtain upward and downward fluctuating envelopes for the fit distributions. Shape uncertainties extracted from these fluctuations are applied on the Z +jets samples for the light and heavy-flavor components.

Events with jets misidentified as leptons can potentially arise in the 2ℓ channel mainly from the $t\bar{t}$ process and in the 3ℓ channel from the $t\bar{t}$ or Z +jets processes. After the $m(\ell\ell)$ and $p_T(\ell\ell)$ cuts, these contributions are estimated to be less than 2% in the signal regions. Following the prescription in Ref. [35], a conservative 25% uncertainty is applied on the normalization of the $t\bar{t}$ ($t\bar{t}$ and Z +jets) events in the 2ℓ (3ℓ) channel. This uncertainty is decorrelated across the control and signal regions in the 2ℓ and 3ℓ channels.

7 Statistical analysis and results

A binned profile likelihood fit in the discriminating variable $p_T(\ell\ell)$ is performed in both channels to test if the data is compatible with the background-only hypothesis. The uncertainties are introduced in the likelihood as nuisance parameters (NP), which are constrained using Gaussian priors. Additional NPs are included to take into account the statistical uncertainties in each bin for each event category due to the limited size of the simulated samples [125]. The likelihood function $L(\mu, \vec{\theta})$ is constructed as a product of Poisson probabilities for each bin of the discriminating variable in the control and signal regions,

$$L(\mu, \vec{\theta}) = \prod_{i=1}^{N_{\text{bins}}} \text{Pois}(n_i^{\text{data}} | b_i + \mu s_i) \times P(\vec{\theta}), \quad (4)$$

where N_{bins} is the total number of bins in control and signal regions. The parameters, n_i^{data} , b_i , s_i , represent the number of observed data, expected background and signal events respectively in the i -th bin. The product of prior distributions for the NPs, $P(\vec{\theta})$, is given by $P(\vec{\theta})$. The expected number of events in each bin depends on these NPs as well as the signal strength, μ , which acts as a scaling factor for the signal cross-section.

The background and signal templates are fitted to the observed data to obtain the best estimate of signal and background contributions in the control and signal regions. The fitted values of μ , $\vec{\theta}$ are propagated to the validation regions to test the quality of the fit and the corresponding background modeling. The background-only *post-fit* distributions, obtained by maximizing the likelihood function in Eq. (4) with a fixed choice of $\mu = 0$, are shown for the 2ℓ and 3ℓ control, validation, and signal regions in Figures 6 and 7 respectively. The expected pre-fit signal yields for the $WTZt$ and $ZTZt$ processes with $M_T = 1.5$ TeV and $\kappa = 0.5$ for the singlet and doublet representations of T are also shown in these figures. The contribution of different background processes, expected signal yields, and observed data in different regions for the

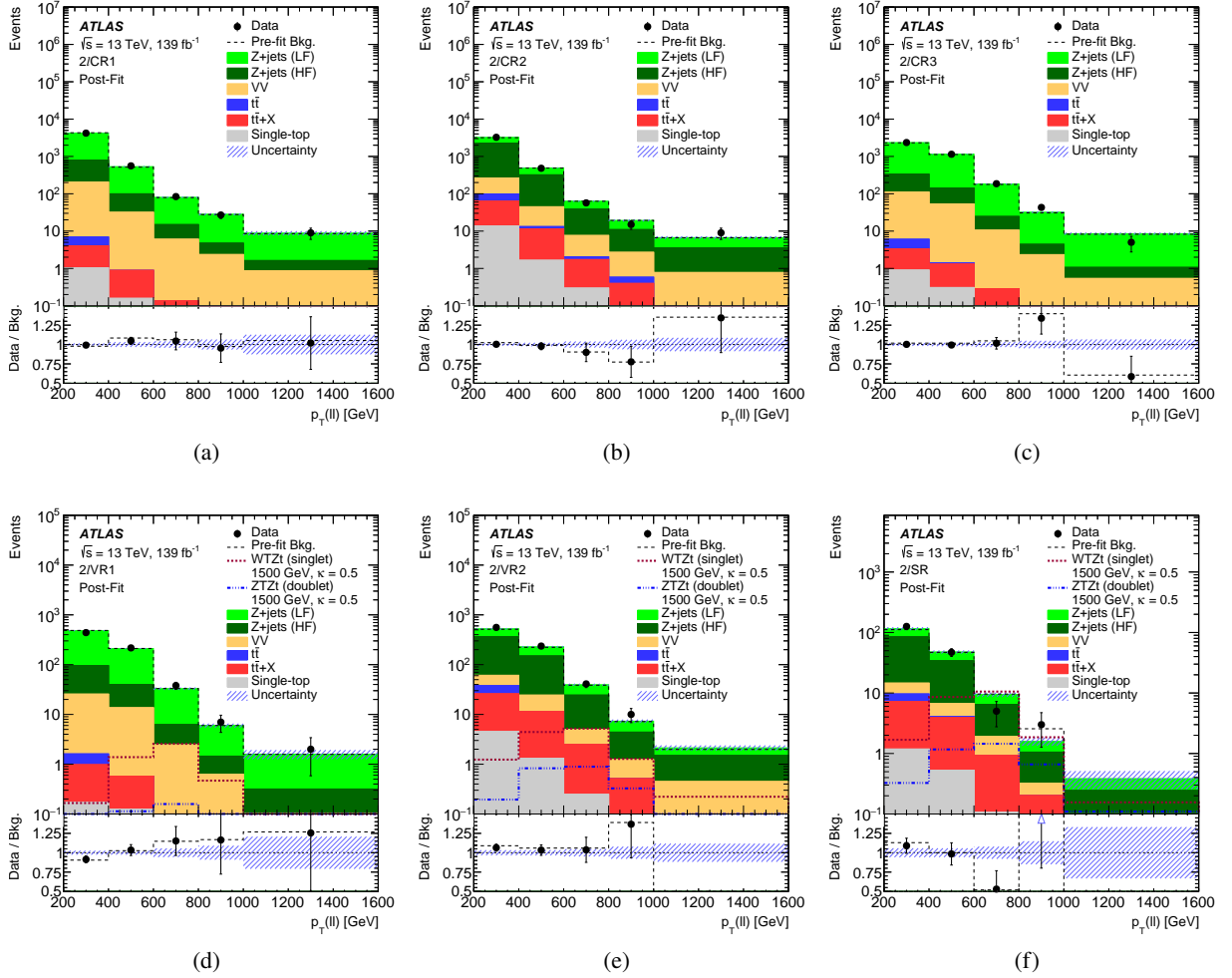


Figure 6: Distribution of the final discriminant, $p_T(\ell\ell)$, for the 2ℓ channel in the control regions (a) $2\ell\text{CR1}$, (b) $2\ell\text{CR2}$, (c) $2\ell\text{CR3}$, the validation regions (d) $2\ell\text{VR1}$, (e) $2\ell\text{VR2}$, and the signal region (f) $2\ell\text{SR}$. The distributions are shown after the background-only fit in the 2ℓ channel. The black, dashed line shows the total pre-fit background distribution and the corresponding data-over-background ratio in the bottom panel. The blue arrows in the bottom panel indicate points that are outside the vertical range of the figure. The overlaid red and blue dotted lines in (d)-(f) show the expected signal contributions in the corresponding regions from $WTZt$ and $ZTZt$ processes with $M_T = 1.5$ TeV and $\kappa = 0.5$ in singlet and doublet representations respectively. Expected signal contributions in the control regions are negligible. The last bin in each distribution contains the overflow.

2ℓ and 3ℓ channels are summarized in Tables 3 and 4 respectively. The post-fit background contribution shows reasonable agreement in all regions with the observed data within the uncertainties.

To test whether the observed data is compatible with the background-only hypothesis, tests are performed with RooStats [126] with statistical models implemented using RooFit [127] and HistFactory [128]. No significant excess over the background expectation is observed. Hence, the results were used to set upper limits on the top partner total production cross-section $\sigma(WTZt + ZTZt)$ at 95% confidence level (CL) using the CL_s method [129, 130]. These limits were calculated with the asymptotic approximation [131] of the test statistic and validated against the limits obtained using pseudoexperiments for benchmark signal samples with $M_T = 1200, 1500,$ and 2100 GeV. For all these benchmarks, the expected and observed

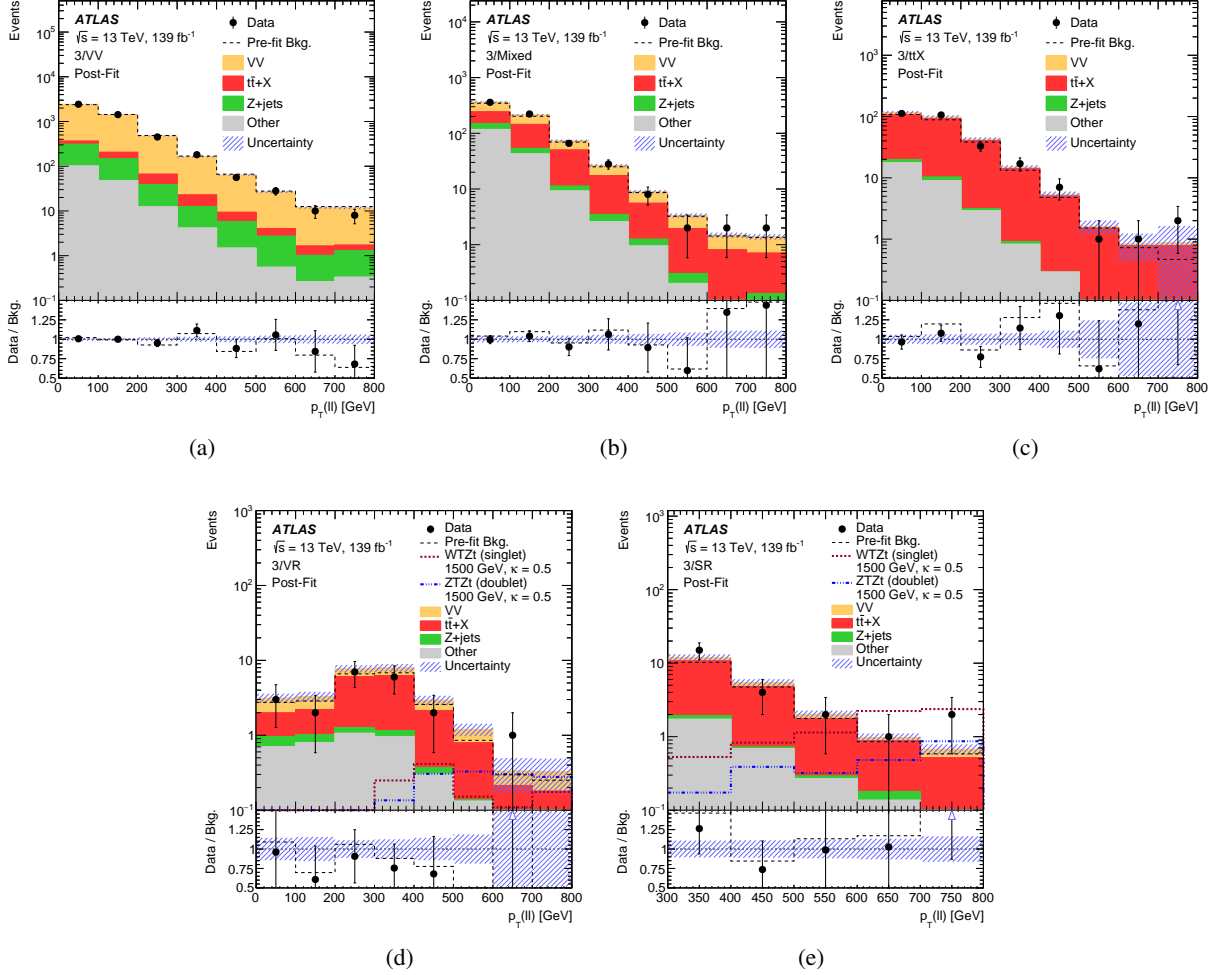


Figure 7: Distribution of the final discriminant, $p_T(\ell\ell)$, for the 3ℓ channel in the control regions (a) 3ℓ VV, (b) 3ℓ Mixed, (c) 3ℓ ttX, the validation region (d) 3ℓ VR, and the signal region (e) 3ℓ SR. The distributions are shown after the background-only fit in the 3ℓ channel. The black, dashed line shows the total pre-fit background distribution and the corresponding data-over-background ratio in the bottom panel. The blue arrows in the bottom panel indicate points that are outside the vertical range of the figure. The overlaid red and blue dotted lines in (d)-(e) show the expected signal contributions in the corresponding regions from $WTZt$ and $ZTZt$ processes with $M_T = 1.5$ TeV and $\kappa = 0.5$ in singlet and doublet representations respectively. Expected signal contributions in the control regions are negligible. The last bin in each distribution contains the overflow.

Table 3: Observed number of events in data and post-fit number of background events in the control, validation, and signal regions for the 2ℓ channel. The fit was performed under a background-only hypothesis. Statistical uncertainties from the limited size of MC samples and systematic uncertainties are added in quadrature. Systematic uncertainties take the correlations among nuisance parameters into account. The $WTZt$ and $ZTZt$ signal yields correspond to pre-fit yields.

	$2\ell\text{CR1}$	$2\ell\text{CR2}$	$2\ell\text{CR3}$	$2\ell\text{VR1}$	$2\ell\text{VR2}$	$2\ell\text{SR}$
$WTZt$ (singlet) $M_T = 1.5$ TeV, $\kappa = 0.5$	3.9 ± 0.5	9.8 ± 0.9	3.6 ± 0.5	4.7 ± 0.6	12.4 ± 1.1	22.8 ± 1.7
$ZTZt$ (doublet) $M_T = 1.5$ TeV, $\kappa = 0.5$	0.34 ± 0.04	1.64 ± 0.16	0.19 ± 0.04	0.32 ± 0.05	2.28 ± 0.22	3.72 ± 0.24
Z+jets (LF)	3980 ± 90	1170 ± 110	3220 ± 80	589 ± 16	258 ± 27	48 ± 6
Z+jets (HF)	660 ± 60	2330 ± 140	330 ± 50	101 ± 9	452 ± 28	103 ± 10
VV	238 ± 35	206 ± 25	169 ± 26	40 ± 6	40 ± 7	8.7 ± 1.6
$t\bar{t}$	2.8 ± 3.4	38 ± 20	2.8 ± 1.9	0.6 ± 0.6	12 ± 5	2.6 ± 1.6
$t\bar{t} + X$	3.9 ± 1.0	61 ± 23	3.8 ± 0.8	1.34 ± 0.28	34 ± 12	10 ± 4
Single-top	1.23 ± 0.17	15.6 ± 1.8	1.27 ± 0.15	0.33 ± 0.09	6.1 ± 0.8	1.85 ± 0.26
Total background	4886 ± 70	3821 ± 60	3727 ± 60	732 ± 16	802 ± 24	174 ± 9
Data	4887	3818	3735	704	846	181

Table 4: Observed number of events in data and post-fit number of background events in the control, validation, and signal regions for the 3ℓ channel. The fit was performed under a background-only hypothesis. Statistical uncertainties from the limited size of MC samples and systematic uncertainties are added in quadrature. Systematic uncertainties take the correlations among nuisance parameters into account. The $WTZt$ and $ZTZt$ signal yields correspond to pre-fit yields.

	$3\ell\text{VV}$	$3\ell\text{Mixed}$	$3\ell\text{ttX}$	$3\ell\text{VR}$	$3\ell\text{SR}$
$WTZt$ (singlet) $M_T = 1.5$ TeV, $\kappa = 0.5$	3.2 ± 0.4	0.85 ± 0.19	0.58 ± 0.14	1.21 ± 0.24	8.3 ± 0.8
$ZTZt$ (doublet) $M_T = 1.5$ TeV, $\kappa = 0.5$	0.84 ± 0.24	0.68 ± 0.12	0.40 ± 0.12	2.0 ± 0.8	2.04 ± 0.32
VV	3920 ± 160	230 ± 40	21 ± 4	7.1 ± 1.5	2.4 ± 0.5
$t\bar{t} + X$	156 ± 27	245 ± 28	225 ± 20	14.9 ± 2.5	15.4 ± 2.2
Z+jets	350 ± 120	45 ± 13	3.8 ± 1.5	1.0 ± 0.4	0.31 ± 0.11
$t\bar{t}$	82 ± 30	93 ± 16	5 ± 6	0.9 ± 1.1	0.005 ± 0.007
single-top	63.1 ± 2.6	77.9 ± 1.6	25.8 ± 0.8	2.99 ± 0.17	2.88 ± 0.17
VVV	22.6 ± 1.2	1.22 ± 0.09	0.087 ± 0.012	0.078 ± 0.015	0.023 ± 0.004
Total Bkg.	4594 ± 70	692 ± 26	281 ± 16	27.0 ± 3.0	21.0 ± 2.2
Data	4590	690	279	21	24

limits obtained from pseudoexperiments at 95% CL agreed with the limits obtained using the asymptotic approximation within 5%. The largest difference, close to 30%, in the results obtained with the two methods was observed in the -1σ and -2σ bands for the 2100 GeV mass point.

The overall impact of the systematic uncertainties introduced in Section 6 on the final result is found to be small. Considering only statistical uncertainties, the limits on the total cross-section of the $WTZt$ and $ZTZt$ processes are reduced by less than 14%.

Given that the signal efficiencies for the $WTZt$ and $ZTZt$ signal modes can be different, limits were independently calculated for different combinations of top partner mass, coupling, and branching ratios, under the assumption that $\xi_Z = \xi_H$. The latter is motivated by the Goldstone equivalence theorem [132], which states that the asymptotic branching ratios of T decaying into Zt and Ht become similar in the large M_T limit under the narrow-width approximation.

To maximize the sensitivity of the search, the results from both channels were statistically combined. All experimental uncertainties are treated as fully correlated across the channels while the theoretical and modeling uncertainties are taken to be uncorrelated. The corresponding limits on the signal strength translate into limits on the total cross-section of the $WTZt$ and $ZTZt$ processes for the corresponding choice of coupling and branching ratio. Limits corresponding to $\kappa = 0.3, 0.5$, and 0.7 for the singlet and doublet representations are shown in Figure 8. The combined expected limit is significantly stronger than limits obtained independently from the 2ℓ and 3ℓ channels. For the singlet representation with $\kappa = 0.5$, top partner masses less than 1825 GeV are excluded. The doublet representation only receives contribution from the $ZTZt$ process that has a much smaller cross-section because of the suppressed matrix element contribution from the gluon splitting into $t\bar{t}$ (Figure 1). Hence, the doublet exclusion limits are found to be considerably weaker than the singlet limits and none of the considered T masses are excluded for $\kappa \leq 0.5$.

The cross-section limits calculated for different choices of coupling can be reinterpreted as limits on the plane of (M_T, κ) , as shown in Figures 9(a) and 9(b) for the singlet and doublet representations only. Following the prescription of Ref. [133], this interpretation is only applied for the parametric subspace where the top partner's relative decay width, $\frac{\Gamma_T}{M_T}$ is smaller than 50%. The correction factors for finite width and non-resonant contributions [98, 99] are also valid for the same parametric subspace. Hence, the limits in Figure 9 beyond $\frac{\Gamma_T}{M_T} > 50\%$ are omitted for phenomenological consistency.

To further generalize the interpretation of the search results for any possible combination of top partner branching ratios, the semi-analytical interpretation strategy presented in Ref. [98] was adopted in Figure 10 to represent the excluded top partner mass as a function of its relative decay width and ξ_W , the asymptotic branching ratio for the $T \rightarrow Wb$ decay mode. The ξ parameters for the other two decay modes are determined by the constraint $\xi_Z = \xi_H = \frac{1-\xi_W}{2}$.

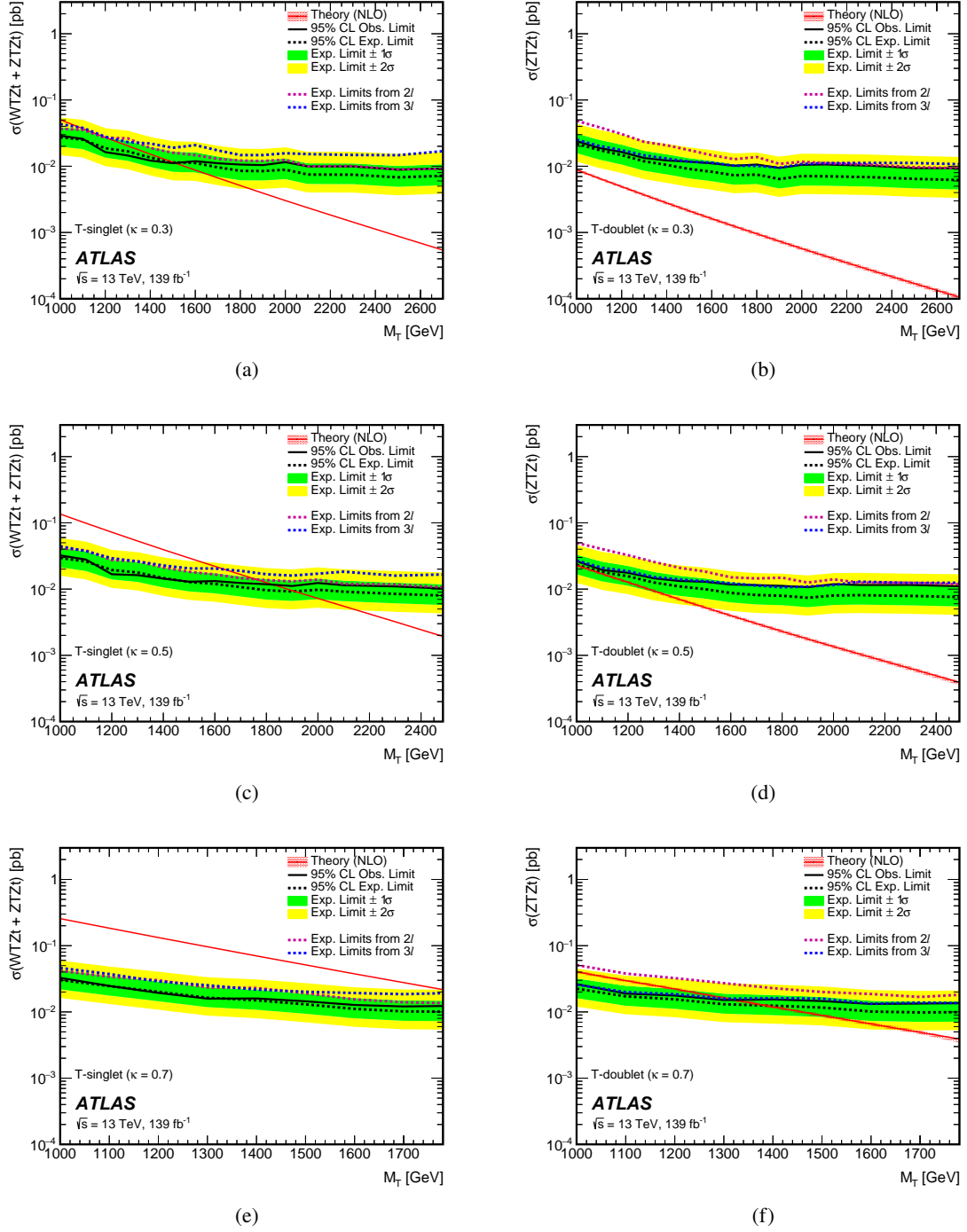


Figure 8: Observed (solid black line) and expected (dashed black line) limits calculated at 95% CL on total cross-section of the $WTZt$ and $ZTZt$ processes as a function of the T mass for a choice of coupling $\kappa = 0.3$ (top row), $\kappa = 0.5$ (middle row), and $\kappa = 0.7$ (bottom row) for singlet (left column) and doublet (right column) representations. Expected limits calculated at 95% CL by independently fitting the 2ℓ and 3ℓ channels are shown as overlaid blue and red dotted lines respectively. The green (yellow) band is the 68% (95%) confidence interval around the median expected limit. The solid red line shows the theory prediction for the NLO cross-section, with the surrounding shaded band representing the corresponding uncertainty. The mass range in these figures is restricted to ensure that the relative decay width $\frac{\Gamma_T}{M_T}$ is limited to less than 50%.

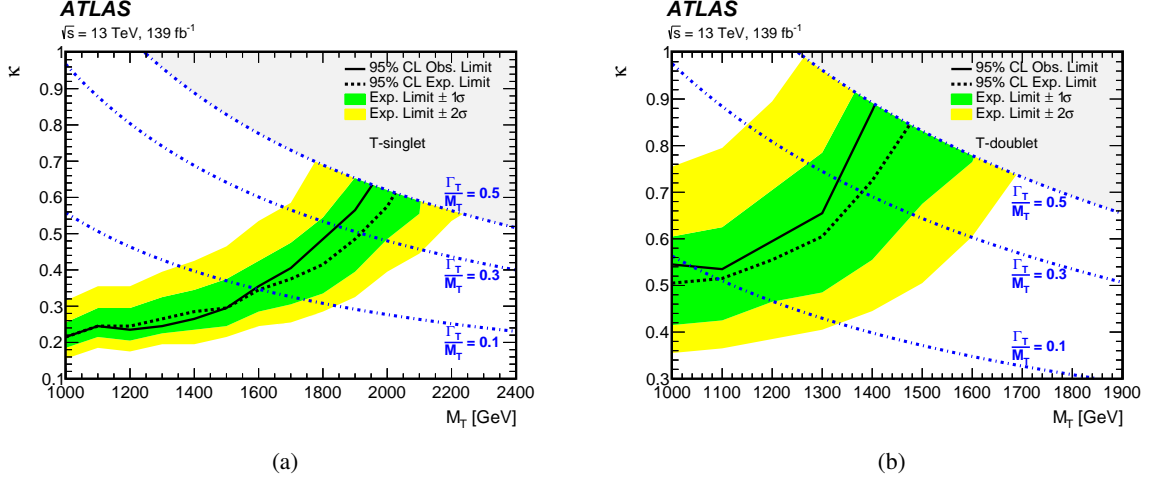


Figure 9: Observed (solid black line) and expected (dashed black line) limits calculated at 95% CL on the top partner coupling as a function of the T mass for (a) singlet and (b) doublet representations. The shaded regions represent the parametric space with $\frac{\Gamma_T}{M_T} > 50\%$. The green (yellow) band is the 68% (95%) confidence interval around the median expected limit. The dotted lines represent contours of equal values in $\frac{\Gamma_T}{M_T}$.

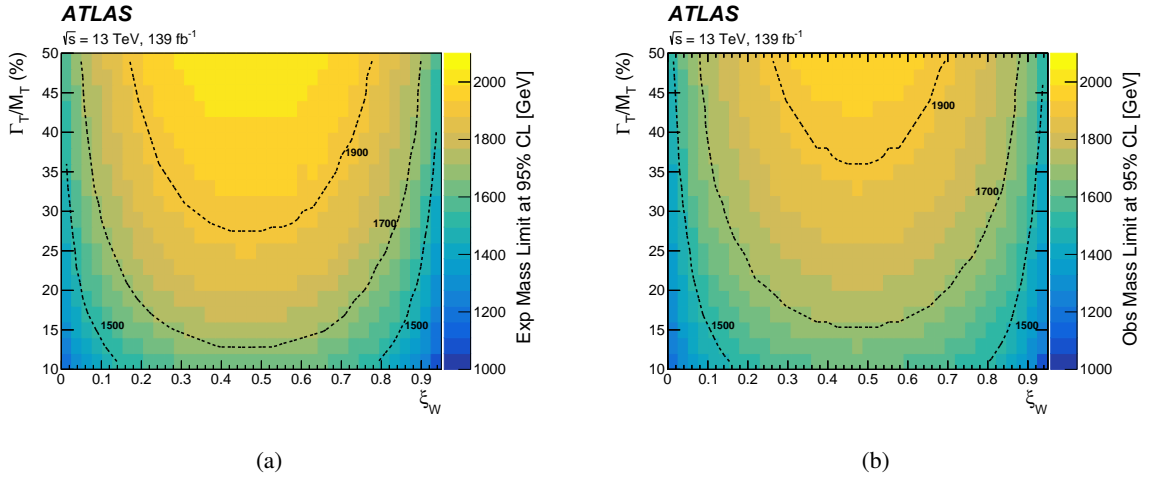


Figure 10: (a) Expected and (b) observed upper limits calculated at 95% CL on the excluded top partner mass as a function of its relative decay width ($\frac{\Gamma_T}{M_T}$) and the relative coupling parameter ξ_W with the assumption of $\xi_Z = \xi_H = \frac{1-\xi_W}{2}$. The dotted contour lines represent exclusion limits of equal mass in units of GeV.

8 Conclusion

A search for the production of a single vector-like quark T with electric charge $\frac{2}{3}e$ and mass greater than 1 TeV in a final state with a leptonically decaying Z boson and a top quark is presented. Two orthogonal channels with two or at least three leptons are separately optimized and their results are statistically combined to obtain the final result. No significant excess over the background expectation is observed, and therefore 95% CL upper limits on the inclusive single- T cross-section are derived for different choices of T mass and couplings. These results are interpreted in terms of limits on the T mass and coupling for different electroweak representations and generalized branching ratio scenarios. For the singlet representation, κ values are excluded between 0.22 and 0.64 for masses of T between 1000 and 1975 GeV. The exclusion range for the doublet representation spans κ values between 0.54 and 0.88 for masses of T between 1000 and 1425 GeV. These limits significantly improve on the previous limits obtained from the 2015–16 data sample. The strongest exclusion is observed for singlet representation with $\xi_W \approx 0.5$ where masses up to 1975 GeV are excluded at relative decay width of $\frac{\Gamma_T}{M_T} = 0.5$ for the top partner. The exclusion of singlet T production with mass and coupling of 1.8 (1.6) TeV and 0.70 (0.35), corresponding to a decay width of 30% (10%), provides the strongest limits from the LHC in these parameter regions.

Acknowledgments

We thank CERN for the very successful operation of the LHC, as well as the support staff from our institutions without whom ATLAS could not be operated efficiently.

We acknowledge the support of ANPCyT, Argentina; YerPhI, Armenia; ARC, Australia; BMWFW and FWF, Austria; ANAS, Azerbaijan; CNPq and FAPESP, Brazil; NSERC, NRC and CFI, Canada; CERN; ANID, Chile; CAS, MOST and NSFC, China; Minciencias, Colombia; MEYS CR, Czech Republic; DNRF and DNSRC, Denmark; IN2P3-CNRS and CEA-DRF/IRFU, France; SRNSFG, Georgia; BMBF, HGF and MPG, Germany; GSRI, Greece; RGC and Hong Kong SAR, China; ISF and Benoziyo Center, Israel; INFN, Italy; MEXT and JSPS, Japan; CNRST, Morocco; NWO, Netherlands; RCN, Norway; MEiN, Poland; FCT, Portugal; MNE/IFA, Romania; MESTD, Serbia; MSSR, Slovakia; ARRS and MIZŠ, Slovenia; DSI/NRF, South Africa; MICINN, Spain; SRC and Wallenberg Foundation, Sweden; SERI, SNSF and Cantons of Bern and Geneva, Switzerland; MOST, Taiwan; TENMAK, Türkiye; STFC, United Kingdom; DOE and NSF, United States of America. In addition, individual groups and members have received support from BCKDF, CANARIE, Compute Canada and CRC, Canada; PRIMUS 21/SCI/017 and UNCE SCI/013, Czech Republic; COST, ERC, ERDF, Horizon 2020 and Marie Skłodowska-Curie Actions, European Union; Investissements d’Avenir Labex, Investissements d’Avenir IDEX and ANR, France; DFG and AvH Foundation, Germany; Herakleitos, Thales and Aristeia programmes co-financed by EU-ESF and the Greek NSRF, Greece; BSF-NSF and MINERVA, Israel; Norwegian Financial Mechanism 2014-2021, Norway; NCN and NAWA, Poland; La Caixa Banking Foundation, CERCA Programme Generalitat de Catalunya and PROMETEO and GenT Programmes Generalitat Valenciana, Spain; Göran Gustafssons Stiftelse, Sweden; The Royal Society and Leverhulme Trust, United Kingdom.

The crucial computing support from all WLCG partners is acknowledged gratefully, in particular from CERN, the ATLAS Tier-1 facilities at TRIUMF (Canada), NDGF (Denmark, Norway, Sweden), CC-IN2P3 (France), KIT/GridKA (Germany), INFN-CNAF (Italy), NL-T1 (Netherlands), PIC (Spain), ASGC (Taiwan), RAL (UK) and BNL (USA), the Tier-2 facilities worldwide and large non-WLCG resource providers. Major contributors of computing resources are listed in Ref. [134].

References

- [1] ATLAS Collaboration, *Observation of a new particle in the search for the Standard Model Higgs boson with the ATLAS detector at the LHC*, *Phys. Lett. B* **716** (2012) 1, arXiv: [1207.7214 \[hep-ex\]](#).
- [2] CMS Collaboration, *Observation of a new boson at a mass of 125 GeV with the CMS experiment at the LHC*, *Phys. Lett. B* **716** (2012) 30, arXiv: [1207.7235 \[hep-ex\]](#).
- [3] L. Susskind, *Dynamics of spontaneous symmetry breaking in the Weinberg-Salam theory*, *Phys. Rev. D* **20** (1979) 2619.
- [4] F. Del Aguila and M. J. Bowick, *The possibility of new fermions with $\Delta I=0$ mass*, *Nucl. Phys. B* **224** (1983) 107.
- [5] D. B. Kaplan, H. Georgi, and S. Dimopoulos, *Composite Higgs scalars*, *Phys. Lett. B* **136** (1984) 187.
- [6] K. Agashe, R. Contino, and A. Pomarol, *The minimal composite Higgs model*, *Nucl. Phys. B* **719** (2005) 165, arXiv: [hep-ph/0412089](#).
- [7] R. Contino, L. Da Rold, and A. Pomarol, *Light custodians in natural composite Higgs models*, *Phys. Rev. D* **75** (2007) 055014, arXiv: [hep-ph/0612048](#).
- [8] N. Arkani-Hamed, A. Cohen, E. Katz, and A. Nelson, *The Littlest Higgs*, *JHEP* **07** (2002) 034, arXiv: [hep-ph/0206021 \[hep-ph\]](#).
- [9] Y. Hosotani, S. Noda, and K. Takenaga, *Dynamical gauge-Higgs unification in the electroweak theory*, *Phys. Lett. B* **607** (2005) 276, arXiv: [hep-ph/0410193](#).
- [10] I. Antoniadis, K. Benakli, and M. Quirós, *Finite Higgs mass without supersymmetry*, *New J. Phys.* **3** (2001) 20, arXiv: [hep-th/0108005](#).
- [11] T. Appelquist, H.-C. Cheng, and B. A. Dobrescu, *Bounds on universal extra dimensions*, *Phys. Rev. D* **64** (2001) 035002, arXiv: [hep-ph/0012100](#).
- [12] F. Del Aguila, L. Ametller, G. L. Kane, and J. Vidal, *Vector-like fermion and standard Higgs production at hadron colliders*, *Nucl. Phys. B* **334** (1990) 1.
- [13] J. Aguilar-Saavedra, *Identifying top partners at LHC*, *JHEP* **11** (2009) 030, arXiv: [0907.3155 \[hep-ph\]](#).
- [14] B. Fuks and H.-S. Shao, *QCD next-to-leading-order predictions matched to parton showers for vector-like quark models*, *Eur. Phys. J. C* **77** (2017) 135, arXiv: [1610.04622](#).
- [15] Y. Okada and L. Panizzi, *LHC Signatures of Vector-Like Quarks*, *Adv. High Energy Phys.* **2013** (2013) 364936, arXiv: [1207.5607](#).
- [16] J. A. Aguilar-Saavedra, R. Benbrik, S. Heinemeyer, and M. Pérez-Victoria, *Handbook of vectorlike quarks: Mixing and single production*, *Phys. Rev. D* **88** (2013) 094010, arXiv: [1306.0572](#).
- [17] ATLAS Collaboration, *Search for production of vector-like quark pairs and of four top quarks in the lepton-plus-jets final state in pp collisions at $\sqrt{s} = 8$ TeV with the ATLAS detector*, *JHEP* **08** (2015) 105, arXiv: [1505.04306 \[hep-ex\]](#).

- [18] ATLAS Collaboration, *Search for vectorlike B quarks in events with one isolated lepton, missing transverse momentum, and jets at $\sqrt{s} = 8$ TeV with the ATLAS detector*, [Phys. Rev. D **91** \(2015\) 112011](#), arXiv: [1503.05425 \[hep-ex\]](#).
- [19] ATLAS Collaboration, *Search for pair and single production of new heavy quarks that decay to a Z boson and a third-generation quark in pp collisions at $\sqrt{s} = 8$ TeV with the ATLAS detector*, [JHEP **11** \(2014\) 104](#), arXiv: [1409.5500 \[hep-ex\]](#).
- [20] CMS Collaboration, *Search for vectorlike charge 2/3 T quarks in proton–proton collisions at $\sqrt{s} = 8$ TeV*, [Phys. Rev. D **93** \(2016\) 012003](#), arXiv: [1509.04177 \[hep-ex\]](#).
- [21] CMS Collaboration, *Search for pair-produced vectorlike B quarks in proton–proton collisions at $\sqrt{s} = 8$ TeV*, [Phys. Rev. D **93** \(2016\) 112009](#), arXiv: [1507.07129 \[hep-ex\]](#).
- [22] CMS Collaboration, *Search for top-quark partners with charge 5/3 in the same-sign dilepton final state*, [Phys. Rev. Lett. **112** \(2014\) 171801](#), arXiv: [1312.2391 \[hep-ex\]](#).
- [23] ATLAS Collaboration, *Search for single production of vector-like quarks decaying into Wb in pp collisions at $\sqrt{s} = 8$ TeV with the ATLAS detector*, [Eur. Phys. J. C **76** \(2016\) 442](#), arXiv: [1602.05606 \[hep-ex\]](#).
- [24] ATLAS Collaboration, *Search for pair production of up-type vector-like quarks and for four-top-quark events in final states with multiple b-jets with the ATLAS detector*, [JHEP **07** \(2018\) 089](#), arXiv: [1803.09678 \[hep-ex\]](#).
- [25] ATLAS Collaboration, *Search for pair production of heavy vector-like quarks decaying to high- p_T W bosons and b quarks in the lepton-plus-jets final state in pp collisions at $\sqrt{s} = 13$ TeV with the ATLAS detector*, [JHEP **10** \(2017\) 141](#), arXiv: [1707.03347 \[hep-ex\]](#).
- [26] ATLAS Collaboration, *Search for pair production of vector-like top quarks in events with one lepton, jets, and missing transverse momentum in $\sqrt{s} = 13$ TeV pp collisions with the ATLAS detector*, [JHEP **08** \(2017\) 052](#), arXiv: [1705.10751 \[hep-ex\]](#).
- [27] ATLAS Collaboration, *Search for new phenomena in events with same-charge leptons and b-jets in pp collisions at $\sqrt{s} = 13$ TeV with the ATLAS detector*, [JHEP **12** \(2018\) 039](#), arXiv: [1807.11883 \[hep-ex\]](#).
- [28] ATLAS Collaboration, *Search for pair production of heavy vector-like quarks decaying into hadronic final states in pp collisions at $\sqrt{s} = 13$ TeV with the ATLAS detector*, [Phys. Rev. D **98** \(2018\) 092005](#), arXiv: [1808.01771 \[hep-ex\]](#).
- [29] ATLAS Collaboration, *Combination of the searches for pair-produced vector-like partners of the third-generation quarks at $\sqrt{s} = 13$ TeV with the ATLAS detector*, [Phys. Rev. Lett. **121** \(2018\) 211801](#), arXiv: [1808.02343 \[hep-ex\]](#).
- [30] ATLAS collaboration, *Search for pair-production of vector-like quarks in pp collision events at $\sqrt{s} = 13$ TeV with at least one leptonically decaying Z boson and a third-generation quark with the ATLAS detector*, [arXiv:2210.15413 \(2022\)](#).

- [31] CMS Collaboration, *Search for pair production of vector-like T and B quarks in single-lepton final states using boosted jet substructure techniques at $\sqrt{s} = 13$ TeV*, *JHEP* **11** (2017) 085, arXiv: [1706.03408 \[hep-ex\]](#).
- [32] CMS Collaboration, *Search for pair production of vector-like quarks in the $bW\bar{b}W$ channel from proton–proton collisions at $\sqrt{s} = 13$ TeV*, *Phys. Lett. B* **779** (2018) 82, arXiv: [1710.01539 \[hep-ex\]](#).
- [33] CMS Collaboration, *Search for vector-like T and B quark pairs in final states with leptons at $\sqrt{s} = 13$ TeV*, *JHEP* **08** (2018) 177, arXiv: [1805.04758 \[hep-ex\]](#).
- [34] CMS Collaboration, *Search for pair production of vector-like quarks in leptonic final states in proton–proton collisions at $\sqrt{s} = 13$ TeV*, arXiv: [2209.07327 \(2022\)](#).
- [35] ATLAS Collaboration, *Search for pair- and single-production of vector-like quarks in final states with at least one Z boson decaying into a pair of electrons or muons in pp collision data collected with the ATLAS detector*, *Phys. Rev. D* **98** (2018) 112010, arXiv: [1806.10555 \[hep-ex\]](#).
- [36] ATLAS Collaboration, *Search for single production of vector-like quarks decaying into Wb in pp collisions at $\sqrt{s} = 13$ TeV with the ATLAS detector*, *JHEP* **05** (2019) 164, arXiv: [1812.07343 \[hep-ex\]](#).
- [37] ATLAS Collaboration, *Search for large missing transverse momentum in association with one top-quark in proton–proton collisions at $\sqrt{s} = 13$ TeV with the ATLAS detector*, *JHEP* **05** (2019) 041, arXiv: [1812.09743 \[hep-ex\]](#).
- [38] CMS Collaboration, *Search for single production of a vector-like T quark decaying to a Z boson and a top quark in proton–proton collisions at $\sqrt{s} = 13$ TeV*, *Phys. Lett. B* **781** (2018) 574, arXiv: [1708.01062 \[hep-ex\]](#).
- [39] CMS Collaboration, *Search for single production of vector-like quarks decaying to a top quark and a W boson in proton–proton collisions at $\sqrt{s} = 13$ TeV*, *Eur. Phys. J. C* **79** (2019) 90, arXiv: [1809.08597 \[hep-ex\]](#).
- [40] CMS Collaboration, *Search for single production of vector-like quarks decaying to a b quark and a Higgs boson*, *JHEP* **06** (2018) 031, arXiv: [1802.01486 \[hep-ex\]](#).
- [41] CMS Collaboration, *Search for electroweak production of a vector-like T quark using fully hadronic final states*, *JHEP* **01** (2020) 036, arXiv: [1909.04721 \[hep-ex\]](#).
- [42] CMS Collaboration, *Search for single production of a vector-like T quark decaying to a top quark and a Z boson in the final state with jets and missing transverse momentum at $\sqrt{s} = 13$ TeV*, *JHEP* **05** (2022) 093, arXiv: [2201.02227](#).
- [43] CMS Collaboration, *Search for a vector-like quark $T' \rightarrow tH$ via the diphoton decay mode of the Higgs boson in proton–proton collisions at $\sqrt{s} = 13$ TeV*, arXiv: [2302.12802 \(2023\)](#).
- [44] ATLAS Collaboration, *Search for single production of a vectorlike T quark decaying into a Higgs boson and top quark with fully hadronic final states using the ATLAS detector*, *Phys. Rev. D* **105** (2022) 092012, arXiv: [2201.07045](#).
- [45] ATLAS Collaboration, *Search for single production of vector-like T quarks decaying into Ht or Zt in pp collisions at $\sqrt{s} = 13$ TeV with the ATLAS detector*, arXiv: [2305.03401 \(2023\)](#).

- [46] A. Atre et al., *Model-independent searches for new quarks at the LHC*, **JHEP** **2011** (2011) 80, arXiv: [1102.1987](#).
- [47] M. Buchkremer, G. Cacciapaglia, A. Deandrea, and L. Panizzi, *Model-independent framework for searches of top partners*, **Nucl. Phys. B** **876** (2013) 376, arXiv: [1305.4172](#).
- [48] O. Matsedonskyi, G. Panico, and A. Wulzer, *On the interpretation of Top partners searches*, **JHEP** **2014** (2014) 97, arXiv: [1409.0100](#).
- [49] ATLAS Collaboration, *The ATLAS Experiment at the CERN Large Hadron Collider*, **JINST** **3** (2008) S08003.
- [50] B. Abbott et al., *Production and integration of the ATLAS Insertable B-Layer*, **JINST** **13** (2018) T05008, arXiv: [1803.00844](#) [[physics.ins-det](#)].
- [51] ATLAS Collaboration, *Performance of the ATLAS trigger system in 2015*, **Eur. Phys. J. C** **77** (2017) 317, arXiv: [1611.09661](#) [[hep-ex](#)].
- [52] ATLAS Collaboration, *The ATLAS Collaboration Software and Firmware*, ATL-SOFT-PUB-2021-001, 2021, URL: <https://cds.cern.ch/record/2767187>.
- [53] ATLAS Collaboration, *The ATLAS Simulation Infrastructure*, **Eur. Phys. J. C** **70** (2010) 823, arXiv: [1005.4568](#) [[physics.ins-det](#)].
- [54] S. Agostinelli et al., *GEANT4 – a simulation toolkit*, **Nucl. Instrum. Meth. A** **506** (2003) 250.
- [55] T. Sjöstrand, S. Mrenna, and P. Skands, *A brief introduction to PYTHIA 8.1*, **Comput. Phys. Commun.** **178** (2008) 852, arXiv: [0710.3820](#) [[hep-ph](#)].
- [56] NNPDF Collaboration, R. D. Ball, et al., *Parton distributions with LHC data*, **Nucl. Phys. B** **867** (2013) 244, arXiv: [1207.1303](#) [[hep-ph](#)].
- [57] ATLAS Collaboration, *The Pythia 8 A3 tune description of ATLAS minimum bias and inelastic measurements incorporating the Donnachie–Landshoff diffractive model*, ATL-PHYS-PUB-2016-017, 2016, URL: <https://cds.cern.ch/record/2206965>.
- [58] E. Bothmann et al., *Event generation with Sherpa 2.2*, **SciPost Phys.** **7** (2019) 034, arXiv: [1905.09127](#) [[hep-ph](#)].
- [59] The NNPDF Collaboration, R. D. Ball, et al., *Parton distributions for the LHC run II*, **JHEP** **04** (2015) 040, arXiv: [1410.8849](#) [[hep-ph](#)].
- [60] C. Anastasiou, L. Dixon, K. Melnikov, and F. Petriello, *High-precision QCD at hadron colliders: Electroweak gauge boson rapidity distributions at next-to-next-to leading order*, **Phys. Rev. D** **69** (2004) 094008, arXiv: [hep-ph/0312266](#).
- [61] T. Gleisberg and S. Höche, *Comix, a new matrix element generator*, **JHEP** **12** (2008) 039, arXiv: [0808.3674](#) [[hep-ph](#)].
- [62] F. Buccioni et al., *OpenLoops 2*, **Eur. Phys. J. C** **79** (2019) 866, arXiv: [1907.13071](#) [[hep-ph](#)].
- [63] F. Cascioli, P. Maierhöfer, and S. Pozzorini, *Scattering Amplitudes with Open Loops*, **Phys. Rev. Lett.** **108** (2012) 111601, arXiv: [1111.5206](#) [[hep-ph](#)].
- [64] A. Denner, S. Dittmaier, and L. Hofer, *COLLIER: A fortran-based complex one-loop library in extended regularizations*, **Comput. Phys. Commun.** **212** (2017) 220, arXiv: [1604.06792](#) [[hep-ph](#)].

- [65] S. Schumann and F. Krauss,
A parton shower algorithm based on Catani–Seymour dipole factorisation, **JHEP** **03** (2008) 038,
arXiv: [0709.1027 \[hep-ph\]](#).
- [66] S. Höche, F. Krauss, M. Schönherr, and F. Siegert,
A critical appraisal of NLO+PS matching methods, **JHEP** **09** (2012) 049,
arXiv: [1111.1220 \[hep-ph\]](#).
- [67] S. Höche, F. Krauss, M. Schönherr, and F. Siegert,
QCD matrix elements + parton showers. The NLO case, **JHEP** **04** (2013) 027,
arXiv: [1207.5030 \[hep-ph\]](#).
- [68] S. Catani, F. Krauss, B. R. Webber, and R. Kuhn, *QCD Matrix Elements + Parton Showers*,
JHEP **11** (2001) 063, arXiv: [hep-ph/0109231](#).
- [69] S. Höche, F. Krauss, S. Schumann, and F. Siegert, *QCD matrix elements and truncated showers*,
JHEP **05** (2009) 053, arXiv: [0903.1219 \[hep-ph\]](#).
- [70] J. Alwall et al., *The automated computation of tree-level and next-to-leading order differential cross sections, and their matching to parton shower simulations*, **JHEP** **07** (2014) 079,
arXiv: [1405.0301 \[hep-ph\]](#).
- [71] T. Sjöstrand et al., *An introduction to PYTHIA 8.2*, **Comput. Phys. Commun.** **191** (2015) 159,
arXiv: [1410.3012 \[hep-ph\]](#).
- [72] ATLAS Collaboration, *ATLAS Pythia 8 tunes to 7 TeV data*, ATL-PHYS-PUB-2014-021, 2014,
URL: <https://cds.cern.ch/record/1966419>.
- [73] P. Nason, *A new method for combining NLO QCD with shower Monte Carlo algorithms*,
JHEP **11** (2004) 040, arXiv: [hep-ph/0409146](#).
- [74] S. Frixione, P. Nason, and C. Oleari,
Matching NLO QCD computations with parton shower simulations: the POWHEG method,
JHEP **11** (2007) 070, arXiv: [0709.2092 \[hep-ph\]](#).
- [75] S. Alioli, P. Nason, C. Oleari, and E. Re, *A general framework for implementing NLO calculations in shower Monte Carlo programs: the POWHEG BOX*, **JHEP** **06** (2010) 043,
arXiv: [1002.2581 \[hep-ph\]](#).
- [76] J. M. Campbell, R. K. Ellis, P. Nason, and E. Re,
Top-Pair production and decay at NLO matched with parton showers, **JHEP** **04** (2015) 114,
arXiv: [1412.1828 \[hep-ph\]](#).
- [77] M. Czakon and A. Mitov,
Top++: A program for the calculation of the top-pair cross-section at hadron colliders,
Comput. Phys. Commun. **185** (2014) 2930, arXiv: [1112.5675 \[hep-ph\]](#).
- [78] M. Czakon, P. Fiedler, and A. Mitov,
Total Top-Quark Pair-Production Cross Section at Hadron Colliders Through $O(\alpha_S^4)$,
Phys. Rev. Lett. **110** (2013) 252004, arXiv: [1303.6254 \[hep-ph\]](#).
- [79] M. Beneke, P. Falgari, S. Klein, and C. Schwinn,
Hadronic top-quark pair production with NNLL threshold resummation,
Nucl. Phys. B **855** (2012) 695, arXiv: [1109.1536 \[hep-ph\]](#).
- [80] M. Cacciari, M. Czakon, M. Mangano, A. Mitov, and P. Nason, *Top-pair production at hadron colliders with next-to-next-to-leading logarithmic soft-gluon resummation*,
Phys. Lett. B **710** (2012) 612, arXiv: [1111.5869 \[hep-ph\]](#).

- [81] M. Czakon and A. Mitov, *NNLO corrections to top pair production at hadron colliders: the quark-gluon reaction*, *JHEP* **01** (2013) 080, arXiv: [1210.6832 \[hep-ph\]](#).
- [82] M. Czakon and A. Mitov, *NNLO corrections to top-pair production at hadron colliders: the all-fermionic scattering channels*, *JHEP* **12** (2012) 054, arXiv: [1207.0236 \[hep-ph\]](#).
- [83] P. Bärnreuther, M. Czakon, and A. Mitov, *Percent-Level-Precision Physics at the Tevatron: Next-to-Next-to-Leading Order QCD Corrections to $q\bar{q} \rightarrow t\bar{t} + X$* , *Phys. Rev. Lett.* **109** (2012) 132001, arXiv: [1204.5201 \[hep-ph\]](#).
- [84] J. Bellm et al., *Herwig 7.0/Herwig++ 3.0 release note*, *Eur. Phys. J. C* **76** (2016) 196, arXiv: [1512.01178 \[hep-ph\]](#).
- [85] R. Frederix, D. Pagani, and M. Zaro, *Large NLO corrections in $t\bar{t}W^\pm$ and $t\bar{t}\bar{t}$ hadroproduction from supposedly subleading EW contributions*, *JHEP* **02** (2018) 031, arXiv: [1711.02116](#).
- [86] S. Frixione, V. Hirschi, D. Pagani, H.-S. Shao, and M. Zaro, *Electroweak and QCD corrections to top-pair hadroproduction in association with heavy bosons*, *JHEP* **2015** (2015) 184, arXiv: [1504.03446](#).
- [87] R. Frederix, E. Re, and P. Torrielli, *Single-top t -channel hadroproduction in the four-flavour scheme with POWHEG and aMC@NLO*, *JHEP* **09** (2012) 130, arXiv: [1207.5391 \[hep-ph\]](#).
- [88] E. Re, *Single-top Wt -channel production matched with parton showers using the POWHEG method*, *Eur. Phys. J. C* **71** (2011) 1547, arXiv: [1009.2450 \[hep-ph\]](#).
- [89] M. Aliev et al., *HATHOR – HAdronic Top and Heavy quarks crOss section calculatoR*, *Comput. Phys. Commun.* **182** (2011) 1034, arXiv: [1007.1327 \[hep-ph\]](#).
- [90] P. Kant et al., *HatHor for single top-quark production: Updated predictions and uncertainty estimates for single top-quark production in hadronic collisions*, *Comput. Phys. Commun.* **191** (2015) 74, arXiv: [1406.4403 \[hep-ph\]](#).
- [91] N. Kidonakis, *Next-to-next-to-leading-order collinear and soft gluon corrections for t -channel single top quark production*, *Phys. Rev. D* **83** (2011) 091503, arXiv: [1103.2792 \[hep-ph\]](#).
- [92] N. Kidonakis, *Two-loop soft anomalous dimensions for single top quark associated production with a W^- or H^-* , *Phys. Rev. D* **82** (2010) 054018, arXiv: [1005.4451 \[hep-ph\]](#).
- [93] N. Kidonakis, *Next-to-next-to-leading logarithm resummation for s -channel single top quark production*, *Phys. Rev. D* **81** (2010) 054028, arXiv: [1001.5034 \[hep-ph\]](#).
- [94] S. Frixione, E. Laenen, P. Motylinski, C. White, and B. R. Webber, *Single-top hadroproduction in association with a W boson*, *JHEP* **07** (2008) 029, arXiv: [0805.3067 \[hep-ph\]](#).
- [95] C. Degrande et al., *UFO–The Universal FeynRules Output*, *Comput. Phys. Commun.* **183** (2012) 1201, arXiv: [1108.2040](#).
- [96] O. Mattelaer, *On the maximal use of Monte Carlo samples: re-weighting events at NLO accuracy*, *Eur. Phys. J. C* **76** (2016) 1, arXiv: [1607.00763](#).

- [97] G. Cacciapaglia et al., *Next-to-leading-order predictions for single vector-like quark production at the LHC*, [Phys. Lett. B **793** \(2019\) 206](#), arXiv: [1811.05055](#).
- [98] A. Roy, N. Nikiforou, N. Castro, and T. Andeen, *Novel interpretation strategy for searches of singly produced vectorlike quarks at the LHC*, [Phys. Rev. D **101** \(2020\) 115027](#), arXiv: [2003.00640 \[hep-ph\]](#).
- [99] A. Roy and T. Andeen, *Non-resonant diagrams for single production of top and bottom partners*, [Phys. Lett. B **833** \(2022\) 137330](#), arXiv: [2202.02640](#).
- [100] ATLAS Collaboration, *Electron and photon performance measurements with the ATLAS detector using the 2015–2017 LHC proton–proton collision data*, [JINST **14** \(2019\) P12006](#), arXiv: [1908.00005 \[hep-ex\]](#).
- [101] ATLAS Collaboration, *Muon reconstruction and identification efficiency in ATLAS using the full Run 2 pp collision data set at $\sqrt{s} = 13$ TeV*, [Eur. Phys. J. C **81** \(2021\) 578](#), arXiv: [2012.00578 \[hep-ex\]](#).
- [102] ATLAS Collaboration, *Jet reconstruction and performance using particle flow with the ATLAS Detector*, [Eur. Phys. J. C **77** \(2017\) 466](#), arXiv: [1703.10485](#).
- [103] M. Cacciari, G. P. Salam, and G. Soyez, *The anti- k_t jet clustering algorithm*, [JHEP **04** \(2008\) 063](#), arXiv: [0802.1189 \[hep-ph\]](#).
- [104] M. Cacciari, G. P. Salam, and G. Soyez, *FastJet user manual*, [Eur. Phys. J. C **72** \(2012\) 1896](#), arXiv: [1111.6097 \[hep-ph\]](#).
- [105] ATLAS Collaboration, *Jet energy scale and resolution measured in proton–proton collisions at $\sqrt{s} = 13$ TeV with the ATLAS detector*, [Eur. Phys. J. C **81** \(2021\) 689](#), arXiv: [2007.02645](#).
- [106] ATLAS Collaboration, *Performance of pile-up mitigation techniques for jets in pp collisions at $\sqrt{s} = 8$ TeV using the ATLAS detector*, [Eur. Phys. J. C **76** \(2016\) 581](#), arXiv: [1510.03823 \[hep-ex\]](#).
- [107] ATLAS Collaboration, *ATLAS flavour-tagging algorithms for the LHC Run 2 pp collision dataset*, (2022), arXiv: [2211.16345 \[physics.data-an\]](#).
- [108] ATLAS Collaboration, *E_T^{miss} performance in the ATLAS detector using 2015–2016 LHC pp collisions*, ATLAS-CONF-2018-023, 2018, URL: <https://cds.cern.ch/record/2625233>.
- [109] D. Krohn, J. Thaler, and L.-T. Wang, *Jets with variable R*, [JHEP **06** \(2009\) 059](#), arXiv: [0903.0392](#).
- [110] T. Lapsien, R. Kogler, and J. Haller, *A new tagger for hadronically decaying heavy particles at the LHC*, [Eur. Phys. J. C **76** \(2016\) 600](#), arXiv: [1606.04961](#).
- [111] ATLAS Collaboration, *Performance of the ATLAS muon triggers in Run 2*, [JINST **15** \(2020\) P09015](#), arXiv: [2004.13447 \[hep-ex\]](#).
- [112] ATLAS Collaboration, *Performance of electron and photon triggers in ATLAS during LHC Run 2*, [Eur. Phys. J. C **80** \(2020\) 47](#), arXiv: [1909.00761 \[hep-ex\]](#).
- [113] ATLAS Collaboration, *ATLAS simulation of boson plus jets processes in Run 2*, ATL-PHYS-PUB-2017-006, 2017, URL: <https://cds.cern.ch/record/2261937>.

- [114] ATLAS Collaboration, *ATLAS b-jet identification performance and efficiency measurement with $t\bar{t}$ events in pp collisions at $\sqrt{s} = 13$ TeV*, *Eur. Phys. J. C* **79** (2019) 970, arXiv: [1907.05120 \[hep-ex\]](#).
- [115] ATLAS Collaboration, *Measurement of the c-jet mistagging efficiency in $t\bar{t}$ events using pp collision data at $\sqrt{s} = 13$ TeV collected with the ATLAS detector*, *Eur. Phys. J. C* **82** (2021) 95, arXiv: [2109.10627 \[hep-ex\]](#).
- [116] *Calibration of the light-flavour jet mistagging efficiency of the b-tagging algorithms with Z+jets events using 139 fb^{-1} of ATLAS proton-proton collision data at $\sqrt{s} = 13$ TeV*, (), arXiv: [2301.06319 \[hep-ex\]](#).
- [117] ATLAS Collaboration, *Performance of missing transverse momentum reconstruction with the ATLAS detector using proton-proton collisions at $\sqrt{s} = 13$ TeV*, *Eur. Phys. J. C* **78** (2018) 903, arXiv: [1802.08168 \[hep-ex\]](#).
- [118] ATLAS Collaboration, *Luminosity determination in pp collisions at $\sqrt{s} = 13$ TeV using the ATLAS detector at the LHC*, ATLAS-CONF-2019-021, 2019, URL: <https://cds.cern.ch/record/2677054>.
- [119] G. Avoni et al., *The new LUCID-2 detector for luminosity measurement and monitoring in ATLAS*, *JINST* **13** (2018) P07017.
- [120] ATLAS Collaboration, *Measurements of the production cross section of a Z boson in association with jets in pp collisions at $\sqrt{s} = 13$ TeV with the ATLAS detector*, *Eur. Phys. J. C* **77** (2017) 361, arXiv: [1702.05725 \[hep-ex\]](#).
- [121] J. M. Campbell and R. K. Ellis, *Update on vector boson pair production at hadron colliders*, *Phys. Rev. D* **60** (1999) 113006, arXiv: [hep-ph/9905386](#).
- [122] ATLAS Collaboration, *Measurements of the inclusive and differential production cross sections of a top-quark-antiquark pair in association with a Z boson at $\sqrt{s} = 13$ TeV with the ATLAS detector*, *Eur. Phys. J. C* **81** (2021) 737, arXiv: [2103.12603 \[hep-ex\]](#).
- [123] J. Butterworth et al., *PDF4LHC recommendations for LHC Run II*, *J. Phys. G* **43** (2016) 023001, arXiv: [1510.03865 \[hep-ph\]](#).
- [124] ATLAS Collaboration, *Measurement of Higgs boson decay into b-quarks in associated production with a top-quark pair in pp collisions at $\sqrt{s} = 13$ TeV with the ATLAS detector*, *JHEP* **06** (2021) 097, arXiv: [2111.06712 \[hep-ex\]](#).
- [125] R. Barlow and C. Beeston, *Fitting using finite Monte Carlo samples*, *Comput. Phys. Commun.* **77** (1993) 219.
- [126] L. Moneta et al., *The RooStats Project*, *PoS ACAT2010* (2010) 057, ed. by T. Speer et al., arXiv: [1009.1003 \[physics.data-an\]](#).
- [127] W. Verkerke and D. Kirkby, *The RooFit toolkit for data modeling*, 2003, arXiv: [physics/0306116 \[physics.data-an\]](#).
- [128] K. Cranmer, G. Lewis, L. Moneta, A. Shibata, and W. Verkerke, *HistFactory: A tool for creating statistical models for use with RooFit and RooStats*, tech. rep., CERN-OPEN-2012-016, 2012, URL: <https://cds.cern.ch/record/1456844>.
- [129] T. Junk, *Confidence level computation for combining searches with small statistics*, *Nucl. Instrum. Meth. A* **434** (1999) 435, arXiv: [hep-ex/9902006 \[hep-ex\]](#).
- [130] A. L. Read, *Presentation of search results: the CL_S technique*, *J. Phys. G* **28** (2002) 2693.

- [131] G. Cowan, K. Cranmer, E. Gross, and O. Vitells, *Asymptotic formulae for likelihood-based tests of new physics*, *Eur. Phys. J. C* **71** (2011) 1554, arXiv: [1007.1727](https://arxiv.org/abs/1007.1727) [[physics.data-an](https://arxiv.org/archive/physics)], Erratum: *Eur. Phys. J. C* **73** (2013) 2501.
- [132] M. S. Chanowitz and M. K. Gaillard, *The TeV physics of strongly interacting W's and Z's*, *Nucl. Phys. B* **261** (1985) 379.
- [133] A. Deandrea, T. Flacke, B. Fuks, L. Panizzi, and H.-S. Shao, *Single production of vector-like quarks: the effects of large width, interference and NLO corrections*, *JHEP* **08** (2021) 107, arXiv: [2105.08745](https://arxiv.org/abs/2105.08745).
- [134] ATLAS Collaboration, *ATLAS Computing Acknowledgements*, ATL-SOFT-PUB-2021-003, 2021, URL: <https://cds.cern.ch/record/2776662>.

The ATLAS Collaboration

G. Aad ¹⁰², B. Abbott ¹²⁰, K. Abeling ⁵⁵, N.J. Abicht ⁴⁹, S.H. Abidi ²⁹, A. Aboulhorma ^{35e}, H. Abramowicz ¹⁵¹, H. Abreu ¹⁵⁰, Y. Abulaiti ¹¹⁷, A.C. Abusleme Hoffman ^{137a}, B.S. Acharya ^{69a,69b,n}, C. Adam Bourdarios ⁴, L. Adamczyk ^{86a}, L. Adamek ¹⁵⁵, S.V. Addepalli ²⁶, M.J. Addison ¹⁰¹, J. Adelman ¹¹⁵, A. Adiguzel ^{21c}, T. Adye ¹³⁴, A.A. Affolder ¹³⁶, Y. Afik ³⁶, M.N. Agaras ¹³, J. Agarwala ^{73a,73b}, A. Aggarwal ¹⁰⁰, C. Agheorghiesei ^{27c}, A. Ahmad ³⁶, F. Ahmadov ^{38,z}, W.S. Ahmed ¹⁰⁴, S. Ahuja ⁹⁵, X. Ai ^{62a}, G. Aielli ^{76a,76b}, M. Ait Tamliah ^{35e}, B. Aitbenkikh ^{35a}, I. Aizenberg ¹⁶⁹, M. Akbiyik ¹⁰⁰, T.P.A. Åkesson ⁹⁸, A.V. Akimov ³⁷, D. Akiyama ¹⁶⁸, N.N. Akolkar ²⁴, K. Al Houry ⁴¹, G.L. Alberghi ^{23b}, J. Albert ¹⁶⁵, P. Albicocco ⁵³, G.L. Albouy ⁶⁰, S. Alderweireldt ⁵², M. Aleksa ³⁶, I.N. Aleksandrov ³⁸, C. Alexa ^{27b}, T. Alexopoulos ¹⁰, A. Alfonsi ¹¹⁴, F. Alfonsi ^{23b}, M. Algren ⁵⁶, M. Alhroob ¹²⁰, B. Ali ¹³², H.M.J. Ali ⁹¹, S. Ali ¹⁴⁸, S.W. Alibocus ⁹², M. Aliev ³⁷, G. Alimonti ^{71a}, W. Alkahi ⁵⁵, C. Allaire ⁶⁶, B.M.M. Allbrooke ¹⁴⁶, J.F. Allen ⁵², C.A. Allendes Flores ^{137f}, P.P. Allport ²⁰, A. Aloisio ^{72a,72b}, F. Alonso ⁹⁰, C. Alpigiani ¹³⁸, M. Alvarez Estevez ⁹⁹, A. Alvarez Fernandez ¹⁰⁰, M. Alves Cardoso ⁵⁶, M.G. Alviggi ^{72a,72b}, M. Aly ¹⁰¹, Y. Amaral Coutinho ^{83b}, A. Ambler ¹⁰⁴, C. Amelung ³⁶, M. Amerl ¹⁰¹, C.G. Ames ¹⁰⁹, D. Amidei ¹⁰⁶, S.P. Amor Dos Santos ^{130a}, K.R. Amos ¹⁶³, V. Ananiev ¹²⁵, C. Anastopoulos ¹³⁹, T. Andeen ¹¹, J.K. Anders ³⁶, S.Y. Andreev ^{47a,47b}, A. Andreatta ^{71a,71b}, S. Angelidakis ⁹, A. Angerami ^{41,ac}, A.V. Anisenkov ³⁷, A. Annovi ^{74a}, C. Antel ⁵⁶, M.T. Anthony ¹³⁹, E. Antipov ¹⁴⁵, M. Antonelli ⁵³, D.J.A. Antrim ^{17a}, F. Anulli ^{75a}, M. Aoki ⁸⁴, T. Aoki ¹⁵³, J.A. Aparisi Pozo ¹⁶³, M.A. Aparo ¹⁴⁶, L. Aperio Bella ⁴⁸, C. Appelt ¹⁸, A. Apyan ²⁶, N. Aranzabal ³⁶, C. Arcangeletti ⁵³, A.T.H. Arce ⁵¹, E. Arena ⁹², J-F. Arguin ¹⁰⁸, S. Argyropoulos ⁵⁴, J.-H. Arling ⁴⁸, O. Arnaez ⁴, H. Arnold ¹¹⁴, Z.P. Arrubarrena Tame ¹⁰⁹, G. Artoni ^{75a,75b}, H. Asada ¹¹¹, K. Asai ¹¹⁸, S. Asai ¹⁵³, N.A. Asbah ⁶¹, K. Assamagan ²⁹, R. Astalos ^{28a}, S. Atashi ¹⁶⁰, R.J. Atkin ^{33a}, M. Atkinson ¹⁶², N.B. Atlay ¹⁸, H. Atmani ^{62b}, P.A. Atlasiddha ¹⁰⁶, K. Augsten ¹³², S. Auricchio ^{72a,72b}, A.D. Aurio ²⁰, V.A. Austrup ¹⁰¹, G. Avolio ³⁶, K. Axiotis ⁵⁶, G. Azuelos ^{108,ag}, D. Babal ^{28b}, H. Bachacou ¹³⁵, K. Bachas ^{152,q}, A. Bachiu ³⁴, F. Backman ^{47a,47b}, A. Badea ⁶¹, P. Bagnaia ^{75a,75b}, M. Bahmani ¹⁸, A.J. Bailey ¹⁶³, V.R. Bailey ¹⁶², J.T. Baines ¹³⁴, L. Baines ⁹⁴, C. Bakalis ¹⁰, O.K. Baker ¹⁷², E. Bakos ¹⁵, D. Bakshi Gupta ⁸, R. Balasubramanian ¹¹⁴, E.M. Baldin ³⁷, P. Balek ^{86a}, E. Ballabene ^{23b,23a}, F. Balli ¹³⁵, L.M. Baltes ^{63a}, W.K. Balunas ³², J. Balz ¹⁰⁰, E. Banas ⁸⁷, M. Bandieramonte ¹²⁹, A. Bandyopadhyay ²⁴, S. Bansal ²⁴, L. Barak ¹⁵¹, M. Barakat ⁴⁸, E.L. Barberio ¹⁰⁵, D. Barberis ^{57b,57a}, M. Barbero ¹⁰², G. Barbour ⁹⁶, K.N. Barends ^{33a}, T. Barillari ¹¹⁰, M-S. Barisits ³⁶, T. Barklow ¹⁴³, P. Baron ¹²², D.A. Baron Moreno ¹⁰¹, A. Baroncelli ^{62a}, G. Barone ²⁹, A.J. Barr ¹²⁶, J.D. Barr ⁹⁶, L. Barranco Navarro ^{47a,47b}, F. Barreiro ⁹⁹, J. Barreiro Guimarães da Costa ^{14a}, U. Barron ¹⁵¹, M.G. Barros Teixeira ^{130a}, S. Barsov ³⁷, F. Bartels ^{63a}, R. Bartoldus ¹⁴³, A.E. Barton ⁹¹, P. Bartos ^{28a}, A. Basan ¹⁰⁰, M. Baselga ⁴⁹, A. Bassalat ^{66,b}, M.J. Basso ^{156a}, C.R. Basson ¹⁰¹, R.L. Bates ⁵⁹, S. Batlamous ^{35e}, J.R. Batley ³², B. Batool ¹⁴¹, M. Battaglia ¹³⁶, D. Battulga ¹⁸, M. Baucé ^{75a,75b}, M. Bauer ³⁶, P. Bauer ²⁴, L.T. Bazzano Hurrell ³⁰, J.B. Beacham ⁵¹, T. Beau ¹²⁷, P.H. Beauchemin ¹⁵⁸, F. Becherer ⁵⁴, P. Bechtel ²⁴, H.P. Beck ^{19,p}, K. Becker ¹⁶⁷, A.J. Beddall ⁸², V.A. Bednyakov ³⁸, C.P. Bee ¹⁴⁵, L.J. Beemster ¹⁵, T.A. Beermann ³⁶, M. Begalli ^{83d}, M. Begel ²⁹, A. Behera ¹⁴⁵, J.K. Behr ⁴⁸, J.F. Beirer ⁵⁵, F. Beisiegel ²⁴, M. Belfkir ¹⁵⁹, G. Bella ¹⁵¹, L. Bellagamba ^{23b}, A. Bellerive ³⁴, P. Bellos ²⁰, K. Beloborodov ³⁷, N.L. Belyaev ³⁷, D. Bencheikroun ^{35a}, F. Bendebba ^{35a},

Y. Benhammou ¹⁵¹, M. Benoit ²⁹, J.R. Bensingher ²⁶, S. Bentvelsen ¹¹⁴, L. Beresford ⁴⁸,
 M. Beretta ⁵³, E. Bergeaas Kuutmann ¹⁶¹, N. Berger ⁴, B. Bergmann ¹³², J. Beringer ^{17a},
 G. Bernardi ⁵, C. Bernius ¹⁴³, F.U. Bernlochner ²⁴, F. Bernon ^{36,102}, T. Berry ⁹⁵, P. Berta ¹³³,
 A. Berthold ⁵⁰, I.A. Bertram ⁹¹, S. Bethke ¹¹⁰, A. Betti ^{75a,75b}, A.J. Bevan ⁹⁴, M. Bhamjee ^{33c},
 S. Bhatta ¹⁴⁵, D.S. Bhattacharya ¹⁶⁶, P. Bhattarai ²⁶, V.S. Bhopatkar ¹²¹, R. Bi ^{29,ai},
 R.M. Bianchi ¹²⁹, G. Bianco ^{23b,23a}, O. Biebel ¹⁰⁹, R. Bielski ¹²³, M. Biglietti ^{77a},
 T.R.V. Billoud ¹³², M. Bindi ⁵⁵, A. Bingul ^{21b}, C. Bini ^{75a,75b}, A. Biondini ⁹²,
 C.J. Birch-sykes ¹⁰¹, G.A. Bird ^{20,134}, M. Birman ¹⁶⁹, M. Biros ¹³³, T. Bisanz ⁴⁹,
 E. Bisceglie ^{43b,43a}, D. Biswas ¹⁴¹, A. Bitadze ¹⁰¹, K. Bjørke ¹²⁵, I. Bloch ⁴⁸, C. Blocker ²⁶,
 A. Blue ⁵⁹, U. Blumenschein ⁹⁴, J. Blumenthal ¹⁰⁰, G.J. Bobbink ¹¹⁴, V.S. Bobrovnikov ³⁷,
 M. Boehler ⁵⁴, B. Boehm ¹⁶⁶, D. Bogavac ³⁶, A.G. Bogdanchikov ³⁷, C. Bohm ^{47a},
 V. Boisvert ⁹⁵, P. Bokan ⁴⁸, T. Bold ^{86a}, M. Bomben ⁵, M. Bona ⁹⁴, M. Boonekamp ¹³⁵,
 C.D. Booth ⁹⁵, A.G. Borbély ⁵⁹, I.S. Bordulev ³⁷, H.M. Borecka-Bielska ¹⁰⁸, L.S. Borgna ⁹⁶,
 G. Borisso ⁹¹, D. Bortoletto ¹²⁶, D. Boscherini ^{23b}, M. Bosman ¹³, J.D. Bossio Sola ³⁶,
 K. Bouaouda ^{35a}, N. Bouchhar ¹⁶³, J. Boudreau ¹²⁹, E.V. Bouhova-Thacker ⁹¹, D. Boumediene ⁴⁰,
 R. Bouquet ⁵, A. Boveia ¹¹⁹, J. Boyd ³⁶, D. Boye ²⁹, I.R. Boyko ³⁸, J. Bracinik ²⁰,
 N. Brahim ^{62d}, G. Brandt ¹⁷¹, O. Brandt ³², F. Braren ⁴⁸, B. Brau ¹⁰³, J.E. Brau ¹²³,
 R. Brenner ¹⁶⁹, L. Brenner ¹¹⁴, R. Brenner ¹⁶¹, S. Bressler ¹⁶⁹, D. Britton ⁵⁹, D. Britzger ¹¹⁰,
 I. Brock ²⁴, G. Brooijmans ⁴¹, W.K. Brooks ^{137f}, E. Brost ²⁹, L.M. Brown ¹⁶⁵, L.E. Bruce ⁶¹,
 T.L. Bruckler ¹²⁶, P.A. Bruckman de Renstrom ⁸⁷, B. Brüers ⁴⁸, D. Bruncko ^{28b,*}, A. Bruni ^{23b},
 G. Bruni ^{23b}, M. Bruschi ^{23b}, N. Brusino ^{75a,75b}, T. Buanes ¹⁶, Q. Buat ¹³⁸, D. Buchin ¹¹⁰,
 A.G. Buckley ⁵⁹, M.K. Bugge ¹²⁵, O. Bulekov ³⁷, B.A. Bullard ¹⁴³, S. Burdin ⁹²,
 C.D. Burgard ⁴⁹, A.M. Burger ⁴⁰, B. Burghgrave ⁸, O. Burlayenko ⁵⁴, J.T.P. Burr ³²,
 C.D. Burton ¹¹, J.C. Burzynski ¹⁴², E.L. Busch ⁴¹, V. Büscher ¹⁰⁰, P.J. Bussey ⁵⁹, J.M. Butler ²⁵,
 C.M. Buttar ⁵⁹, J.M. Butterworth ⁹⁶, W. Buttinger ¹³⁴, C.J. Buxo Vazquez ¹⁰⁷, A.R. Buzykaev ³⁷,
 G. Cabras ^{23b}, S. Cabrera Urbán ¹⁶³, L. Cadamuro ⁶⁶, D. Caforio ⁵⁸, H. Cai ¹²⁹, Y. Cai ^{14a,14e},
 V.M.M. Cairo ³⁶, O. Cakir ^{3a}, N. Calace ³⁶, P. Calafiura ^{17a}, G. Calderini ¹²⁷, P. Calfayan ⁶⁸,
 G. Callea ⁵⁹, L.P. Caloba ^{83b}, D. Calvet ⁴⁰, S. Calvet ⁴⁰, T.P. Calvet ¹⁰², M. Calvetti ^{74a,74b},
 R. Camacho Toro ¹²⁷, S. Camarda ³⁶, D. Camarero Munoz ²⁶, P. Camarri ^{76a,76b},
 M.T. Camerlingo ^{72a,72b}, D. Cameron ¹²⁵, C. Camincher ¹⁶⁵, M. Campanelli ⁹⁶, A. Camplani ⁴²,
 V. Canale ^{72a,72b}, A. Canesse ¹⁰⁴, M. Cano Bret ⁸⁰, J. Cantero ¹⁶³, Y. Cao ¹⁶², F. Capocasa ²⁶,
 M. Capua ^{43b,43a}, A. Carbone ^{71a,71b}, R. Cardarelli ^{76a}, J.C.J. Cardenas ⁸, F. Cardillo ¹⁶³,
 T. Carli ³⁶, G. Carlino ^{72a}, J.I. Carlotto ¹³, B.T. Carlson ^{129,r}, E.M. Carlson ^{165,156a},
 L. Carminati ^{71a,71b}, A. Carnelli ¹³⁵, M. Carnesale ^{75a,75b}, S. Caron ¹¹³, E. Carquin ^{137f},
 S. Carrá ^{71a}, G. Carratta ^{23b,23a}, F. Carrio Argos ^{33g}, J.W.S. Carter ¹⁵⁵, T.M. Carter ⁵²,
 M.P. Casado ^{13,i}, M. Caspar ⁴⁸, E.G. Castiglia ¹⁷², F.L. Castillo ⁴, L. Castillo Garcia ¹³,
 V. Castillo Gimenez ¹⁶³, N.F. Castro ^{130a,130e}, A. Catinaccio ³⁶, J.R. Catmore ¹²⁵, V. Cavaliere ²⁹,
 N. Cavalli ^{23b,23a}, V. Cavalinni ^{74a,74b}, Y.C. Cekmecelioglu ⁴⁸, E. Celebi ^{21a}, F. Celli ¹²⁶,
 M.S. Centonze ^{70a,70b}, K. Cerny ¹²², A.S. Cerqueira ^{83a}, A. Cerri ¹⁴⁶, L. Cerrito ^{76a,76b},
 F. Cerutti ^{17a}, B. Cervato ¹⁴¹, A. Cervelli ^{23b}, G. Cesarini ⁵³, S.A. Cetin ⁸², Z. Chadi ^{35a},
 D. Chakraborty ¹¹⁵, M. Chala ^{130f}, J. Chan ¹⁷⁰, W.Y. Chan ¹⁵³, J.D. Chapman ³², E. Chapon ¹³⁵,
 B. Chargeishvili ^{149b}, D.G. Charlton ²⁰, T.P. Charman ⁹⁴, M. Chatterjee ¹⁹, C. Chauhan ¹³³,
 S. Chekanov ⁶, S.V. Chekulaev ^{156a}, G.A. Chelkov ^{38,a}, A. Chen ¹⁰⁶, B. Chen ¹⁵¹, B. Chen ¹⁶⁵,
 H. Chen ^{14c}, H. Chen ²⁹, J. Chen ^{62c}, J. Chen ¹⁴², M. Chen ¹²⁶, S. Chen ¹⁵³, S.J. Chen ^{14c},
 X. Chen ^{62c}, X. Chen ^{14b,af}, Y. Chen ^{62a}, C.L. Cheng ¹⁷⁰, H.C. Cheng ^{64a}, S. Cheong ¹⁴³,
 A. Cheplakov ³⁸, E. Cheremushkina ⁴⁸, E. Cherepanova ¹¹⁴, R. Cherkaoui El Moursli ^{35e},
 E. Cheu ⁷, K. Cheung ⁶⁵, L. Chevalier ¹³⁵, V. Chiarella ⁵³, G. Chiarelli ^{74a}, N. Chiedde ¹⁰²,

G. Chiodini ^{70a}, A.S. Chisholm ²⁰, A. Chitan ^{27b}, M. Chitishvili ¹⁶³, M.V. Chizhov ³⁸, K. Choi ¹¹, A.R. Chomont ^{75a,75b}, Y. Chou ¹⁰³, E.Y.S. Chow ¹¹⁴, T. Chowdhury ^{33g}, K.L. Chu ¹⁶⁹, M.C. Chu ^{64a}, X. Chu ^{14a,14e}, J. Chudoba ¹³¹, J.J. Chwastowski ⁸⁷, D. Cieri ¹¹⁰, K.M. Ciesla ^{86a}, V. Cindro ⁹³, A. Ciocio ^{17a}, F. Cirotto ^{72a,72b}, Z.H. Citron ^{169,1}, M. Citterio ^{71a}, D.A. Ciubotaru ^{27b}, B.M. Ciungu ¹⁵⁵, A. Clark ⁵⁶, P.J. Clark ⁵², J.M. Clavijo Columbie ⁴⁸, S.E. Clawson ⁴⁸, C. Clement ^{47a,47b}, J. Clercx ⁴⁸, Y. Coadou ¹⁰², M. Cobal ^{69a,69c}, A. Coccaro ^{57b}, R.F. Coelho Barrue ^{130a}, R. Coelho Lopes De Sa ¹⁰³, S. Coelli ^{71a}, H. Cohen ¹⁵¹, A.E.C. Coimbra ^{71a,71b}, B. Cole ⁴¹, J. Collot ⁶⁰, P. Conde Muiño ^{130a,130g}, M.P. Connell ^{33c}, S.H. Connell ^{33c}, I.A. Connelly ⁵⁹, E.I. Conroy ¹²⁶, F. Conventi ^{72a,ah}, H.G. Cooke ²⁰, A.M. Cooper-Sarkar ¹²⁶, A. Cordeiro Oudot Choi ¹²⁷, F. Cormier ¹⁶⁴, L.D. Corpe ⁴⁰, M. Corradi ^{75a,75b}, F. Corriveau ^{104,x}, A. Cortes-Gonzalez ¹⁸, M.J. Costa ¹⁶³, F. Costanza ⁴, D. Costanzo ¹³⁹, B.M. Cote ¹¹⁹, G. Cowan ⁹⁵, K. Cranmer ¹⁷⁰, D. Cremonini ^{23b,23a}, S. Crépe-Renaudin ⁶⁰, F. Crescioli ¹²⁷, M. Cristinziani ¹⁴¹, M. Cristoforetti ^{78a,78b}, V. Croft ¹¹⁴, J.E. Crosby ¹²¹, G. Crosetti ^{43b,43a}, A. Cueto ⁹⁹, T. Cuhadar Donszelmann ¹⁶⁰, H. Cui ^{14a,14e}, Z. Cui ⁷, W.R. Cunningham ⁵⁹, F. Curcio ^{43b,43a}, P. Czodrowski ³⁶, M.M. Czurylo ^{63b}, M.J. Da Cunha Sargedas De Sousa ^{62a}, J.V. Da Fonseca Pinto ^{83b}, C. Da Via ¹⁰¹, W. Dabrowski ^{86a}, T. Dado ⁴⁹, S. Dahbi ^{33g}, T. Dai ¹⁰⁶, C. Dallapiccola ¹⁰³, M. Dam ⁴², G. D'amen ²⁹, V. D'Amico ¹⁰⁹, J. Damp ¹⁰⁰, J.R. Dandoy ¹²⁸, M.F. Daneri ³⁰, M. Danninger ¹⁴², V. Dao ³⁶, G. Darbo ^{57b}, S. Darmora ⁶, S.J. Das ^{29,ai}, S. D'Auria ^{71a,71b}, C. David ^{156b}, T. Davidek ¹³³, B. Davis-Purcell ³⁴, I. Dawson ⁹⁴, H.A. Day-hall ¹³², K. De ⁸, R. De Asmundis ^{72a}, N. De Biase ⁴⁸, S. De Castro ^{23b,23a}, N. De Groot ¹¹³, P. de Jong ¹¹⁴, H. De la Torre ¹⁰⁷, A. De Maria ^{14c}, A. De Salvo ^{75a}, U. De Sanctis ^{76a,76b}, A. De Santo ¹⁴⁶, J.B. De Vivie De Regie ⁶⁰, D.V. Dedovich ³⁸, J. Degens ¹¹⁴, A.M. Deiana ⁴⁴, F. Del Corso ^{23b,23a}, J. Del Peso ⁹⁹, F. Del Rio ^{63a}, F. Deliot ¹³⁵, C.M. Delitzsch ⁴⁹, M. Della Pietra ^{72a,72b}, D. Della Volpe ⁵⁶, A. Dell'Acqua ³⁶, L. Dell'Asta ^{71a,71b}, M. Delmastro ⁴, P.A. Delsart ⁶⁰, S. Demers ¹⁷², M. Demichev ³⁸, S.P. Denisov ³⁷, L. D'Eramo ⁴⁰, D. Derendarz ⁸⁷, F. Derue ¹²⁷, P. Dervan ⁹², K. Desch ²⁴, C. Deutsch ²⁴, F.A. Di Bello ^{57b,57a}, A. Di Ciaccio ^{76a,76b}, L. Di Ciaccio ⁴, A. Di Domenico ^{75a,75b}, C. Di Donato ^{72a,72b}, A. Di Girolamo ³⁶, G. Di Gregorio ⁵, A. Di Luca ^{78a,78b}, B. Di Micco ^{77a,77b}, R. Di Nardo ^{77a,77b}, C. Diaconu ¹⁰², M. Diamantopoulou ³⁴, F.A. Dias ¹¹⁴, T. Dias Do Vale ¹⁴², M.A. Diaz ^{137a,137b}, F.G. Diaz Capriles ²⁴, M. Didenko ¹⁶³, E.B. Diehl ¹⁰⁶, L. Diehl ⁵⁴, S. Díez Cornell ⁴⁸, C. Diez Pardos ¹⁴¹, C. Dimitriadi ^{161,24,161}, A. Dimitrievska ^{17a}, J. Dingfelder ²⁴, I-M. Dinu ^{27b}, S.J. Dittmeier ^{63b}, F. Dittus ³⁶, F. Djama ¹⁰², T. Djobava ^{149b}, J.I. Djuvsland ¹⁶, C. Doglioni ^{101,98}, J. Dolejsi ¹³³, Z. Dolezal ¹³³, M. Donadelli ^{83c}, B. Dong ¹⁰⁷, J. Donini ⁴⁰, A. D'Onofrio ^{77a,77b}, M. D'Onofrio ⁹², J. Dopke ¹³⁴, A. Doria ^{72a}, N. Dos Santos Fernandes ^{130a}, M.T. Dova ⁹⁰, A.T. Doyle ⁵⁹, M.A. Dragnet ¹²⁶, E. Dreyer ¹⁶⁹, I. Drivas-koulouris ¹⁰, A.S. Drobac ¹⁵⁸, M. Drozdova ⁵⁶, D. Du ^{62a}, T.A. du Pree ¹¹⁴, F. Dubinin ³⁷, M. Dubovsky ^{28a}, E. Duchovni ¹⁶⁹, G. Duckeck ¹⁰⁹, O.A. Ducu ^{27b}, D. Duda ⁵², A. Dudarev ³⁶, E.R. Duden ²⁶, M. D'uffizi ¹⁰¹, L. Duflot ⁶⁶, M. Dührssen ³⁶, C. Dülsen ¹⁷¹, A.E. Dumitriu ^{27b}, M. Dunford ^{63a}, S. Dungs ⁴⁹, K. Dunne ^{47a,47b}, A. Duperrin ¹⁰², H. Duran Yildiz ^{3a}, M. Düren ⁵⁸, A. Durglishvili ^{149b}, B.L. Dwyer ¹¹⁵, G.I. Dyckes ^{17a}, M. Dyndal ^{86a}, S. Dysch ¹⁰¹, B.S. Dziedzic ⁸⁷, Z.O. Earnshaw ¹⁴⁶, G.H. Eberwein ¹²⁶, B. Eckerova ^{28a}, S. Eggebrecht ⁵⁵, M.G. Eggleston ⁵¹, E. Egidio Purcino De Souza ¹²⁷, L.F. Ehrke ⁵⁶, G. Eigen ¹⁶, K. Einsweiler ^{17a}, T. Ekelof ¹⁶¹, P.A. Ekman ⁹⁸, S. El Farkh ^{35b}, Y. El Ghazali ^{35b}, H. El Jarrari ^{35e,148}, A. El Moussaouy ^{35a}, V. Ellajosyula ¹⁶¹, M. Ellert ¹⁶¹, F. Ellinghaus ¹⁷¹, A.A. Elliot ⁹⁴, N. Ellis ³⁶, J. Elmsheuser ²⁹, M. Elsing ³⁶, D. Emelianov ¹³⁴, Y. Enari ¹⁵³, I. Ene ^{17a}, S. Epari ¹³, J. Erdmann ⁴⁹, P.A. Erland ⁸⁷, M. Errenst ¹⁷¹, M. Escalier ⁶⁶, C. Escobar ¹⁶³,

E. Etzion ¹⁵¹, G. Evans ^{130a}, H. Evans ⁶⁸, L.S. Evans ⁹⁵, M.O. Evans ¹⁴⁶, A. Ezhilov ³⁷,
 S. Ezzartouni ^{35a}, F. Fabbri ⁵⁹, L. Fabbri ^{23b,23a}, G. Facini ⁹⁶, V. Fadeyev ¹³⁶,
 R.M. Fakhrutdinov ³⁷, S. Falciano ^{75a}, L.F. Falda Ulhoa Coelho ³⁶, P.J. Falke ²⁴, J. Faltova ¹³³,
 C. Fan ¹⁶², Y. Fan ^{14a}, Y. Fang ^{14a,14e}, M. Fanti ^{71a,71b}, M. Faraj ^{69a,69b}, Z. Farazpay ⁹⁷,
 A. Farbin ⁸, A. Farilla ^{77a}, T. Farooque ¹⁰⁷, S.M. Farrington ⁵², F. Fassi ^{35e}, D. Fassouliotis ⁹,
 M. Faucci Giannelli ^{76a,76b}, W.J. Fawcett ³², L. Fayard ⁶⁶, P. Federic ¹³³, P. Federicova ¹³¹,
 O.L. Fedin ^{37,a}, G. Fedotov ³⁷, M. Feickert ¹⁷⁰, L. Feligioni ¹⁰², D.E. Fellers ¹²³, C. Feng ^{62b},
 M. Feng ^{14b}, Z. Feng ¹¹⁴, M.J. Fenton ¹⁶⁰, A.B. Fenyuk ³⁷, L. Ferencz ⁴⁸, R.A.M. Ferguson ⁹¹,
 S.I. Fernandez Luengo ^{137f}, M.J.V. Fernoux ¹⁰², J. Ferrando ⁴⁸, A. Ferrari ¹⁶¹, P. Ferrari ^{114,113},
 R. Ferrari ^{73a}, D. Ferrere ⁵⁶, C. Ferretti ¹⁰⁶, F. Fiedler ¹⁰⁰, A. Filipčić ⁹³, E.K. Filmer ¹,
 F. Filthaut ¹¹³, M.C.N. Fiolhais ^{130a,130c,c}, L. Fiorini ¹⁶³, W.C. Fisher ¹⁰⁷, T. Fitschen ¹⁰¹,
 P.M. Fitzhugh ¹³⁵, I. Fleck ¹⁴¹, P. Fleischmann ¹⁰⁶, T. Flick ¹⁷¹, L. Flores ¹²⁸, M. Flores ^{33d,ad},
 L.R. Flores Castillo ^{64a}, L. Flores Sanz De Acedo ³⁶, F.M. Follega ^{78a,78b}, N. Fomin ¹⁶,
 J.H. Foo ¹⁵⁵, B.C. Forland ⁶⁸, A. Formica ¹³⁵, A.C. Forti ¹⁰¹, E. Fortin ³⁶, A.W. Fortman ⁶¹,
 M.G. Foti ^{17a}, L. Fountas ^{9,j}, D. Fournier ⁶⁶, H. Fox ⁹¹, P. Francavilla ^{74a,74b}, S. Francescato ⁶¹,
 S. Franchellucci ⁵⁶, M. Franchini ^{23b,23a}, S. Franchino ^{63a}, D. Francis ³⁶, L. Franco ¹¹³,
 L. Franconi ⁴⁸, M. Franklin ⁶¹, G. Frattari ²⁶, A.C. Freegard ⁹⁴, W.S. Freund ^{83b}, Y.Y. Frid ¹⁵¹,
 N. Fritzsche ⁵⁰, A. Froch ⁵⁴, D. Froidevaux ³⁶, J.A. Frost ¹²⁶, Y. Fu ^{62a}, M. Fujimoto ¹¹⁸,
 E. Fullana Torregrosa ^{163,*}, K.Y. Fung ^{64a}, E. Furtado De Simas Filho ^{83b}, M. Furukawa ¹⁵³,
 J. Fuster ¹⁶³, A. Gabrielli ^{23b,23a}, A. Gabrielli ¹⁵⁵, P. Gadow ³⁶, G. Gagliardi ^{57b,57a},
 L.G. Gagnon ^{17a}, E.J. Gallas ¹²⁶, B.J. Gallop ¹³⁴, K.K. Gan ¹¹⁹, S. Ganguly ¹⁵³, J. Gao ^{62a},
 Y. Gao ⁵², F.M. Garay Walls ^{137a,137b}, B. Garcia ²⁹, C. García ¹⁶³, A. Garcia Alonso ¹¹⁴,
 A.G. Garcia Caffaro ¹⁷², J.E. García Navarro ¹⁶³, M. Garcia-Sciveres ^{17a}, G.L. Gardner ¹²⁸,
 R.W. Gardner ³⁹, N. Garelli ¹⁵⁸, D. Garg ⁸⁰, R.B. Garg ^{143,o}, J.M. Gargan ⁵², C.A. Garner ¹⁵⁵,
 S.J. Gasiorowski ¹³⁸, P. Gaspar ^{83b}, G. Gaudio ^{73a}, V. Gautam ¹³, P. Gauzzi ^{75a,75b},
 I.L. Gavrilenko ³⁷, A. Gavrilyuk ³⁷, C. Gay ¹⁶⁴, G. Gaycken ⁴⁸, E.N. Gazis ¹⁰, A.A. Geanta ^{27b},
 C.M. Gee ¹³⁶, C. Gemme ^{57b}, M.H. Genest ⁶⁰, S. Gentile ^{75a,75b}, S. George ⁹⁵, W.F. George ²⁰,
 T. Geralis ⁴⁶, P. Gessinger-Befurt ³⁶, M.E. Geyik ¹⁷¹, M. Ghneimat ¹⁴¹, K. Ghorbanian ⁹⁴,
 A. Ghosal ¹⁴¹, A. Ghosh ¹⁶⁰, A. Ghosh ⁷, B. Giacobbe ^{23b}, S. Giagu ^{75a,75b}, P. Giannetti ^{74a},
 A. Giannini ^{62a}, S.M. Gibson ⁹⁵, M. Gignac ¹³⁶, D.T. Gil ^{86b}, A.K. Gilbert ^{86a}, B.J. Gilbert ⁴¹,
 D. Gillberg ³⁴, G. Gilles ¹¹⁴, N.E.K. Gillwald ⁴⁸, L. Ginabat ¹²⁷, D.M. Gingrich ^{2,ag},
 M.P. Giordani ^{69a,69c}, P.F. Giraud ¹³⁵, G. Giugliarelli ^{69a,69c}, D. Giugni ^{71a}, F. Giuli ³⁶,
 I. Gkialas ^{9,j}, L.K. Gladilin ³⁷, C. Glasman ⁹⁹, G.R. Gledhill ¹²³, G. Glemža ⁴⁸, M. Glisic ¹²³,
 I. Gnesi ^{43b,f}, Y. Go ^{29,ai}, M. Goblirsch-Kolb ³⁶, B. Gocke ⁴⁹, D. Godin ¹⁰⁸, B. Gokturk ^{21a},
 S. Goldfarb ¹⁰⁵, T. Golling ⁵⁶, M.G.D. Gololo ^{33g}, D. Golubkov ³⁷, J.P. Gombas ¹⁰⁷,
 A. Gomes ^{130a,130b}, G. Gomes Da Silva ¹⁴¹, A.J. Gomez Delegido ¹⁶³, R. Gonçalo ^{130a,130c},
 G. Gonella ¹²³, L. Gonella ²⁰, A. Gongadze ^{149c}, F. Gonnella ²⁰, J.L. Gonski ⁴¹,
 R.Y. González Andana ⁵², S. González de la Hoz ¹⁶³, S. Gonzalez Fernandez ¹³,
 R. Gonzalez Lopez ⁹², C. Gonzalez Renteria ^{17a}, R. Gonzalez Suarez ¹⁶¹, S. Gonzalez-Sevilla ⁵⁶,
 G.R. Gonzalvo Rodriguez ¹⁶³, L. Goossens ³⁶, P.A. Gorbounov ³⁷, B. Gorini ³⁶, E. Gorini ^{70a,70b},
 A. Gorišek ⁹³, T.C. Gosart ¹²⁸, A.T. Goshaw ⁵¹, M.I. Gostkin ³⁸, S. Goswami ¹²¹,
 C.A. Gottardo ³⁶, M. Gouighri ^{35b}, V. Goumarre ⁴⁸, A.G. Goussiou ¹³⁸, N. Govender ^{33c},
 I. Grabowska-Bold ^{86a}, K. Graham ³⁴, E. Gramstad ¹²⁵, S. Grancagnolo ^{70a,70b}, M. Grandi ¹⁴⁶,
 P.M. Gravila ^{27f}, F.G. Gravili ^{70a,70b}, H.M. Gray ^{17a}, M. Greco ^{70a,70b}, C. Grefe ²⁴,
 I.M. Gregor ⁴⁸, P. Grenier ¹⁴³, C. Grieco ¹³, A.A. Grillo ¹³⁶, K. Grimm ³¹, S. Grinstein ^{13,t},
 J.-F. Grivaz ⁶⁶, E. Gross ¹⁶⁹, J. Grosse-Knetter ⁵⁵, C. Grud ¹⁰⁶, J.C. Grundy ¹²⁶, L. Guan ¹⁰⁶,
 W. Guan ²⁹, C. Gubbels ¹⁶⁴, J.G.R. Guerrero Rojas ¹⁶³, G. Guerrieri ^{69a,69c}, F. Guescini ¹¹⁰,

R. Gugel ¹⁰⁰, J.A.M. Guhit ¹⁰⁶, A. Guida ¹⁸, T. Guillemain ⁴, E. Guilloton ^{167,134}, S. Guindon ³⁶, F. Guo ^{14a,14e}, J. Guo ^{62c}, L. Guo ⁴⁸, Y. Guo ¹⁰⁶, R. Gupta ⁴⁸, S. Gurbuz ²⁴, S.S. Gurdasani ⁵⁴, G. Gustavino ³⁶, M. Guth ⁵⁶, P. Gutierrez ¹²⁰, L.F. Gutierrez Zagazeta ¹²⁸, C. Gutschow ⁹⁶, C. Gwenlan ¹²⁶, C.B. Gwilliam ⁹², E.S. Haaland ¹²⁵, A. Haas ¹¹⁷, M. Habedank ⁴⁸, C. Haber ^{17a}, H.K. Hadavand ⁸, A. Hadeef ¹⁰⁰, S. Hadzic ¹¹⁰, J.J. Hahn ¹⁴¹, E.H. Haines ⁹⁶, M. Haleem ¹⁶⁶, J. Haley ¹²¹, J.J. Hall ¹³⁹, G.D. Hallowell ¹⁰², L. Halser ¹⁹, K. Hamano ¹⁶⁵, M. Hamer ²⁴, G.N. Hamity ⁵², E.J. Hampshire ⁹⁵, J. Han ^{62b}, K. Han ^{62a}, L. Han ^{14c}, L. Han ^{62a}, S. Han ^{17a}, Y.F. Han ¹⁵⁵, K. Hanagaki ⁸⁴, M. Hance ¹³⁶, D.A. Hangal ^{41,ac}, H. Hanif ¹⁴², M.D. Hank ¹²⁸, R. Hankache ¹⁰¹, J.B. Hansen ⁴², J.D. Hansen ⁴², P.H. Hansen ⁴², K. Hara ¹⁵⁷, D. Harada ⁵⁶, T. Harenberg ¹⁷¹, S. Harkusha ³⁷, M.L. Harris ¹⁰³, Y.T. Harris ¹²⁶, J. Harrison ¹³, N.M. Harrison ¹¹⁹, P.F. Harrison ¹⁶⁷, N.M. Hartman ¹¹⁰, N.M. Hartmann ¹⁰⁹, Y. Hasegawa ¹⁴⁰, A. Hasib ⁵², S. Haug ¹⁹, R. Hauser ¹⁰⁷, C.M. Hawkes ²⁰, R.J. Hawkings ³⁶, Y. Hayashi ¹⁵³, S. Hayashida ¹¹¹, D. Hayden ¹⁰⁷, C. Hayes ¹⁰⁶, R.L. Hayes ¹¹⁴, C.P. Hays ¹²⁶, J.M. Hays ⁹⁴, H.S. Hayward ⁹², F. He ^{62a}, M. He ^{14a,14e}, Y. He ¹⁵⁴, Y. He ¹²⁷, N.B. Heatley ⁹⁴, V. Hedberg ⁹⁸, A.L. Heggelund ¹²⁵, N.D. Hehir ^{94,*}, C. Heidegger ⁵⁴, K.K. Heidegger ⁵⁴, W.D. Heidorn ⁸¹, J. Heilman ³⁴, S. Heim ⁴⁸, T. Heim ^{17a}, J.G. Heinlein ¹²⁸, J.J. Heinrich ¹²³, L. Heinrich ^{110,ae}, J. Hejbal ¹³¹, L. Helary ⁴⁸, A. Held ¹⁷⁰, S. Hellesund ¹⁶, C.M. Helling ¹⁶⁴, S. Hellman ^{47a,47b}, R.C.W. Henderson ⁹¹, L. Henkelmann ³², A.M. Henriques Correia ³⁶, H. Herde ⁹⁸, Y. Hernández Jiménez ¹⁴⁵, L.M. Herrmann ²⁴, T. Herrmann ⁵⁰, G. Herten ⁵⁴, R. Hertenberger ¹⁰⁹, L. Hervas ³⁶, M.E. Hespings ¹⁰⁰, N.P. Hessey ^{156a}, H. Hibi ⁸⁵, S.J. Hillier ²⁰, J.R. Hinds ¹⁰⁷, F. Hinterkeuser ²⁴, M. Hirose ¹²⁴, S. Hirose ¹⁵⁷, D. Hirschbuehl ¹⁷¹, T.G. Hitchings ¹⁰¹, B. Hiti ⁹³, J. Hobbs ¹⁴⁵, R. Hobincu ^{27e}, N. Hod ¹⁶⁹, M.C. Hodgkinson ¹³⁹, B.H. Hodgkinson ³², A. Hoecker ³⁶, J. Hofer ⁴⁸, T. Holm ²⁴, M. Holzbock ¹¹⁰, L.B.A.H. Hommels ³², B.P. Honan ¹⁰¹, J. Hong ^{62c}, T.M. Hong ¹²⁹, B.H. Hooberman ¹⁶², W.H. Hopkins ⁶, Y. Horii ¹¹¹, S. Hou ¹⁴⁸, A.S. Howard ⁹³, J. Howarth ⁵⁹, J. Hoya ⁶, M. Hrabovsky ¹²², A. Hrynevich ⁴⁸, T. Hryn'ova ⁴, P.J. Hsu ⁶⁵, S.-C. Hsu ¹³⁸, Q. Hu ⁴¹, Y.F. Hu ^{14a,14e}, S. Huang ^{64b}, X. Huang ^{14c}, Y. Huang ¹³⁹, Y. Huang ^{14a}, Z. Huang ¹⁰¹, Z. Hubacek ¹³², M. Huebner ²⁴, F. Hugging ²⁴, T.B. Huffman ¹²⁶, C.A. Hugli ⁴⁸, M. Huhtinen ³⁶, S.K. Huiberts ¹⁶, R. Hulsken ¹⁰⁴, N. Huseynov ^{12,a}, J. Huston ¹⁰⁷, J. Huth ⁶¹, R. Hyneman ¹⁴³, G. Iacobucci ⁵⁶, G. Iakovidis ²⁹, I. Ibragimov ¹⁴¹, L. Iconomidou-Fayard ⁶⁶, P. Iengo ^{72a,72b}, R. Iguchi ¹⁵³, T. Iizawa ⁸⁴, Y. Ikegami ⁸⁴, N. Ilic ¹⁵⁵, H. Imam ^{35a}, M. Ince Lezki ⁵⁶, T. Ingebretsen Carlson ^{47a,47b}, G. Introzzi ^{73a,73b}, M. Iodice ^{77a}, V. Ippolito ^{75a,75b}, R.K. Irwin ⁹², M. Ishino ¹⁵³, W. Islam ¹⁷⁰, C. Issever ^{18,48}, S. Istin ^{21a,ak}, H. Ito ¹⁶⁸, J.M. Iturbe Ponce ^{64a}, R. Iuppa ^{78a,78b}, A. Ivina ¹⁶⁹, J.M. Izen ⁴⁵, V. Izzo ^{72a}, P. Jacka ^{131,132}, P. Jackson ¹, R.M. Jacobs ⁴⁸, B.P. Jaeger ¹⁴², C.S. Jagfeld ¹⁰⁹, P. Jain ⁵⁴, G. Jäkel ¹⁷¹, K. Jakobs ⁵⁴, T. Jakoubek ¹⁶⁹, J. Jamieson ⁵⁹, K.W. Janas ^{86a}, A.E. Jaspan ⁹², M. Javurkova ¹⁰³, F. Jeanneau ¹³⁵, L. Jeanty ¹²³, J. Jejelava ^{149a,aa}, P. Jenni ^{54,g}, C.E. Jessiman ³⁴, S. Jézéquel ⁴, C. Jia ^{62b}, J. Jia ¹⁴⁵, X. Jia ⁶¹, X. Jia ^{14a,14e}, Z. Jia ^{14c}, Y. Jiang ^{62a}, S. Jiggins ⁴⁸, J. Jimenez Pena ¹³, S. Jin ^{14c}, A. Jinaru ^{27b}, O. Jinnouchi ¹⁵⁴, P. Johansson ¹³⁹, K.A. Johns ⁷, J.W. Johnson ¹³⁶, D.M. Jones ³², E. Jones ⁴⁸, P. Jones ³², R.W.L. Jones ⁹¹, T.J. Jones ⁹², R. Joshi ¹¹⁹, J. Jovicevic ¹⁵, X. Ju ^{17a}, J.J. Junggeburth ³⁶, T. Junkermann ^{63a}, A. Juste Rozas ^{13,t}, M.K. Juzek ⁸⁷, S. Kabana ^{137e}, A. Kaczmarek ⁸⁷, M. Kado ¹¹⁰, H. Kagan ¹¹⁹, M. Kagan ¹⁴³, A. Kahn ⁴¹, A. Kahn ¹²⁸, C. Kahra ¹⁰⁰, T. Kaji ¹⁶⁸, E. Kajomovitz ¹⁵⁰, N. Kakati ¹⁶⁹, I. Kalaitzidou ⁵⁴, C.W. Calderon ²⁹, A. Kamenshchikov ¹⁵⁵, S. Kanayama ¹⁵⁴, N.J. Kang ¹³⁶, D. Kar ^{33g}, K. Karava ¹²⁶, M.J. Kareem ^{156b}, E. Karentzos ⁵⁴, I. Karknias ¹⁵², O. Karkout ¹¹⁴, S.N. Karpov ³⁸, Z.M. Karpova ³⁸, V. Kartvelishvili ⁹¹, A.N. Karyukhin ³⁷, E. Kasimi ¹⁵², J. Katzy ⁴⁸, S. Kaur ³⁴, K. Kawade ¹⁴⁰, M.P. Kawale ¹²⁰, T. Kawamoto ¹³⁵, E.F. Kay ³⁶, F.I. Kaya ¹⁵⁸, S. Kazakos ¹⁰⁷, V.F. Kazanin ³⁷, Y. Ke ¹⁴⁵,

J.M. Keaveney ^{133a}, R. Keeler ¹⁶⁵, G.V. Kehris ⁶¹, J.S. Keller ³⁴, A.S. Kelly ⁹⁶, J.J. Kempster ¹⁴⁶, K.E. Kennedy ⁴¹, P.D. Kennedy ¹⁰⁰, O. Kepka ¹³¹, B.P. Kerridge ¹⁶⁷, S. Kersten ¹⁷¹, B.P. Kerševan ⁹³, S. Keshri ⁶⁶, L. Keszeghova ^{28a}, S. Ketabchi Haghghat ¹⁵⁵, M. Khandoga ¹²⁷, A. Khanov ¹²¹, A.G. Kharlamov ³⁷, T. Kharlamova ³⁷, E.E. Khoda ¹³⁸, T.J. Khoo ¹⁸, G. Khoriauli ¹⁶⁶, J. Khubua ^{149b}, Y.A.R. Khwaira ⁶⁶, A. Kilgallon ¹²³, D.W. Kim ^{47a,47b}, Y.K. Kim ³⁹, N. Kimura ⁹⁶, A. Kirchhoff ⁵⁵, C. Kirfel ²⁴, F. Kirfel ²⁴, J. Kirk ¹³⁴, A.E. Kiryunin ¹¹⁰, C. Kitsaki ¹⁰, O. Kivernyk ²⁴, M. Klassen ^{63a}, C. Klein ³⁴, L. Klein ¹⁶⁶, M.H. Klein ¹⁰⁶, M. Klein ⁹², S.B. Klein ⁵⁶, U. Klein ⁹², P. Klimek ³⁶, A. Klimentov ²⁹, T. Klioutchnikova ³⁶, P. Kluit ¹¹⁴, S. Kluth ¹¹⁰, E. Kneringer ⁷⁹, T.M. Knight ¹⁵⁵, A. Knue ⁵⁴, R. Kobayashi ⁸⁸, S.F. Koch ¹²⁶, M. Kocian ¹⁴³, P. Kodyš ¹³³, D.M. Koeck ¹²³, P.T. Koenig ²⁴, T. Koffas ³⁴, M. Kolb ¹³⁵, I. Koletsou ⁴, T. Komarek ¹²², K. Köneke ⁵⁴, A.X.Y. Kong ¹, T. Kono ¹¹⁸, N. Konstantinidis ⁹⁶, B. Konya ⁹⁸, R. Kopeliansky ⁶⁸, S. Koperny ^{86a}, K. Korcyl ⁸⁷, K. Kordas ^{152,e}, G. Koren ¹⁵¹, A. Korn ⁹⁶, S. Korn ⁵⁵, I. Korolkov ¹³, N. Korotkova ³⁷, B. Kortman ¹¹⁴, O. Kortner ¹¹⁰, S. Kortner ¹¹⁰, W.H. Kostecka ¹¹⁵, V.V. Kostyukhin ¹⁴¹, A. Kotsokechagia ¹³⁵, A. Kotwal ⁵¹, A. Koulouris ³⁶, A. Kourkoumeli-Charalampidi ^{73a,73b}, C. Kourkoumelis ⁹, E. Kourlitis ^{110,ae}, O. Kovanda ¹⁴⁶, R. Kowalewski ¹⁶⁵, W. Kozanecki ¹³⁵, A.S. Kozhin ³⁷, V.A. Kramarenko ³⁷, G. Kramberger ⁹³, P. Kramer ¹⁰⁰, M.W. Krasny ¹²⁷, A. Krasznahorkay ³⁶, J.W. Kraus ¹⁷¹, J.A. Kremer ¹⁰⁰, T. Kresse ⁵⁰, J. Kretschmar ⁹², K. Kreul ¹⁸, P. Krieger ¹⁵⁵, S. Krishnamurthy ¹⁰³, M. Krivos ¹³³, K. Krizka ²⁰, K. Kroeninger ⁴⁹, H. Kroha ¹¹⁰, J. Kroll ¹³¹, J. Kroll ¹²⁸, K.S. Krowpman ¹⁰⁷, U. Kruchonak ³⁸, H. Krüger ²⁴, N. Krumnack ⁸¹, M.C. Kruse ⁵¹, J.A. Krzysiak ⁸⁷, O. Kuchinskaia ³⁷, S. Kuday ^{3a}, S. Kuehn ³⁶, R. Kuesters ⁵⁴, T. Kuhl ⁴⁸, V. Kukhtin ³⁸, Y. Kulchitsky ^{37,a}, S. Kuleshov ^{137d,137b}, M. Kumar ^{33g}, N. Kumari ¹⁰², A. Kupco ¹³¹, T. Kupfer ⁴⁹, A. Kupich ³⁷, O. Kuprash ⁵⁴, H. Kurashige ⁸⁵, L.L. Kurchaninov ^{156a}, O. Kurdysh ⁶⁶, Y.A. Kurochkin ³⁷, A. Kurova ³⁷, M. Kuze ¹⁵⁴, A.K. Kvam ¹⁰³, J. Kvita ¹²², T. Kwan ¹⁰⁴, N.G. Kyriacou ¹⁰⁶, L.A.O. Laatu ¹⁰², C. Lacasta ¹⁶³, F. Lacava ^{75a,75b}, H. Lacker ¹⁸, D. Lacour ¹²⁷, N.N. Lad ⁹⁶, E. Ladygin ³⁸, B. Laforge ¹²⁷, T. Lagouri ^{137e}, S. Lai ⁵⁵, I.K. Lakomic ^{86a}, N. Lalloue ⁶⁰, J.E. Lambert ¹⁶⁵, S. Lammers ⁶⁸, W. Lampl ⁷, C. Lampoudis ^{152,e}, A.N. Lancaster ¹¹⁵, E. Lançon ²⁹, U. Landgraf ⁵⁴, M.P.J. Landon ⁹⁴, V.S. Lang ⁵⁴, R.J. Langenberg ¹⁰³, O.K.B. Langrekken ¹²⁵, A.J. Lankford ¹⁶⁰, F. Lanni ³⁶, K. Lantzsch ²⁴, A. Lanza ^{73a}, A. Lapertosa ^{57b,57a}, J.F. Laporte ¹³⁵, T. Lari ^{71a}, F. Lasagni Manghi ^{23b}, M. Lassnig ³⁶, V. Latonova ¹³¹, A. Laudrain ¹⁰⁰, A. Laurier ¹⁵⁰, S.D. Lawlor ⁹⁵, Z. Lawrence ¹⁰¹, M. Lazzaroni ^{71a,71b}, B. Le ¹⁰¹, E.M. Le Boulicaut ⁵¹, B. Leban ⁹³, A. Lebedev ⁸¹, M. LeBlanc ³⁶, F. Ledroit-Guillon ⁶⁰, A.C.A. Lee ⁹⁶, S.C. Lee ¹⁴⁸, S. Lee ^{47a,47b}, T.F. Lee ⁹², L.L. Leeuw ^{33c}, H.P. Lefebvre ⁹⁵, M. Lefebvre ¹⁶⁵, C. Leggett ^{17a}, G. Lehmann Miotto ³⁶, M. Leigh ⁵⁶, W.A. Leight ¹⁰³, W. Leinonen ¹¹³, A. Leisos ^{152,s}, M.A.L. Leite ^{83c}, C.E. Leitgeb ⁴⁸, R. Leitner ¹³³, K.J.C. Leney ⁴⁴, T. Lenz ²⁴, S. Leone ^{74a}, C. Leonidopoulos ⁵², A. Leopold ¹⁴⁴, C. Leroy ¹⁰⁸, R. Les ¹⁰⁷, C.G. Lester ³², M. Levchenko ³⁷, J. Levêque ⁴, D. Levin ¹⁰⁶, L.J. Levinson ¹⁶⁹, M.P. Lewicki ⁸⁷, D.J. Lewis ⁴, A. Li ⁵, B. Li ^{62b}, C. Li ^{62a}, C-Q. Li ^{62c}, H. Li ^{62a}, H. Li ^{62b}, H. Li ^{14c}, H. Li ^{62b}, K. Li ¹³⁸, L. Li ^{62c}, M. Li ^{14a,14e}, Q.Y. Li ^{62a}, S. Li ^{14a,14e}, S. Li ^{62d,62c,d}, T. Li ⁵, X. Li ¹⁰⁴, Z. Li ¹²⁶, Z. Li ¹⁰⁴, Z. Li ⁹², Z. Li ^{14a,14e}, Z. Liang ^{14a}, M. Liberatore ¹³⁵, B. Liberti ^{76a}, K. Lie ^{64c}, J. Lieber Marin ^{83b}, H. Lien ⁶⁸, K. Lin ¹⁰⁷, R.E. Lindley ⁷, J.H. Lindon ², A. Linss ⁴⁸, E. Lipeles ¹²⁸, A. Lipniacka ¹⁶, A. Lister ¹⁶⁴, J.D. Little ⁴, B. Liu ^{14a}, B.X. Liu ¹⁴², D. Liu ^{62d,62c}, J.B. Liu ^{62a}, J.K.K. Liu ³², K. Liu ^{62d,62c}, M. Liu ^{62a}, M.Y. Liu ^{62a}, P. Liu ^{14a}, Q. Liu ^{62d,138,62c}, X. Liu ^{62a}, Y. Liu ^{14d,14e}, Y.L. Liu ¹⁰⁶, Y.W. Liu ^{62a}, J. Llorente Merino ¹⁴², S.L. Lloyd ⁹⁴, E.M. Lobodzinska ⁴⁸, P. Loch ⁷, S. Loffredo ^{76a,76b}, T. Lohse ¹⁸, K. Lohwasser ¹³⁹, E. Loiacono ⁴⁸, M. Lokajicek ^{131,*}, J.D. Lomas ²⁰,



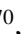














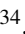

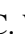




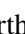


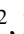






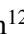
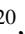













J.D. Long ¹⁶², I. Longarini ¹⁶⁰, L. Longo ^{70a,70b}, R. Longo ¹⁶², I. Lopez Paz ⁶⁷,
A. Lopez Solis ⁴⁸, J. Lorenz ¹⁰⁹, N. Lorenzo Martinez ⁴, A.M. Lory ¹⁰⁹,
G. Löschcke Centeno ¹⁴⁶, O. Loseva ³⁷, X. Lou ^{47a,47b}, X. Lou ^{14a,14e}, A. Lounis ⁶⁶, J. Love ⁶,
P.A. Love ⁹¹, G. Lu ^{14a,14e}, M. Lu ⁸⁰, S. Lu ¹²⁸, Y.J. Lu ⁶⁵, H.J. Lubatti ¹³⁸, C. Luci ^{75a,75b},
F.L. Lucio Alves ^{14c}, A. Lucotte ⁶⁰, F. Luehring ⁶⁸, I. Luise ¹⁴⁵, O. Lukianchuk ⁶⁶,
O. Lundberg ¹⁴⁴, B. Lund-Jensen ¹⁴⁴, N.A. Luongo ¹²³, M.S. Lutz ¹⁵¹, D. Lynn ²⁹, H. Lyons ⁹²,
R. Lysak ¹³¹, E. Lytken ⁹⁸, V. Lyubushkin ³⁸, T. Lyubushkina ³⁸, M.M. Lyukova ¹⁴⁵, H. Ma ²⁹,
K. Ma ^{62a}, L.L. Ma ^{62b}, Y. Ma ¹²¹, D.M. Mac Donell ¹⁶⁵, G. Maccarrone ⁵³, J.C. MacDonald ¹⁰⁰,
R. Madar ⁴⁰, W.F. Mader ⁵⁰, J. Maeda ⁸⁵, T. Maeno ²⁹, M. Maerker ⁵⁰, H. Maguire ¹³⁹,
V. Maiboroda ¹³⁵, A. Maio ^{130a,130b,130d}, K. Maj ^{86a}, O. Majersky ⁴⁸, S. Majewski ¹²³,
N. Makovec ⁶⁶, V. Maksimovic ¹⁵, B. Malaescu ¹²⁷, Pa. Malecki ⁸⁷, V.P. Maleev ³⁷,
F. Malek ⁶⁰, M. Mali ⁹³, D. Malito ⁹⁵, U. Mallik ⁸⁰, S. Maltezos ¹⁰, S. Malyukov ³⁸, J. Mamuzic ¹³,
G. Mancini ⁵³, G. Manco ^{73a,73b}, J.P. Mandalia ⁹⁴, I. Mandić ⁹³,
L. Manhaes de Andrade Filho ^{83a}, I.M. Maniatis ¹⁶⁹, J. Manjarres Ramos ^{102,ab}, D.C. Mankad ¹⁶⁹,
A. Mann ¹⁰⁹, B. Mansoulie ¹³⁵, S. Manzoni ³⁶, A. Marantis ^{152,s}, G. Marchiori ⁵,
M. Marcisovsky ¹³¹, C. Marcon ^{71a}, M. Marinescu ²⁰, M. Marjanovic ¹²⁰, E.J. Marshall ⁹¹,
Z. Marshall ^{17a}, S. Marti-Garcia ¹⁶³, T.A. Martin ¹⁶⁷, V.J. Martin ⁵², B. Martin dit Latour ¹⁶,
L. Martinelli ^{75a,75b}, M. Martinez ^{13,t}, P. Martinez Agullo ¹⁶³, V.I. Martinez Outschoorn ¹⁰³,
P. Martinez Suarez ¹³, S. Martin-Haugh ¹³⁴, V.S. Martoiu ^{27b}, A.C. Martyniuk ⁹⁶, A. Marzin ³⁶,
D. Mascione ^{78a,78b}, L. Masetti ¹⁰⁰, T. Mashimo ¹⁵³, J. Masik ¹⁰¹, A.L. Maslennikov ³⁷,
L. Massa ^{23b}, P. Massarotti ^{72a,72b}, P. Mastrandrea ^{74a,74b}, A. Mastroberardino ^{43b,43a},
T. Masubuchi ¹⁵³, T. Mathisen ¹⁶¹, J. Matousek ¹³³, N. Matsuzawa ¹⁵³, J. Maurer ^{27b}, B. Maček ⁹³,
D.A. Maximov ³⁷, R. Mazini ¹⁴⁸, I. Maznas ¹⁵², M. Mazza ¹⁰⁷, S.M. Mazza ¹³⁶,
E. Mazzeo ^{71a,71b}, C. Mc Ginn ²⁹, J.P. Mc Gowan ¹⁰⁴, S.P. Mc Kee ¹⁰⁶, E.F. McDonald ¹⁰⁵,
A.E. McDougall ¹¹⁴, J.A. Mcfayden ¹⁴⁶, R.P. McGovern ¹²⁸, G. Mchedlidze ^{149b},
R.P. Mckenzie ^{33g}, T.C. Mclachlan ⁴⁸, D.J. Mclaughlin ⁹⁶, K.D. McLean ¹⁶⁵, S.J. McMahon ¹³⁴,
P.C. McNamara ¹⁰⁵, C.M. Mcpartland ⁹², R.A. McPherson ^{165,x}, S. Mehlhase ¹⁰⁹, A. Mehta ⁹²,
D. Melini ¹⁵⁰, B.R. Mellado Garcia ^{33g}, A.H. Melo ⁵⁵, F. Meloni ⁴⁸,
A.M. Mendes Jacques Da Costa ¹⁰¹, H.Y. Meng ¹⁵⁵, L. Meng ⁹¹, S. Menke ¹¹⁰, M. Mentink ³⁶,
E. Meoni ^{43b,43a}, C. Merlassino ¹²⁶, L. Merola ^{72a,72b}, C. Meroni ^{71a,71b}, G. Merz ¹⁰⁶,
O. Meshkov ³⁷, J. Metcalfe ⁶, A.S. Mete ⁶, C. Meyer ⁶⁸, J-P. Meyer ¹³⁵, R.P. Middleton ¹³⁴,
L. Mijović ⁵², G. Mikenberg ¹⁶⁹, M. Mikestikova ¹³¹, M. Mikuž ⁹³, H. Mildner ¹⁰⁰, A. Milic ³⁶,
C.D. Milke ⁴⁴, D.W. Miller ³⁹, L.S. Miller ³⁴, A. Milov ¹⁶⁹, D.A. Milstead ^{47a,47b}, T. Min ^{14c},
A.A. Minaenko ³⁷, I.A. Minashvili ^{149b}, L. Mince ⁵⁹, A.I. Mincer ¹¹⁷, B. Mindur ^{86a},
M. Mineev ³⁸, Y. Mino ⁸⁸, L.M. Mir ¹³, M. Miralles Lopez ¹⁶³, M. Mironova ^{17a}, A. Mishima ¹⁵³,
M.C. Missio ¹¹³, T. Mitani ¹⁶⁸, A. Mitra ¹⁶⁷, V.A. Mitsou ¹⁶³, O. Miu ¹⁵⁵, P.S. Miyagawa ⁹⁴,
Y. Miyazaki ⁸⁹, A. Mizukami ⁸⁴, T. Mkrtchyan ^{63a}, M. Mlinarevic ⁹⁶, T. Mlinarevic ⁹⁶,
M. Mlynarikova ³⁶, S. Mobius ¹⁹, K. Mochizuki ¹⁰⁸, P. Moder ⁴⁸, P. Mogg ¹⁰⁹,
A.F. Mohammed ^{14a,14e}, S. Mohapatra ⁴¹, G. Mokgatitwane ^{33g}, L. Moleri ¹⁶⁹, B. Mondal ¹⁴¹,
S. Mondal ¹³², K. Mönig ⁴⁸, E. Monnier ¹⁰², L. Monsonis Romero ¹⁶³, J. Montejo Berlingen ^{13,84},
M. Montella ¹¹⁹, F. Montereali ^{77a,77b}, F. Monticelli ⁹⁰, S. Monzani ^{69a,69c}, N. Morange ⁶⁶,
A.L. Moreira De Carvalho ^{130a}, M. Moreno Llácer ¹⁶³, C. Moreno Martinez ⁵⁶, P. Morettini ^{57b},
S. Morgenstern ³⁶, M. Morii ⁶¹, M. Morinaga ¹⁵³, A.K. Morley ³⁶, F. Morodei ^{75a,75b},
L. Morvaj ³⁶, P. Moschovakos ³⁶, B. Moser ³⁶, M. Mosidze ^{149b}, T. Moskalets ⁵⁴,
P. Moskvitina ¹¹³, J. Moss ^{31,m}, E.J.W. Moyses ¹⁰³, O. Mtintsilana ^{33g}, S. Muanza ¹⁰²,
J. Mueller ¹²⁹, D. Muenstermann ⁹¹, R. Müller ¹⁹, G.A. Mullier ¹⁶¹, A.J. Mullin ³², J.J. Mullin ¹²⁸,
D.P. Mungo ¹⁵⁵, D. Munoz Perez ¹⁶³, F.J. Munoz Sanchez ¹⁰¹, M. Murin ¹⁰¹, W.J. Murray ^{167,134},

A. Murrone ^{71a,71b}, J.M. Muse ¹²⁰, M. Muškinja ^{17a}, C. Mwewa ²⁹, A.G. Myagkov ^{37,a},
 A.J. Myers ⁸, A.A. Myers ¹²⁹, G. Myers ⁶⁸, M. Myska ¹³², B.P. Nachman ^{17a}, O. Nackenhorst ⁴⁹,
 A. Nag ⁵⁰, K. Nagai ¹²⁶, K. Nagano ⁸⁴, J.L. Nagle ^{29,ai}, E. Nagy ¹⁰², A.M. Nairz ³⁶,
 Y. Nakahama ⁸⁴, K. Nakamura ⁸⁴, K. Nakkalil ⁵, H. Nanjo ¹²⁴, R. Narayan ⁴⁴,
 E.A. Narayanan ¹¹², I. Naryshkin ³⁷, M. Naseri ³⁴, S. Nasri ¹⁵⁹, C. Nass ²⁴, G. Navarro ^{22a},
 J. Navarro-Gonzalez ¹⁶³, R. Nayak ¹⁵¹, A. Nayaz ¹⁸, P.Y. Nechaeva ³⁷, F. Nechansky ⁴⁸,
 L. Nedic ¹²⁶, T.J. Neep ²⁰, A. Negri ^{73a,73b}, M. Negrini ^{23b}, C. Nellist ¹¹⁴, C. Nelson ¹⁰⁴,
 K. Nelson ¹⁰⁶, S. Nemecek ¹³¹, M. Nessi ^{36,h}, M.S. Neubauer ¹⁶², F. Neuhaus ¹⁰⁰,
 J. Neundorff ⁴⁸, R. Newhouse ¹⁶⁴, P.R. Newman ²⁰, C.W. Ng ¹²⁹, Y.W.Y. Ng ⁴⁸, B. Ngair ^{35e},
 H.D.N. Nguyen ¹⁰⁸, R.B. Nickerson ¹²⁶, R. Nicolaidou ¹³⁵, J. Nielsen ¹³⁶, M. Niemeyer ⁵⁵,
 J. Niermann ^{55,36}, N. Nikiforou ³⁶, V. Nikolaenko ^{37,a}, I. Nikolic-Audit ¹²⁷, K. Nikolopoulos ²⁰,
 P. Nilsson ²⁹, I. Ninca ⁴⁸, H.R. Nindhito ⁵⁶, G. Ninio ¹⁵¹, A. Nisati ^{75a}, N. Nishu ²,
 R. Nisius ¹¹⁰, J-E. Nitschke ⁵⁰, E.K. Nkadimeng ^{33g}, S.J. Noacco Rosende ⁹⁰, T. Nobe ¹⁵³,
 D.L. Noel ³², T. Nommensen ¹⁴⁷, M.B. Norfolk ¹³⁹, R.R.B. Norisam ⁹⁶, B.J. Norman ³⁴,
 J. Novak ⁹³, T. Novak ⁴⁸, L. Novotny ¹³², R. Novotny ¹¹², L. Nozka ¹²², K. Ntekas ¹⁶⁰,
 N.M.J. Nunes De Moura Junior ^{83b}, E. Nurse ⁹⁶, J. Ocariz ¹²⁷, A. Ochi ⁸⁵, I. Ochoa ^{130a},
 S. Oerdek ¹⁶¹, J.T. Offermann ³⁹, A. Ogrodnik ¹³³, A. Oh ¹⁰¹, C.C. Ohm ¹⁴⁴, H. Oide ⁸⁴,
 R. Oishi ¹⁵³, M.L. Ojeda ⁴⁸, Y. Okazaki ⁸⁸, M.W. O'Keefe ⁹², Y. Okumura ¹⁵³,
 L.F. Oleiro Seabra ^{130a}, S.A. Olivares Pino ^{137d}, D. Oliveira Damazio ²⁹, D. Oliveira Goncalves ^{83a},
 J.L. Oliver ¹⁶⁰, A. Olszewski ⁸⁷, Ö.O. Öncel ⁵⁴, D.C. O'Neil ¹⁴², A.P. O'Neill ¹⁹,
 A. Onofre ^{130a,130e}, P.U.E. Onyisi ¹¹, M.J. Oreglia ³⁹, G.E. Orellana ⁹⁰, D. Orestano ^{77a,77b},
 N. Orlando ¹³, R.S. Orr ¹⁵⁵, V. O'Shea ⁵⁹, L.M. Osojnak ¹²⁸, R. Ospanov ^{62a},
 G. Otero y Garzon ³⁰, H. Otono ⁸⁹, P.S. Ott ^{63a}, G.J. Ottino ^{17a}, M. Ouchrif ^{35d}, J. Ouellette ²⁹,
 F. Ould-Saada ¹²⁵, M. Owen ⁵⁹, R.E. Owen ¹³⁴, K.Y. Oyulmaz ^{21a}, V.E. Ozcan ^{21a}, N. Ozturk ⁸,
 S. Ozturk ⁸², H.A. Pacey ³², A. Pacheco Pages ¹³, C. Padilla Aranda ¹³, G. Padovano ^{75a,75b},
 S. Pagan Griso ^{17a}, G. Palacino ⁶⁸, A. Palazzo ^{70a,70b}, S. Palestini ³⁶, J. Pan ¹⁷², T. Pan ^{64a},
 D.K. Panchal ¹¹, C.E. Pandini ¹¹⁴, J.G. Panduro Vazquez ⁹⁵, H. Pang ^{14b}, P. Pani ⁴⁸,
 G. Panizzo ^{69a,69c}, L. Paolozzi ⁵⁶, C. Papadatos ¹⁰⁸, S. Parajuli ⁴⁴, A. Paramonov ⁶,
 C. Paraskevopoulos ¹⁰, D. Paredes Hernandez ^{64b}, T.H. Park ¹⁵⁵, M.A. Parker ³², F. Parodi ^{57b,57a},
 E.W. Parrish ¹¹⁵, V.A. Parrish ⁵², J.A. Parsons ⁴¹, U. Parzefall ⁵⁴, B. Pascual Dias ¹⁰⁸,
 L. Pascual Dominguez ¹⁵¹, F. Pasquali ¹¹⁴, E. Pasqualucci ^{75a}, S. Passaggio ^{57b}, F. Pastore ⁹⁵,
 P. Pasuwan ^{47a,47b}, P. Patel ⁸⁷, U.M. Patel ⁵¹, J.R. Pater ¹⁰¹, T. Pauly ³⁶, J. Parkes ¹⁴³,
 M. Pedersen ¹²⁵, R. Pedro ^{130a}, S.V. Peleganchuk ³⁷, O. Penc ³⁶, E.A. Pender ⁵², H. Peng ^{62a},
 K.E. Pensi ¹⁰⁹, M. Penzin ³⁷, B.S. Peralva ^{83d}, A.P. Pereira Peixoto ⁶⁰, L. Pereira Sanchez ^{47a,47b},
 D.V. Perepelitsa ^{29,ai}, E. Perez Codina ^{156a}, M. Perganti ¹⁰, L. Perini ^{71a,71b,*}, H. Pernegger ³⁶,
 O. Perrin ⁴⁰, K. Peters ⁴⁸, R.F.Y. Peters ¹⁰¹, B.A. Petersen ³⁶, T.C. Petersen ⁴², E. Petit ¹⁰²,
 V. Petousis ¹³², C. Petridou ^{152,e}, A. Petrukhin ¹⁴¹, M. Pettee ^{17a}, N.E. Pettersson ³⁶,
 A. Petukhov ³⁷, K. Petukhova ¹³³, A. Peyaud ¹³⁵, R. Pezoa ^{137f}, L. Pezzotti ³⁶, G. Pezzullo ¹⁷²,
 T.M. Pham ¹⁷⁰, T. Pham ¹⁰⁵, P.W. Phillips ¹³⁴, G. Piacquadio ¹⁴⁵, E. Pianori ^{17a},
 F. Piazza ^{71a,71b}, R. Piegai ³⁰, D. Pietreanu ^{27b}, A.D. Pilkington ¹⁰¹, M. Pinamonti ^{69a,69c},
 J.L. Pinfeld ², B.C. Pinheiro Pereira ^{130a}, A.E. Pinto Pinoargote ¹³⁵, K.M. Piper ¹⁴⁶,
 A. Pirttikoski ⁵⁶, C. Pitman Donaldson ⁹⁶, D.A. Pizzi ³⁴, L. Pizzimento ^{64b}, A. Pizzini ¹¹⁴,
 M.-A. Pleier ²⁹, V. Plesanovs ⁵⁴, V. Pleskot ¹³³, E. Plotnikova ³⁸, G. Poddar ⁴, R. Poettgen ⁹⁸,
 L. Poggioli ¹²⁷, I. Pokharel ⁵⁵, S. Polacek ¹³³, G. Polesello ^{73a}, A. Poley ^{142,156a}, R. Polifka ¹³²,
 A. Polini ^{23b}, C.S. Pollard ¹⁶⁷, Z.B. Pollock ¹¹⁹, V. Polychronakos ²⁹, E. Pompa Pacchi ^{75a,75b},
 D. Ponomarenko ¹¹³, L. Pontecorvo ³⁶, S. Popa ^{27a}, G.A. Popeneciu ^{27d}, A. Poreba ³⁶,
 D.M. Portillo Quintero ^{156a}, S. Pospisil ¹³², M.A. Postill ¹³⁹, P. Postolache ^{27c}, K. Potamianos ¹⁶⁷,

P.A. Potepa ^{86a}, I.N. Potrap ³⁸, C.J. Potter ³², H. Potti ¹, T. Poulsen ⁴⁸, J. Poveda ¹⁶³,
 M.E. Pozo Astigarraga ³⁶, A. Prades Ibanez ¹⁶³, J. Pretel ⁵⁴, D. Price ¹⁰¹, M. Primavera ^{70a},
 M.A. Principe Martin ⁹⁹, R. Privara ¹²², T. Procter ⁵⁹, M.L. Proffitt ¹³⁸, N. Proklova ¹²⁸,
 K. Prokofiev ^{64c}, G. Proto ¹¹⁰, S. Protopopescu ²⁹, J. Proudfoot ⁶, M. Przybycien ^{86a},
 W.W. Przygoda ^{86b}, J.E. Puddefoot ¹³⁹, D. Pudzha ³⁷, D. Pyatiizbyantseva ³⁷, J. Qian ¹⁰⁶,
 D. Qichen ¹⁰¹, Y. Qin ¹⁰¹, T. Qiu ⁵², A. Quadt ⁵⁵, M. Queitsch-Maitland ¹⁰¹, G. Quetant ⁵⁶,
 G. Rabanal Bolanos ⁶¹, D. Rafanoharana ⁵⁴, F. Ragusa ^{71a,71b}, J.L. Rainbolt ³⁹, J.A. Raine ⁵⁶,
 S. Rajagopalan ²⁹, E. Ramakoti ³⁷, K. Ran ^{48,14c}, N.P. Rapheeha ^{33g}, H. Rasheed ^{27b},
 V. Raskina ¹²⁷, D.F. Rassloff ^{63a}, S. Rave ¹⁰⁰, B. Ravina ⁵⁵, I. Ravinovich ¹⁶⁹, M. Raymond ³⁶,
 A.L. Read ¹²⁵, N.P. Readioff ¹³⁹, D.M. Rebutzi ^{73a,73b}, G. Redlinger ²⁹, A.S. Reed ¹¹⁰,
 K. Reeves ²⁶, J.A. Reidelsturz ¹⁷¹, D. Reikher ¹⁵¹, A. Rej ¹⁴¹, C. Rembser ³⁶, A. Renardi ⁴⁸,
 M. Renda ^{27b}, M.B. Rendel ¹¹⁰, F. Renner ⁴⁸, A.G. Rennie ⁵⁹, S. Resconi ^{71a},
 M. Ressegotti ^{57b,57a}, S. Rettie ³⁶, J.G. Reyes Rivera ¹⁰⁷, B. Reynolds ¹¹⁹, E. Reynolds ^{17a},
 O.L. Rezanova ³⁷, P. Reznicek ¹³³, N. Ribaric ⁹¹, E. Ricci ^{78a,78b}, R. Richter ¹¹⁰,
 S. Richter ^{47a,47b}, E. Richter-Was ^{86b}, M. Ridel ¹²⁷, S. Ridouani ^{35d}, P. Rieck ¹¹⁷, P. Riedler ³⁶,
 M. Rijssenbeek ¹⁴⁵, A. Rimoldi ^{73a,73b}, M. Rimoldi ⁴⁸, L. Rinaldi ^{23b,23a}, T.T. Rinn ²⁹,
 M.P. Rinnagel ¹⁰⁹, G. Ripellino ¹⁶¹, I. Riu ¹³, P. Rivadeneira ⁴⁸, J.C. Rivera Vergara ¹⁶⁵,
 F. Rizatdinova ¹²¹, E. Rizvi ⁹⁴, B.A. Roberts ¹⁶⁷, B.R. Roberts ^{17a}, S.H. Robertson ^{104,x},
 M. Robin ⁴⁸, D. Robinson ³², C.M. Robles Gajardo ^{137f}, M. Robles Manzano ¹⁰⁰, A. Robson ⁵⁹,
 A. Rocchi ^{76a,76b}, C. Roda ^{74a,74b}, S. Rodriguez Bosca ^{63a}, Y. Rodriguez Garcia ^{22a},
 A. Rodriguez Rodriguez ⁵⁴, A.M. Rodríguez Vera ^{156b}, S. Roe ³⁶, J.T. Roemer ¹⁶⁰,
 A.R. Roepe-Gier ¹³⁶, J. Roggel ¹⁷¹, O. Røhne ¹²⁵, R.A. Rojas ¹⁰³, C.P.A. Roland ⁶⁸, J. Roloff ²⁹,
 A. Romaniouk ³⁷, E. Romano ^{73a,73b}, M. Romano ^{23b}, A.C. Romero Hernandez ¹⁶²,
 N. Rompotis ⁹², L. Roos ¹²⁷, S. Rosati ^{75a}, B.J. Rosser ³⁹, E. Rossi ¹²⁶, E. Rossi ^{72a,72b},
 L.P. Rossi ^{57b}, L. Rossini ⁴⁸, R. Rosten ¹¹⁹, M. Rotaru ^{27b}, B. Rottler ⁵⁴, C. Rougier ^{102,ab},
 D. Rousseau ⁶⁶, D. Rousso ³², A. Roy ¹⁶², S. Roy-Garand ¹⁵⁵, A. Rozanov ¹⁰², Y. Rozen ¹⁵⁰,
 X. Ruan ^{33g}, A. Rubio Jimenez ¹⁶³, A.J. Ruby ⁹², V.H. Ruelas Rivera ¹⁸, T.A. Ruggeri ¹,
 A. Ruggiero ¹²⁶, A. Ruiz-Martinez ¹⁶³, A. Rummler ³⁶, Z. Rurikova ⁵⁴, N.A. Rusakovich ³⁸,
 H.L. Russell ¹⁶⁵, G. Russo ^{75a,75b}, J.P. Rutherford ⁷, S. Rutherford Colmenares ³², K. Rybacki ⁹¹,
 M. Rybar ¹³³, E.B. Rye ¹²⁵, A. Ryzhov ⁴⁴, J.A. Sabater Iglesias ⁵⁶, P. Sabatini ¹⁶³,
 L. Sabetta ^{75a,75b}, H.F-W. Sadrozinski ¹³⁶, F. Safai Tehrani ^{75a}, B. Safarzadeh Samani ¹⁴⁶,
 M. Safdari ¹⁴³, S. Saha ¹⁶⁵, M. Sahinsoy ¹¹⁰, M. Saimpert ¹³⁵, M. Saito ¹⁵³, T. Saito ¹⁵³,
 D. Salamani ³⁶, A. Salnikov ¹⁴³, J. Salt ¹⁶³, A. Salvador Salas ¹³, D. Salvatore ^{43b,43a},
 F. Salvatore ¹⁴⁶, A. Salzburger ³⁶, D. Sammel ⁵⁴, D. Sampsonidis ^{152,e}, D. Sampsonidou ¹²³,
 J. Sánchez ¹⁶³, A. Sanchez Pineda ⁴, V. Sanchez Sebastian ¹⁶³, H. Sandaker ¹²⁵, C.O. Sander ⁴⁸,
 J.A. Sandesara ¹⁰³, M. Sandhoff ¹⁷¹, C. Sandoval ^{22b}, D.P.C. Sankey ¹³⁴, T. Sano ⁸⁸,
 A. Sansoni ⁵³, L. Santi ^{75a,75b}, C. Santoni ⁴⁰, H. Santos ^{130a,130b}, S.N. Santpur ^{17a}, A. Santra ¹⁶⁹,
 K.A. Saoucha ¹³⁹, J.G. Saraiva ^{130a,130d}, J. Sardain ⁷, O. Sasaki ⁸⁴, K. Sato ¹⁵⁷, C. Sauer ^{63b},
 F. Sauerburger ⁵⁴, E. Sauvan ⁴, P. Savard ^{155,ag}, R. Sawada ¹⁵³, C. Sawyer ¹³⁴, L. Sawyer ⁹⁷,
 I. Sayago Galvan ¹⁶³, C. Sbarra ^{23b}, A. Sbrizzi ^{23b,23a}, T. Scanlon ⁹⁶, J. Schaarschmidt ¹³⁸,
 P. Schacht ¹¹⁰, D. Schaefer ³⁹, U. Schäfer ¹⁰⁰, A.C. Schaffer ^{66,44}, D. Schaile ¹⁰⁹,
 R.D. Schamberger ¹⁴⁵, C. Scharf ¹⁸, M.M. Schefer ¹⁹, V.A. Schegelsky ³⁷, D. Scheirich ¹³³,
 F. Schenck ¹⁸, M. Schernau ¹⁶⁰, C. Scheulen ⁵⁵, C. Schiavi ^{57b,57a}, E.J. Schioppa ^{70a,70b},
 M. Schioppa ^{43b,43a}, B. Schlag ^{143,o}, K.E. Schleicher ⁵⁴, S. Schlenker ³⁶, J. Schmeing ¹⁷¹,
 M.A. Schmidt ¹⁷¹, K. Schmieden ¹⁰⁰, C. Schmitt ¹⁰⁰, S. Schmitt ⁴⁸, L. Schoeffel ¹³⁵,
 A. Schoening ^{63b}, P.G. Scholer ⁵⁴, E. Schopf ¹²⁶, M. Schott ¹⁰⁰, J. Schovancova ³⁶,
 S. Schramm ⁵⁶, F. Schroeder ¹⁷¹, T. Schroer ⁵⁶, H-C. Schultz-Coulon ^{63a}, M. Schumacher ⁵⁴,

B.A. Schumm [ID136](#), Ph. Schune [ID135](#), A.J. Schuy [ID138](#), H.R. Schwartz [ID136](#), A. Schwartzman [ID143](#),
 T.A. Schwarz [ID106](#), Ph. Schwemling [ID135](#), R. Schwienhorst [ID107](#), A. Sciandra [ID136](#), G. Sciolla [ID26](#),
 F. Scuri [ID74a](#), C.D. Sebastiani [ID92](#), K. Sedlaczek [ID115](#), P. Seema [ID18](#), S.C. Seidel [ID112](#), A. Seiden [ID136](#),
 B.D. Seidlitz [ID41](#), C. Seitz [ID48](#), J.M. Seixas [ID83b](#), G. Sekhniaidze [ID72a](#), S.J. Sekula [ID44](#), L. Selem [ID60](#),
 N. Semprini-Cesari [ID23b,23a](#), D. Sengupta [ID56](#), V. Senthilkumar [ID163](#), L. Serin [ID66](#), L. Serkin [ID69a,69b](#),
 M. Sessa [ID76a,76b](#), H. Severini [ID120](#), F. Sforza [ID57b,57a](#), A. Sfyrla [ID56](#), E. Shabalina [ID55](#), R. Shaheen [ID144](#),
 J.D. Shahinian [ID128](#), D. Shaked Renous [ID169](#), L.Y. Shan [ID14a](#), M. Shapiro [ID17a](#), A. Sharma [ID36](#),
 A.S. Sharma [ID164](#), P. Sharma [ID80](#), S. Sharma [ID48](#), P.B. Shatalov [ID37](#), K. Shaw [ID146](#), S.M. Shaw [ID101](#),
 A. Shcherbakova [ID37](#), Q. Shen [ID62c,5](#), P. Sherwood [ID96](#), L. Shi [ID96](#), X. Shi [ID14a](#), C.O. Shimmin [ID172](#),
 Y. Shimogama [ID168](#), J.D. Shinner [ID95](#), I.P.J. Shipsey [ID126](#), S. Shirabe [ID56,h](#), M. Shiyakova [ID38,v](#),
 J. Shlomi [ID169](#), M.J. Shochet [ID39](#), J. Shojaii [ID105](#), D.R. Shope [ID125](#), B. Shrestha [ID120](#), S. Shrestha [ID119,aj](#),
 E.M. Shrif [ID33g](#), M.J. Shroff [ID165](#), P. Sicho [ID131](#), A.M. Sickles [ID162](#), E. Sideras Haddad [ID33g](#),
 A. Sidoti [ID23b](#), F. Siegert [ID50](#), Dj. Sijacki [ID15](#), R. Sikora [ID86a](#), F. Sili [ID90](#), J.M. Silva [ID20](#),
 M.V. Silva Oliveira [ID29](#), S.B. Silverstein [ID47a](#), S. Simion [ID66](#), R. Simoniello [ID36](#), E.L. Simpson [ID59](#),
 H. Simpson [ID146](#), L.R. Simpson [ID106](#), N.D. Simpson [ID98](#), S. Simsek [ID82](#), S. Sindhu [ID55](#), P. Sinervo [ID155](#),
 S. Singh [ID155](#), S. Sinha [ID48](#), S. Sinha [ID101](#), M. Sioli [ID23b,23a](#), I. Siral [ID36](#), E. Sitnikova [ID48](#),
 S.Yu. Sivoklov [ID37,*](#), J. Sjölin [ID47a,47b](#), A. Skaf [ID55](#), E. Skorda [ID20](#), P. Skubic [ID120](#), M. Slawinska [ID87](#),
 V. Smakhtin [ID169](#), B.H. Smart [ID134](#), J. Smiesko [ID36](#), S.Yu. Smirnov [ID37](#), Y. Smirnov [ID37](#),
 L.N. Smirnova [ID37,a](#), O. Smirnova [ID98](#), A.C. Smith [ID41](#), E.A. Smith [ID39](#), H.A. Smith [ID126](#),
 J.L. Smith [ID92](#), R. Smith [ID143](#), M. Smizanska [ID91](#), K. Smolek [ID132](#), A.A. Snesarev [ID37](#), S.R. Snider [ID155](#),
 H.L. Snoek [ID114](#), S. Snyder [ID29](#), R. Sobie [ID165,x](#), A. Soffer [ID151](#), C.A. Solans Sanchez [ID36](#),
 E.Yu. Soldatov [ID37](#), U. Soldevila [ID163](#), A.A. Solodkov [ID37](#), S. Solomon [ID26](#), A. Soloshenko [ID38](#),
 K. Solovieva [ID54](#), O.V. Solovyanov [ID40](#), V. Solovyev [ID37](#), P. Sommer [ID36](#), A. Sonay [ID13](#),
 W.Y. Song [ID156b](#), J.M. Sonneveld [ID114](#), A. Sopczak [ID132](#), A.L. Sopio [ID96](#), F. Sopkova [ID28b](#),
 V. Sothilingam [ID63a](#), S. Sottocornola [ID68](#), R. Soualah [ID116b](#), Z. Soumami [ID35e](#), D. South [ID48](#),
 S. Spagnolo [ID70a,70b](#), M. Spalla [ID110](#), D. Sperlich [ID54](#), G. Spigo [ID36](#), M. Spina [ID146](#), S. Spinali [ID91](#),
 D.P. Spiteri [ID59](#), M. Spousta [ID133](#), E.J. Staats [ID34](#), A. Stabile [ID71a,71b](#), R. Stamen [ID63a](#),
 M. Stamenkovic [ID114](#), A. Stampekis [ID20](#), M. Standke [ID24](#), E. Stanecka [ID87](#), M.V. Stange [ID50](#),
 B. Stanislaus [ID17a](#), M.M. Stanitzki [ID48](#), B. Stapf [ID48](#), E.A. Starchenko [ID37](#), G.H. Stark [ID136](#),
 J. Stark [ID102,ab](#), D.M. Starko [ID156b](#), P. Staroba [ID131](#), P. Starovoitov [ID63a](#), S. Stärz [ID104](#), R. Staszewski [ID87](#),
 G. Stavropoulos [ID46](#), J. Steentoft [ID161](#), P. Steinberg [ID29](#), B. Stelzer [ID142,156a](#), H.J. Stelzer [ID129](#),
 O. Stelzer-Chilton [ID156a](#), H. Stenzel [ID58](#), T.J. Stevenson [ID146](#), G.A. Stewart [ID36](#), J.R. Stewart [ID121](#),
 M.C. Stockton [ID36](#), G. Stoicea [ID27b](#), M. Stolarski [ID130a](#), S. Stonjek [ID110](#), A. Straessner [ID50](#),
 J. Strandberg [ID144](#), S. Strandberg [ID47a,47b](#), M. Strauss [ID120](#), T. Strebler [ID102](#), P. Strizenec [ID28b](#),
 R. Ströhmer [ID166](#), D.M. Strom [ID123](#), L.R. Strom [ID48](#), R. Stroynowski [ID44](#), A. Strubig [ID47a,47b](#),
 S.A. Stucci [ID29](#), B. Stugu [ID16](#), J. Stupak [ID120](#), N.A. Styles [ID48](#), D. Su [ID143](#), S. Su [ID62a](#), W. Su [ID62d](#),
 X. Su [ID62a,66](#), K. Sugizaki [ID153](#), V.V. Sulin [ID37](#), M.J. Sullivan [ID92](#), D.M.S. Sultan [ID78a,78b](#),
 L. Sultanaliev [ID37](#), S. Sultansoy [ID3b](#), T. Sumida [ID88](#), S. Sun [ID106](#), S. Sun [ID170](#),
 O. Sunneborn Gudnadottir [ID161](#), N. Sur [ID102](#), M.R. Sutton [ID146](#), H. Suzuki [ID157](#), M. Svatos [ID131](#),
 M. Swiatlowski [ID156a](#), T. Swirski [ID166](#), I. Sykora [ID28a](#), M. Sykora [ID133](#), T. Sykora [ID133](#), D. Ta [ID100](#),
 K. Tackmann [ID48,u](#), A. Taffard [ID160](#), R. Tafirout [ID156a](#), J.S. Tafoya Vargas [ID66](#), E.P. Takeva [ID52](#),
 Y. Takubo [ID84](#), M. Talby [ID102](#), A.A. Talyshev [ID37](#), K.C. Tam [ID64b](#), N.M. Tamir [ID151](#), A. Tanaka [ID153](#),
 J. Tanaka [ID153](#), R. Tanaka [ID66](#), M. Tanasini [ID57b,57a](#), Z. Tao [ID164](#), S. Tapia Araya [ID137f](#),
 S. Tapprogge [ID100](#), A. Tarek Abouelfadl Mohamed [ID107](#), S. Tarem [ID150](#), K. Tariq [ID14a](#), G. Tarna [ID102,27b](#),
 G.F. Tartarelli [ID71a](#), P. Tas [ID133](#), M. Tasevsky [ID131](#), E. Tassi [ID43b,43a](#), A.C. Tate [ID162](#), G. Tateno [ID153](#),
 Y. Tayalati [ID35e,w](#), G.N. Taylor [ID105](#), W. Taylor [ID156b](#), H. Teagle [ID92](#), A.S. Tee [ID170](#),
 R. Teixeira De Lima [ID143](#), P. Teixeira-Dias [ID95](#), J.J. Teoh [ID155](#), K. Terashi [ID153](#), J. Terron [ID99](#),

S. Terzo ¹³, M. Testa ⁵³, R.J. Teuscher ^{155,x}, A. Thaler ⁷⁹, O. Theiner ⁵⁶, N. Themistokleous ⁵²,
 T. Thevenaux-Pelzer ¹⁰², O. Thielmann ¹⁷¹, D.W. Thomas ⁹⁵, J.P. Thomas ²⁰, E.A. Thompson ^{17a},
 P.D. Thompson ²⁰, E. Thomson ¹²⁸, Y. Tian ⁵⁵, V. Tikhomirov ^{37,a}, Yu.A. Tikhonov ³⁷,
 S. Timoshenko ³⁷, D. Timoshyn ¹³³, E.X.L. Ting ¹, P. Tipton ¹⁷², S.H. Tlou ^{33g}, A. Tnourji ⁴⁰,
 K. Todome ^{23b,23a}, S. Todorova-Nova ¹³³, S. Todt ⁵⁰, M. Togawa ⁸⁴, J. Tojo ⁸⁹, S. Tokár ^{28a},
 K. Tokushuku ⁸⁴, O. Toldaiev ⁶⁸, R. Tombs ³², M. Tomoto ^{84,111}, L. Tompkins ^{143,o},
 K.W. Topolnicki ^{86b}, E. Torrence ¹²³, H. Torres ^{102,ab}, E. Torró Pastor ¹⁶³, M. Toscani ³⁰,
 C. Toscirì ³⁹, M. Tost ¹¹, D.R. Tovey ¹³⁹, A. Traeet ¹⁶, I.S. Trandafir ^{27b}, T. Trefzger ¹⁶⁶,
 A. Tricoli ²⁹, I.M. Trigger ^{156a}, S. Trincaz-Duvold ¹²⁷, D.A. Trischuk ²⁶, B. Trocmé ⁶⁰,
 C. Troncon ^{71a}, L. Truong ^{33c}, M. Trzebinski ⁸⁷, A. Trzupiek ⁸⁷, F. Tsai ¹⁴⁵, M. Tsai ¹⁰⁶,
 A. Tsiamis ^{152,e}, P.V. Tsiarehka ³⁷, S. Tsigaridas ^{156a}, A. Tsirigotis ^{152,s}, V. Tsiskaridze ¹⁵⁵,
 E.G. Tskhadadze ^{149a}, M. Tsopoulou ^{152,e}, Y. Tsujikawa ⁸⁸, I.I. Tsukerman ³⁷, V. Tsulaia ^{17a},
 S. Tsuno ⁸⁴, O. Tsur ¹⁵⁰, K. Tsurì ¹¹⁸, D. Tsybychev ¹⁴⁵, Y. Tu ^{64b}, A. Tudorache ^{27b},
 V. Tudorache ^{27b}, A.N. Tuna ³⁶, S. Turchikhin ³⁸, I. Turk Cakir ^{3a}, R. Turra ^{71a},
 T. Turtuvshin ^{38,y}, P.M. Tuts ⁴¹, S. Tzamarias ^{152,e}, P. Tzanis ¹⁰, E. Tzovara ¹⁰⁰, K. Uchida ¹⁵³,
 F. Ukegawa ¹⁵⁷, P.A. Ulloa Poblete ^{137c,137b}, E.N. Umaka ²⁹, G. Unal ³⁶, M. Unal ¹¹,
 A. Undrus ²⁹, G. Unel ¹⁶⁰, J. Urban ^{28b}, P. Urquijo ¹⁰⁵, G. Usai ⁸, R. Ushioda ¹⁵⁴,
 M. Usman ¹⁰⁸, Z. Uysal ^{21b}, L. Vacavant ¹⁰², V. Vacek ¹³², B. Vachon ¹⁰⁴, K.O.H. Vadla ¹²⁵,
 T. Vafeiadis ³⁶, A. Vaitkus ⁹⁶, C. Valderanis ¹⁰⁹, E. Valdes Santurio ^{47a,47b}, M. Valente ^{156a},
 S. Valentinetti ^{23b,23a}, A. Valero ¹⁶³, E. Valiente Moreno ¹⁶³, A. Vallier ^{102,ab},
 J.A. Valls Ferrer ¹⁶³, D.R. Van Arneman ¹¹⁴, T.R. Van Daalen ¹³⁸, A. Van Der Graaf ⁴⁹,
 P. Van Gemmeren ⁶, M. Van Rijnbach ^{125,36}, S. Van Stroud ⁹⁶, I. Van Vulpen ¹¹⁴,
 M. Vanadia ^{76a,76b}, W. Vandelli ³⁶, M. Vandenbroucke ¹³⁵, E.R. Vandewall ¹²¹, D. Vannicola ¹⁵¹,
 L. Vannoli ^{57b,57a}, R. Vari ^{75a}, E.W. Varnes ⁷, C. Varni ^{17b}, T. Varol ¹⁴⁸, D. Varouchas ⁶⁶,
 L. Varriale ¹⁶³, K.E. Varvell ¹⁴⁷, M.E. Vasile ^{27b}, L. Vaslin ⁴⁰, G.A. Vasquez ¹⁶⁵, F. Vazeille ⁴⁰,
 T. Vazquez Schroeder ³⁶, J. Veatch ³¹, V. Vecchio ¹⁰¹, M.J. Veen ¹⁰³, I. Veliscek ¹²⁶,
 L.M. Veloce ¹⁵⁵, F. Veloso ^{130a,130c}, S. Veneziano ^{75a}, A. Ventura ^{70a,70b}, A. Verbytskyi ¹¹⁰,
 M. Verducci ^{74a,74b}, C. Vergis ²⁴, M. Verissimo De Araujo ^{83b}, W. Verkerke ¹¹⁴,
 J.C. Vermeulen ¹¹⁴, C. Vernieri ¹⁴³, M. Vessella ¹⁰³, M.C. Vetterli ^{142,ag}, A. Vgenopoulos ^{152,e},
 N. Viaux Maira ^{137f}, T. Vickey ¹³⁹, O.E. Vickey Boeriu ¹³⁹, G.H.A. Viehhauser ¹²⁶, L. Vignani ^{63b},
 M. Villa ^{23b,23a}, M. Villaplana Perez ¹⁶³, E.M. Villhauer ⁵², E. Vilucchi ⁵³, M.G. Vincter ³⁴,
 G.S. Virdee ²⁰, A. Vishwakarma ⁵², A. Visibile ¹¹⁴, C. Vittori ³⁶, I. Vivarelli ¹⁴⁶, V. Vladimirov ¹⁶⁷,
 E. Voevodina ¹¹⁰, F. Vogel ¹⁰⁹, P. Vokac ¹³², J. Von Ahnen ⁴⁸, E. Von Toerne ²⁴,
 B. Vormwald ³⁶, V. Vorobel ¹³³, K. Vorobev ³⁷, M. Vos ¹⁶³, K. Voss ¹⁴¹, J.H. Vossebeld ⁹²,
 M. Vozak ¹¹⁴, L. Vozdecky ⁹⁴, N. Vranjes ¹⁵, M. Vranjes Milosavljevic ¹⁵, M. Vreeswijk ¹¹⁴,
 R. Vuillermet ³⁶, O. Vujinovic ¹⁰⁰, I. Vukotic ³⁹, S. Wada ¹⁵⁷, C. Wagner ¹⁰³, J.M. Wagner ^{17a},
 W. Wagner ¹⁷¹, S. Wahdan ¹⁷¹, H. Wahlberg ⁹⁰, R. Wakasa ¹⁵⁷, M. Wakida ¹¹¹, J. Walder ¹³⁴,
 R. Walker ¹⁰⁹, W. Walkowiak ¹⁴¹, A. Wall ¹²⁸, T. Wamorkar ⁶, A.Z. Wang ¹⁷⁰, C. Wang ¹⁰⁰,
 C. Wang ^{62c}, H. Wang ^{17a}, J. Wang ^{64a}, R.-J. Wang ¹⁰⁰, R. Wang ⁶¹, R. Wang ⁶,
 S.M. Wang ¹⁴⁸, S. Wang ^{62b}, T. Wang ^{62a}, W.T. Wang ⁸⁰, W. Wang ^{14a}, X. Wang ^{14c},
 X. Wang ¹⁶², X. Wang ^{62c}, Y. Wang ^{62d}, Y. Wang ^{14c}, Z. Wang ¹⁰⁶, Z. Wang ^{62d,51,62c},
 Z. Wang ¹⁰⁶, A. Warburton ¹⁰⁴, R.J. Ward ²⁰, N. Warrack ⁵⁹, A.T. Watson ²⁰, H. Watson ⁵⁹,
 M.F. Watson ²⁰, E. Watton ^{59,134}, G. Watts ¹³⁸, B.M. Waugh ⁹⁶, C. Weber ²⁹, H.A. Weber ¹⁸,
 M.S. Weber ¹⁹, S.M. Weber ^{63a}, C. Wei ^{62a}, Y. Wei ¹²⁶, A.R. Weidberg ¹²⁶, E.J. Weik ¹¹⁷,
 J. Weingarten ⁴⁹, M. Weirich ¹⁰⁰, C. Weiser ⁵⁴, C.J. Wells ⁴⁸, T. Wenaus ²⁹, B. Wendland ⁴⁹,
 T. Wengler ³⁶, N.S. Wenke ¹¹⁰, N. Wermes ²⁴, M. Wessels ^{63a}, K. Whalen ¹²³, A.M. Wharton ⁹¹,
 A.S. White ⁶¹, A. White ⁸, M.J. White ¹, D. Whiteson ¹⁶⁰, L. Wickremasinghe ¹²⁴,

W. Wiedenmann ¹⁷⁰, C. Wiel ⁵⁰, M. Wielers ¹³⁴, C. Wiglesworth ⁴², D.J. Wilbern ¹²⁰, H.G. Wilkens ³⁶, D.M. Williams ⁴¹, H.H. Williams ¹²⁸, S. Williams ³², S. Willocq ¹⁰³, B.J. Wilson ¹⁰¹, P.J. Windischhofer ³⁹, F.I. Winkel ³⁰, F. Winklmeier ¹²³, B.T. Winter ⁵⁴, J.K. Winter ¹⁰¹, M. Wittgen ¹⁴³, M. Wobisch ⁹⁷, Z. Wolffs ¹¹⁴, R. Wölker ¹²⁶, J. Wollrath ¹⁶⁰, M.W. Wolter ⁸⁷, H. Wolters ^{130a,130c}, A.F. Wongel ⁴⁸, S.D. Worm ⁴⁸, B.K. Wosiek ⁸⁷, K.W. Woźniak ⁸⁷, S. Wozniewski ⁵⁵, K. Wraight ⁵⁹, C. Wu ²⁰, J. Wu ^{14a,14e}, M. Wu ^{64a}, M. Wu ¹¹³, S.L. Wu ¹⁷⁰, X. Wu ⁵⁶, Y. Wu ^{62a}, Z. Wu ¹³⁵, J. Wuerzinger ^{110,ae}, T.R. Wyatt ¹⁰¹, B.M. Wynne ⁵², S. Xella ⁴², L. Xia ^{14c}, M. Xia ^{14b}, J. Xiang ^{64c}, X. Xiao ¹⁰⁶, M. Xie ^{62a}, X. Xie ^{62a}, S. Xin ^{14a,14e}, J. Xiong ^{17a}, D. Xu ^{14a}, H. Xu ^{62a}, L. Xu ^{62a}, R. Xu ¹²⁸, T. Xu ¹⁰⁶, Y. Xu ^{14b}, Z. Xu ⁵², Z. Xu ^{14a}, B. Yabsley ¹⁴⁷, S. Yacoob ^{33a}, N. Yamaguchi ⁸⁹, Y. Yamaguchi ¹⁵⁴, E. Yamashita ¹⁵³, H. Yamauchi ¹⁵⁷, T. Yamazaki ^{17a}, Y. Yamazaki ⁸⁵, J. Yan ^{62c}, S. Yan ¹²⁶, Z. Yan ²⁵, H.J. Yang ^{62c,62d}, H.T. Yang ^{62a}, S. Yang ^{62a}, T. Yang ^{64c}, X. Yang ^{62a}, X. Yang ^{14a}, Y. Yang ⁴⁴, Y. Yang ^{62a}, Z. Yang ^{62a}, W-M. Yao ^{17a}, Y.C. Yap ⁴⁸, H. Ye ^{14c}, H. Ye ⁵⁵, J. Ye ⁴⁴, S. Ye ²⁹, X. Ye ^{62a}, Y. Yeh ⁹⁶, I. Yeletsikh ³⁸, B.K. Yeo ^{17b}, M.R. Yexley ⁹⁶, P. Yin ⁴¹, K. Yorita ¹⁶⁸, S. Younas ^{27b}, C.J.S. Young ³⁶, C. Young ¹⁴³, Y. Yu ^{62a}, M. Yuan ¹⁰⁶, R. Yuan ^{62b,k}, L. Yue ⁹⁶, M. Zaazoua ^{62a}, B. Zabinski ⁸⁷, E. Zaid ⁵², T. Zakareishvili ^{149b}, N. Zakharchuk ³⁴, S. Zambito ⁵⁶, J.A. Zamora Saa ^{137d,137b}, J. Zang ¹⁵³, D. Zanzi ⁵⁴, O. Zaplatilek ¹³², C. Zeitnitz ¹⁷¹, H. Zeng ^{14a}, J.C. Zeng ¹⁶², D.T. Zenger Jr ²⁶, O. Zenin ³⁷, T. Ženiš ^{28a}, S. Zenz ⁹⁴, S. Zerradi ^{35a}, D. Zerwas ⁶⁶, M. Zhai ^{14a,14e}, B. Zhang ^{14c}, D.F. Zhang ¹³⁹, J. Zhang ^{62b}, J. Zhang ⁶, K. Zhang ^{14a,14e}, L. Zhang ^{14c}, P. Zhang ^{14a,14e}, R. Zhang ¹⁷⁰, S. Zhang ¹⁰⁶, T. Zhang ¹⁵³, X. Zhang ^{62c}, X. Zhang ^{62b}, Y. Zhang ^{62c,5}, Y. Zhang ⁹⁶, Z. Zhang ^{17a}, Z. Zhang ⁶⁶, H. Zhao ¹³⁸, P. Zhao ⁵¹, T. Zhao ^{62b}, Y. Zhao ¹³⁶, Z. Zhao ^{62a}, A. Zhemchugov ³⁸, K. Zheng ¹⁶², X. Zheng ^{62a}, Z. Zheng ¹⁴³, D. Zhong ¹⁶², B. Zhou ¹⁰⁶, H. Zhou ⁷, N. Zhou ^{62c}, Y. Zhou ⁷, C.G. Zhu ^{62b}, J. Zhu ¹⁰⁶, Y. Zhu ^{62c}, Y. Zhu ^{62a}, X. Zhuang ^{14a}, K. Zhukov ³⁷, V. Zhulanov ³⁷, N.I. Zimine ³⁸, J. Zinsser ^{63b}, M. Ziolkowski ¹⁴¹, L. Živković ¹⁵, A. Zoccoli ^{23b,23a}, K. Zoch ⁵⁶, T.G. Zorbas ¹³⁹, O. Zormpa ⁴⁶, W. Zou ⁴¹, L. Zwalinski ³⁶.

¹Department of Physics, University of Adelaide, Adelaide; Australia.

²Department of Physics, University of Alberta, Edmonton AB; Canada.

³(^a)Department of Physics, Ankara University, Ankara; (^b)Division of Physics, TOBB University of Economics and Technology, Ankara; Türkiye.

⁴LAPP, Université Savoie Mont Blanc, CNRS/IN2P3, Annecy; France.

⁵APC, Université Paris Cité, CNRS/IN2P3, Paris; France.

⁶High Energy Physics Division, Argonne National Laboratory, Argonne IL; United States of America.

⁷Department of Physics, University of Arizona, Tucson AZ; United States of America.

⁸Department of Physics, University of Texas at Arlington, Arlington TX; United States of America.

⁹Physics Department, National and Kapodistrian University of Athens, Athens; Greece.

¹⁰Physics Department, National Technical University of Athens, Zografou; Greece.

¹¹Department of Physics, University of Texas at Austin, Austin TX; United States of America.

¹²Institute of Physics, Azerbaijan Academy of Sciences, Baku; Azerbaijan.

¹³Institut de Física d'Altes Energies (IFAE), Barcelona Institute of Science and Technology, Barcelona; Spain.

¹⁴(^a)Institute of High Energy Physics, Chinese Academy of Sciences, Beijing; (^b)Physics Department, Tsinghua University, Beijing; (^c)Department of Physics, Nanjing University, Nanjing; (^d)School of Science, Shenzhen Campus of Sun Yat-sen University; (^e)University of Chinese Academy of Science (UCAS), Beijing; China.

- ¹⁵Institute of Physics, University of Belgrade, Belgrade; Serbia.
- ¹⁶Department for Physics and Technology, University of Bergen, Bergen; Norway.
- ¹⁷(^a)Physics Division, Lawrence Berkeley National Laboratory, Berkeley CA;(^b)University of California, Berkeley CA; United States of America.
- ¹⁸Institut für Physik, Humboldt Universität zu Berlin, Berlin; Germany.
- ¹⁹Albert Einstein Center for Fundamental Physics and Laboratory for High Energy Physics, University of Bern, Bern; Switzerland.
- ²⁰School of Physics and Astronomy, University of Birmingham, Birmingham; United Kingdom.
- ²¹(^a)Department of Physics, Bogazici University, Istanbul;(^b)Department of Physics Engineering, Gaziantep University, Gaziantep;(^c)Department of Physics, Istanbul University, Istanbul; Türkiye.
- ²²(^a)Facultad de Ciencias y Centro de Investigaciones, Universidad Antonio Nariño, Bogotá;(^b)Departamento de Física, Universidad Nacional de Colombia, Bogotá; Colombia.
- ²³(^a)Dipartimento di Fisica e Astronomia A. Righi, Università di Bologna, Bologna;(^b)INFN Sezione di Bologna; Italy.
- ²⁴Physikalisches Institut, Universität Bonn, Bonn; Germany.
- ²⁵Department of Physics, Boston University, Boston MA; United States of America.
- ²⁶Department of Physics, Brandeis University, Waltham MA; United States of America.
- ²⁷(^a)Transilvania University of Brasov, Brasov;(^b)Horia Hulubei National Institute of Physics and Nuclear Engineering, Bucharest;(^c)Department of Physics, Alexandru Ioan Cuza University of Iasi, Iasi;(^d)National Institute for Research and Development of Isotopic and Molecular Technologies, Physics Department, Cluj-Napoca;(^e)National University of Science and Technology Politehnica, Bucharest;(^f)West University in Timisoara, Timisoara;(^g)Faculty of Physics, University of Bucharest, Bucharest; Romania.
- ²⁸(^a)Faculty of Mathematics, Physics and Informatics, Comenius University, Bratislava;(^b)Department of Subnuclear Physics, Institute of Experimental Physics of the Slovak Academy of Sciences, Kosice; Slovak Republic.
- ²⁹Physics Department, Brookhaven National Laboratory, Upton NY; United States of America.
- ³⁰Universidad de Buenos Aires, Facultad de Ciencias Exactas y Naturales, Departamento de Física, y CONICET, Instituto de Física de Buenos Aires (IFIBA), Buenos Aires; Argentina.
- ³¹California State University, CA; United States of America.
- ³²Cavendish Laboratory, University of Cambridge, Cambridge; United Kingdom.
- ³³(^a)Department of Physics, University of Cape Town, Cape Town;(^b)iThemba Labs, Western Cape;(^c)Department of Mechanical Engineering Science, University of Johannesburg, Johannesburg;(^d)National Institute of Physics, University of the Philippines Diliman (Philippines);(^e)University of South Africa, Department of Physics, Pretoria;(^f)University of Zululand, KwaDlangezwa;(^g)School of Physics, University of the Witwatersrand, Johannesburg; South Africa.
- ³⁴Department of Physics, Carleton University, Ottawa ON; Canada.
- ³⁵(^a)Faculté des Sciences Ain Chock, Réseau Universitaire de Physique des Hautes Energies - Université Hassan II, Casablanca;(^b)Faculté des Sciences, Université Ibn-Tofail, Kénitra;(^c)Faculté des Sciences Semlalia, Université Cadi Ayyad, LPHEA-Marrakech;(^d)LPMR, Faculté des Sciences, Université Mohamed Premier, Oujda;(^e)Faculté des sciences, Université Mohammed V, Rabat;(^f)Institute of Applied Physics, Mohammed VI Polytechnic University, Ben Guerir; Morocco.
- ³⁶CERN, Geneva; Switzerland.
- ³⁷Affiliated with an institute covered by a cooperation agreement with CERN.
- ³⁸Affiliated with an international laboratory covered by a cooperation agreement with CERN.
- ³⁹Enrico Fermi Institute, University of Chicago, Chicago IL; United States of America.
- ⁴⁰LPC, Université Clermont Auvergne, CNRS/IN2P3, Clermont-Ferrand; France.
- ⁴¹Nevis Laboratory, Columbia University, Irvington NY; United States of America.

- ⁴²Niels Bohr Institute, University of Copenhagen, Copenhagen; Denmark.
- ⁴³(^a)Dipartimento di Fisica, Università della Calabria, Rende; (^b)INFN Gruppo Collegato di Cosenza, Laboratori Nazionali di Frascati; Italy.
- ⁴⁴Physics Department, Southern Methodist University, Dallas TX; United States of America.
- ⁴⁵Physics Department, University of Texas at Dallas, Richardson TX; United States of America.
- ⁴⁶National Centre for Scientific Research "Demokritos", Agia Paraskevi; Greece.
- ⁴⁷(^a)Department of Physics, Stockholm University; (^b)Oskar Klein Centre, Stockholm; Sweden.
- ⁴⁸Deutsches Elektronen-Synchrotron DESY, Hamburg and Zeuthen; Germany.
- ⁴⁹Fakultät Physik , Technische Universität Dortmund, Dortmund; Germany.
- ⁵⁰Institut für Kern- und Teilchenphysik, Technische Universität Dresden, Dresden; Germany.
- ⁵¹Department of Physics, Duke University, Durham NC; United States of America.
- ⁵²SUPA - School of Physics and Astronomy, University of Edinburgh, Edinburgh; United Kingdom.
- ⁵³INFN e Laboratori Nazionali di Frascati, Frascati; Italy.
- ⁵⁴Physikalisches Institut, Albert-Ludwigs-Universität Freiburg, Freiburg; Germany.
- ⁵⁵II. Physikalisches Institut, Georg-August-Universität Göttingen, Göttingen; Germany.
- ⁵⁶Département de Physique Nucléaire et Corpusculaire, Université de Genève, Genève; Switzerland.
- ⁵⁷(^a)Dipartimento di Fisica, Università di Genova, Genova; (^b)INFN Sezione di Genova; Italy.
- ⁵⁸II. Physikalisches Institut, Justus-Liebig-Universität Giessen, Giessen; Germany.
- ⁵⁹SUPA - School of Physics and Astronomy, University of Glasgow, Glasgow; United Kingdom.
- ⁶⁰LPSC, Université Grenoble Alpes, CNRS/IN2P3, Grenoble INP, Grenoble; France.
- ⁶¹Laboratory for Particle Physics and Cosmology, Harvard University, Cambridge MA; United States of America.
- ⁶²(^a)Department of Modern Physics and State Key Laboratory of Particle Detection and Electronics, University of Science and Technology of China, Hefei; (^b)Institute of Frontier and Interdisciplinary Science and Key Laboratory of Particle Physics and Particle Irradiation (MOE), Shandong University, Qingdao; (^c)School of Physics and Astronomy, Shanghai Jiao Tong University, Key Laboratory for Particle Astrophysics and Cosmology (MOE), SKLPPC, Shanghai; (^d)Tsun-Dao Lee Institute, Shanghai; China.
- ⁶³(^a)Kirchhoff-Institut für Physik, Ruprecht-Karls-Universität Heidelberg, Heidelberg; (^b)Physikalisches Institut, Ruprecht-Karls-Universität Heidelberg, Heidelberg; Germany.
- ⁶⁴(^a)Department of Physics, Chinese University of Hong Kong, Shatin, N.T., Hong Kong; (^b)Department of Physics, University of Hong Kong, Hong Kong; (^c)Department of Physics and Institute for Advanced Study, Hong Kong University of Science and Technology, Clear Water Bay, Kowloon, Hong Kong; China.
- ⁶⁵Department of Physics, National Tsing Hua University, Hsinchu; Taiwan.
- ⁶⁶IJCLab, Université Paris-Saclay, CNRS/IN2P3, 91405, Orsay; France.
- ⁶⁷Centro Nacional de Microelectrónica (IMB-CNM-CSIC), Barcelona; Spain.
- ⁶⁸Department of Physics, Indiana University, Bloomington IN; United States of America.
- ⁶⁹(^a)INFN Gruppo Collegato di Udine, Sezione di Trieste, Udine; (^b)ICTP, Trieste; (^c)Dipartimento Politecnico di Ingegneria e Architettura, Università di Udine, Udine; Italy.
- ⁷⁰(^a)INFN Sezione di Lecce; (^b)Dipartimento di Matematica e Fisica, Università del Salento, Lecce; Italy.
- ⁷¹(^a)INFN Sezione di Milano; (^b)Dipartimento di Fisica, Università di Milano, Milano; Italy.
- ⁷²(^a)INFN Sezione di Napoli; (^b)Dipartimento di Fisica, Università di Napoli, Napoli; Italy.
- ⁷³(^a)INFN Sezione di Pavia; (^b)Dipartimento di Fisica, Università di Pavia, Pavia; Italy.
- ⁷⁴(^a)INFN Sezione di Pisa; (^b)Dipartimento di Fisica E. Fermi, Università di Pisa, Pisa; Italy.
- ⁷⁵(^a)INFN Sezione di Roma; (^b)Dipartimento di Fisica, Sapienza Università di Roma, Roma; Italy.
- ⁷⁶(^a)INFN Sezione di Roma Tor Vergata; (^b)Dipartimento di Fisica, Università di Roma Tor Vergata, Roma; Italy.
- ⁷⁷(^a)INFN Sezione di Roma Tre; (^b)Dipartimento di Matematica e Fisica, Università Roma Tre, Roma;

Italy.

^{78(a)}INFN-TIFPA;^(b)Università degli Studi di Trento, Trento; Italy.

⁷⁹Universität Innsbruck, Department of Astro and Particle Physics, Innsbruck; Austria.

⁸⁰University of Iowa, Iowa City IA; United States of America.

⁸¹Department of Physics and Astronomy, Iowa State University, Ames IA; United States of America.

⁸²Istinye University, Sariyer, Istanbul; Türkiye.

^{83(a)}Departamento de Engenharia Elétrica, Universidade Federal de Juiz de Fora (UFJF), Juiz de Fora;^(b)Universidade Federal do Rio De Janeiro COPPE/EE/IF, Rio de Janeiro;^(c)Instituto de Física, Universidade de São Paulo, São Paulo;^(d)Rio de Janeiro State University, Rio de Janeiro; Brazil.

⁸⁴KEK, High Energy Accelerator Research Organization, Tsukuba; Japan.

⁸⁵Graduate School of Science, Kobe University, Kobe; Japan.

^{86(a)}AGH University of Krakow, Faculty of Physics and Applied Computer Science, Krakow;^(b)Marian Smoluchowski Institute of Physics, Jagiellonian University, Krakow; Poland.

⁸⁷Institute of Nuclear Physics Polish Academy of Sciences, Krakow; Poland.

⁸⁸Faculty of Science, Kyoto University, Kyoto; Japan.

⁸⁹Research Center for Advanced Particle Physics and Department of Physics, Kyushu University, Fukuoka ; Japan.

⁹⁰Instituto de Física La Plata, Universidad Nacional de La Plata and CONICET, La Plata; Argentina.

⁹¹Physics Department, Lancaster University, Lancaster; United Kingdom.

⁹²Oliver Lodge Laboratory, University of Liverpool, Liverpool; United Kingdom.

⁹³Department of Experimental Particle Physics, Jožef Stefan Institute and Department of Physics, University of Ljubljana, Ljubljana; Slovenia.

⁹⁴School of Physics and Astronomy, Queen Mary University of London, London; United Kingdom.

⁹⁵Department of Physics, Royal Holloway University of London, Egham; United Kingdom.

⁹⁶Department of Physics and Astronomy, University College London, London; United Kingdom.

⁹⁷Louisiana Tech University, Ruston LA; United States of America.

⁹⁸Fysiska institutionen, Lunds universitet, Lund; Sweden.

⁹⁹Departamento de Física Teórica C-15 and CIAFF, Universidad Autónoma de Madrid, Madrid; Spain.

¹⁰⁰Institut für Physik, Universität Mainz, Mainz; Germany.

¹⁰¹School of Physics and Astronomy, University of Manchester, Manchester; United Kingdom.

¹⁰²CPPM, Aix-Marseille Université, CNRS/IN2P3, Marseille; France.

¹⁰³Department of Physics, University of Massachusetts, Amherst MA; United States of America.

¹⁰⁴Department of Physics, McGill University, Montreal QC; Canada.

¹⁰⁵School of Physics, University of Melbourne, Victoria; Australia.

¹⁰⁶Department of Physics, University of Michigan, Ann Arbor MI; United States of America.

¹⁰⁷Department of Physics and Astronomy, Michigan State University, East Lansing MI; United States of America.

¹⁰⁸Group of Particle Physics, University of Montreal, Montreal QC; Canada.

¹⁰⁹Fakultät für Physik, Ludwig-Maximilians-Universität München, München; Germany.

¹¹⁰Max-Planck-Institut für Physik (Werner-Heisenberg-Institut), München; Germany.

¹¹¹Graduate School of Science and Kobayashi-Maskawa Institute, Nagoya University, Nagoya; Japan.

¹¹²Department of Physics and Astronomy, University of New Mexico, Albuquerque NM; United States of America.

¹¹³Institute for Mathematics, Astrophysics and Particle Physics, Radboud University/Nikhef, Nijmegen; Netherlands.

¹¹⁴Nikhef National Institute for Subatomic Physics and University of Amsterdam, Amsterdam; Netherlands.

- ¹¹⁵Department of Physics, Northern Illinois University, DeKalb IL; United States of America.
- ¹¹⁶^(a)New York University Abu Dhabi, Abu Dhabi;^(b)University of Sharjah, Sharjah; United Arab Emirates.
- ¹¹⁷Department of Physics, New York University, New York NY; United States of America.
- ¹¹⁸Ochanomizu University, Otsuka, Bunkyo-ku, Tokyo; Japan.
- ¹¹⁹Ohio State University, Columbus OH; United States of America.
- ¹²⁰Homer L. Dodge Department of Physics and Astronomy, University of Oklahoma, Norman OK; United States of America.
- ¹²¹Department of Physics, Oklahoma State University, Stillwater OK; United States of America.
- ¹²²Palacký University, Joint Laboratory of Optics, Olomouc; Czech Republic.
- ¹²³Institute for Fundamental Science, University of Oregon, Eugene, OR; United States of America.
- ¹²⁴Graduate School of Science, Osaka University, Osaka; Japan.
- ¹²⁵Department of Physics, University of Oslo, Oslo; Norway.
- ¹²⁶Department of Physics, Oxford University, Oxford; United Kingdom.
- ¹²⁷LPNHE, Sorbonne Université, Université Paris Cité, CNRS/IN2P3, Paris; France.
- ¹²⁸Department of Physics, University of Pennsylvania, Philadelphia PA; United States of America.
- ¹²⁹Department of Physics and Astronomy, University of Pittsburgh, Pittsburgh PA; United States of America.
- ¹³⁰^(a)Laboratório de Instrumentação e Física Experimental de Partículas - LIP, Lisboa;^(b)Departamento de Física, Faculdade de Ciências, Universidade de Lisboa, Lisboa;^(c)Departamento de Física, Universidade de Coimbra, Coimbra;^(d)Centro de Física Nuclear da Universidade de Lisboa, Lisboa;^(e)Departamento de Física, Universidade do Minho, Braga;^(f)Departamento de Física Teórica y del Cosmos, Universidad de Granada, Granada (Spain);^(g)Departamento de Física, Instituto Superior Técnico, Universidade de Lisboa, Lisboa; Portugal.
- ¹³¹Institute of Physics of the Czech Academy of Sciences, Prague; Czech Republic.
- ¹³²Czech Technical University in Prague, Prague; Czech Republic.
- ¹³³Charles University, Faculty of Mathematics and Physics, Prague; Czech Republic.
- ¹³⁴Particle Physics Department, Rutherford Appleton Laboratory, Didcot; United Kingdom.
- ¹³⁵IRFU, CEA, Université Paris-Saclay, Gif-sur-Yvette; France.
- ¹³⁶Santa Cruz Institute for Particle Physics, University of California Santa Cruz, Santa Cruz CA; United States of America.
- ¹³⁷^(a)Departamento de Física, Pontificia Universidad Católica de Chile, Santiago;^(b)Millennium Institute for Subatomic physics at high energy frontier (SAPHIR), Santiago;^(c)Instituto de Investigación Multidisciplinario en Ciencia y Tecnología, y Departamento de Física, Universidad de La Serena;^(d)Universidad Andres Bello, Department of Physics, Santiago;^(e)Instituto de Alta Investigación, Universidad de Tarapacá, Arica;^(f)Departamento de Física, Universidad Técnica Federico Santa María, Valparaíso; Chile.
- ¹³⁸Department of Physics, University of Washington, Seattle WA; United States of America.
- ¹³⁹Department of Physics and Astronomy, University of Sheffield, Sheffield; United Kingdom.
- ¹⁴⁰Department of Physics, Shinshu University, Nagano; Japan.
- ¹⁴¹Department Physik, Universität Siegen, Siegen; Germany.
- ¹⁴²Department of Physics, Simon Fraser University, Burnaby BC; Canada.
- ¹⁴³SLAC National Accelerator Laboratory, Stanford CA; United States of America.
- ¹⁴⁴Department of Physics, Royal Institute of Technology, Stockholm; Sweden.
- ¹⁴⁵Departments of Physics and Astronomy, Stony Brook University, Stony Brook NY; United States of America.
- ¹⁴⁶Department of Physics and Astronomy, University of Sussex, Brighton; United Kingdom.

- ¹⁴⁷School of Physics, University of Sydney, Sydney; Australia.
- ¹⁴⁸Institute of Physics, Academia Sinica, Taipei; Taiwan.
- ¹⁴⁹^(a)E. Andronikashvili Institute of Physics, Iv. Javakhishvili Tbilisi State University, Tbilisi; ^(b)High Energy Physics Institute, Tbilisi State University, Tbilisi; ^(c)University of Georgia, Tbilisi; Georgia.
- ¹⁵⁰Department of Physics, Technion, Israel Institute of Technology, Haifa; Israel.
- ¹⁵¹Raymond and Beverly Sackler School of Physics and Astronomy, Tel Aviv University, Tel Aviv; Israel.
- ¹⁵²Department of Physics, Aristotle University of Thessaloniki, Thessaloniki; Greece.
- ¹⁵³International Center for Elementary Particle Physics and Department of Physics, University of Tokyo, Tokyo; Japan.
- ¹⁵⁴Department of Physics, Tokyo Institute of Technology, Tokyo; Japan.
- ¹⁵⁵Department of Physics, University of Toronto, Toronto ON; Canada.
- ¹⁵⁶^(a)TRIUMF, Vancouver BC; ^(b)Department of Physics and Astronomy, York University, Toronto ON; Canada.
- ¹⁵⁷Division of Physics and Tomonaga Center for the History of the Universe, Faculty of Pure and Applied Sciences, University of Tsukuba, Tsukuba; Japan.
- ¹⁵⁸Department of Physics and Astronomy, Tufts University, Medford MA; United States of America.
- ¹⁵⁹United Arab Emirates University, Al Ain; United Arab Emirates.
- ¹⁶⁰Department of Physics and Astronomy, University of California Irvine, Irvine CA; United States of America.
- ¹⁶¹Department of Physics and Astronomy, University of Uppsala, Uppsala; Sweden.
- ¹⁶²Department of Physics, University of Illinois, Urbana IL; United States of America.
- ¹⁶³Instituto de Física Corpuscular (IFIC), Centro Mixto Universidad de Valencia - CSIC, Valencia; Spain.
- ¹⁶⁴Department of Physics, University of British Columbia, Vancouver BC; Canada.
- ¹⁶⁵Department of Physics and Astronomy, University of Victoria, Victoria BC; Canada.
- ¹⁶⁶Fakultät für Physik und Astronomie, Julius-Maximilians-Universität Würzburg, Würzburg; Germany.
- ¹⁶⁷Department of Physics, University of Warwick, Coventry; United Kingdom.
- ¹⁶⁸Waseda University, Tokyo; Japan.
- ¹⁶⁹Department of Particle Physics and Astrophysics, Weizmann Institute of Science, Rehovot; Israel.
- ¹⁷⁰Department of Physics, University of Wisconsin, Madison WI; United States of America.
- ¹⁷¹Fakultät für Mathematik und Naturwissenschaften, Fachgruppe Physik, Bergische Universität Wuppertal, Wuppertal; Germany.
- ¹⁷²Department of Physics, Yale University, New Haven CT; United States of America.
- ^a Also Affiliated with an institute covered by a cooperation agreement with CERN.
- ^b Also at An-Najah National University, Nablus; Palestine.
- ^c Also at Borough of Manhattan Community College, City University of New York, New York NY; United States of America.
- ^d Also at Center for High Energy Physics, Peking University; China.
- ^e Also at Center for Interdisciplinary Research and Innovation (CIRI-AUTH), Thessaloniki; Greece.
- ^f Also at Centro Studi e Ricerche Enrico Fermi; Italy.
- ^g Also at CERN, Geneva; Switzerland.
- ^h Also at Département de Physique Nucléaire et Corpusculaire, Université de Genève, Genève; Switzerland.
- ⁱ Also at Departament de Física de la Universitat Autònoma de Barcelona, Barcelona; Spain.
- ^j Also at Department of Financial and Management Engineering, University of the Aegean, Chios; Greece.
- ^k Also at Department of Physics and Astronomy, Michigan State University, East Lansing MI; United States of America.
- ^l Also at Department of Physics, Ben Gurion University of the Negev, Beer Sheva; Israel.

- m* Also at Department of Physics, California State University, Sacramento; United States of America.
- n* Also at Department of Physics, King's College London, London; United Kingdom.
- o* Also at Department of Physics, Stanford University, Stanford CA; United States of America.
- p* Also at Department of Physics, University of Fribourg, Fribourg; Switzerland.
- q* Also at Department of Physics, University of Thessaly; Greece.
- r* Also at Department of Physics, Westmont College, Santa Barbara; United States of America.
- s* Also at Hellenic Open University, Patras; Greece.
- t* Also at Institutio Catalana de Recerca i Estudis Avancats, ICREA, Barcelona; Spain.
- u* Also at Institut für Experimentalphysik, Universität Hamburg, Hamburg; Germany.
- v* Also at Institute for Nuclear Research and Nuclear Energy (INRNE) of the Bulgarian Academy of Sciences, Sofia; Bulgaria.
- w* Also at Institute of Applied Physics, Mohammed VI Polytechnic University, Ben Guerir; Morocco.
- x* Also at Institute of Particle Physics (IPP); Canada.
- y* Also at Institute of Physics and Technology, Mongolian Academy of Sciences, Ulaanbaatar; Mongolia.
- z* Also at Institute of Physics, Azerbaijan Academy of Sciences, Baku; Azerbaijan.
- aa* Also at Institute of Theoretical Physics, Ilia State University, Tbilisi; Georgia.
- ab* Also at L2IT, Université de Toulouse, CNRS/IN2P3, UPS, Toulouse; France.
- ac* Also at Lawrence Livermore National Laboratory, Livermore; United States of America.
- ad* Also at National Institute of Physics, University of the Philippines Diliman (Philippines); Philippines.
- ae* Also at Technical University of Munich, Munich; Germany.
- af* Also at The Collaborative Innovation Center of Quantum Matter (CICQM), Beijing; China.
- ag* Also at TRIUMF, Vancouver BC; Canada.
- ah* Also at Università di Napoli Parthenope, Napoli; Italy.
- ai* Also at University of Colorado Boulder, Department of Physics, Colorado; United States of America.
- aj* Also at Washington College, Chestertown, MD; United States of America.
- ak* Also at Yeditepe University, Physics Department, Istanbul; Türkiye.
- * Deceased